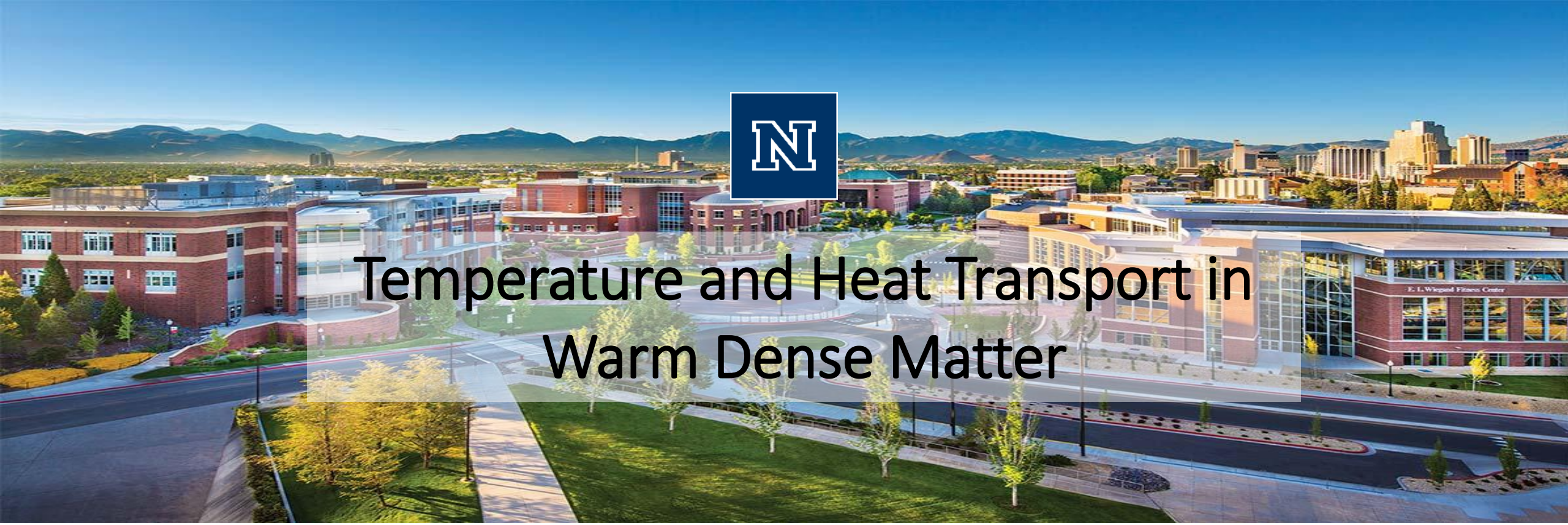

Temperature and Heat Transport in Warm Dense Matter

Tilo Doeppner	LLNL	Larent Divol	LLNL	Hae-Ja Lee	SLAC	Emma McBride	QUB, UK
Cameron Allen	UNR/LANL	Gianluca Gregori	Oxford	Eric Galtier	SLAC	Luke Fletcher	SLAC
Matthew Oliver	CLF, RAL	Chris Spindloe	CLF, RAL	Adrien Descamps	QUB, UK	Karen Appel	European XFEL
Sarah Prins	UNR	Wolfgang Theobald	LLE	Dimitri Khaghani	SLAC	Ulf Zastrau	European XFEL
Dirk Gericke	University of Warwick	G. Elijah Kemp	LLE	Sameen Yunus	SLAC	Sebastian Goede	European XFEL
Otto Landen	LLNL	Daniel Haden	UNR	Eric Cunningham	SLAC	Giulio Monaco	University of Padova
Yuan Ping	LLNL	Travis Griffin	UNR	Jerry Hastings	SLAC	Sebastian Goede	European XFEL
Markus Schoelmerich	LLNL	Bob Nagler	SLAC	Siegfried Glenzer	SLAC	Lennart Wollenweber	European XFEL

Dr Thomas White
University of Nevada, Reno

Michigan Seminar
Wednesday | 5th February 2025

NNSA Award NA0004039

NSF Award PHY-2045718

Discussion topics

- **Heat transport across warm dense matter interfaces**
  - **Observation of *Interfacial Thermal Resistance* at Extreme Conditions**
- Direct ion temperature measurements at free electron lasers
  - Bond strength in non-equilibrium gold
  - Electron ion equilibration in warm dense matter
  - Superheating beyond the entropy catastrophe
- Forward Scattering
  - Sound speed in warm dense methane
  - Phonon dispersion and temperature through detailed balance

Cameron Allen
Now postdoc at LANL

Sarah Shores Prins
3rd year GRA

Key Question: Can we directly measure transport properties in warm dense matter?

"transport coefficients including thermal and electrical conduction, electron–ion coupling, inter-ion diffusion, ion viscosity, and charged particle stopping powers."

L. Stanek *et al.* Phys. Plasmas 31, 052104 (2024)

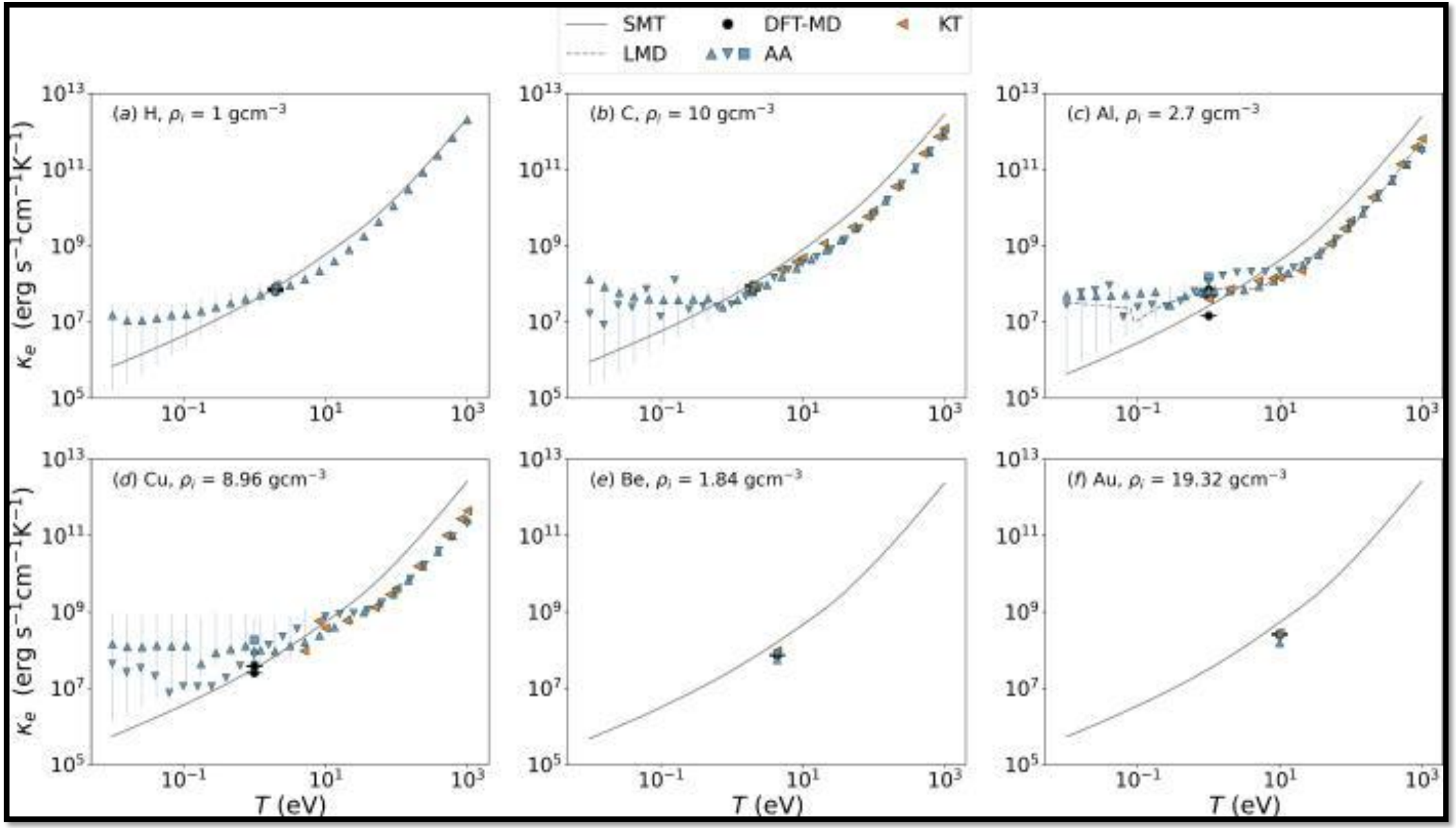

L. Stanek *et al.* Phys. Plasmas 31, 052104 (2024)

Thermal Conductivity affects the temperature profile of a system

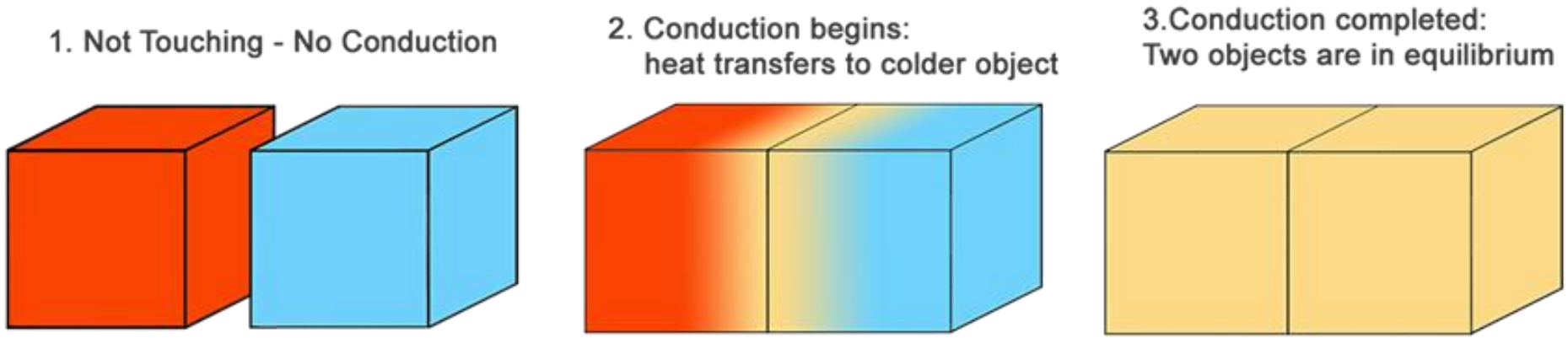

- Thermal conductivity refers to a material's ability to transport heat and is the basic microscopic quantity that governs the atomic level energy transport.
- How much heat is conducted, and how quickly it conducts, are dependent on the materials involved and the initial temperature gradient
- Characteristic scales: $\Delta r \approx \sqrt{\alpha \Delta t}$
  - For WDM materials: $\Delta t \sim ns,\ \alpha = \frac{\kappa}{\rho\, C_P} \sim {}^{cm^2}/_{s} \rightarrow \Delta \boldsymbol{r} \sim \boldsymbol{\mu m}$

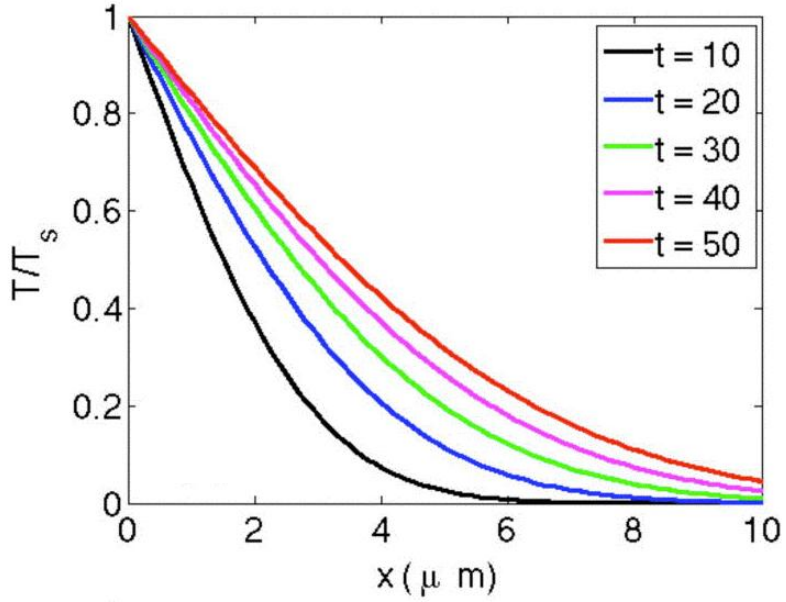

Temperature ratio as a function of distance, at various time delays.
Y. Ping *et al.* Phys. Plasmas 22, 092701 (2015)

A pressure – equilibrated interface allows for investigation of temperature gradients

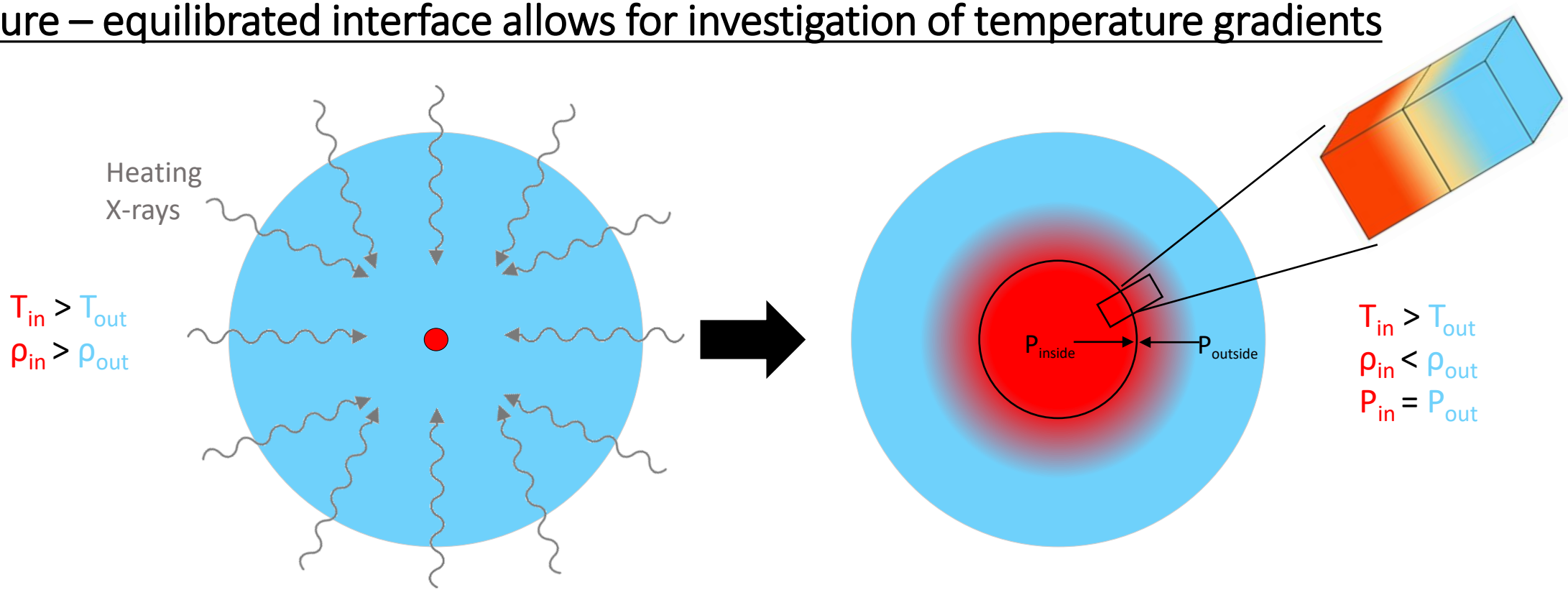

- Isochorically – heating a tamped system – such as a metal wire inside plastic – creates an expanding interface
  - As it expands, we have hot metal next to a cooler plastic, setting up the temperature gradient
- If the tamper can hold the expansion of the inner material, the pressure on either side of the interface is equilibrated –> $P_{inside} = P_{outside}$
  - Of course, we can't see heat, only its effects on density
  - For a constant pressure, a change in the temperature profile will inversely affect the density profile ($P \propto \rho T$)

Thermal conduction will alter density gradients – how much?

- At a pressure – equilibrated interface, the temperature profile is continuous, but the density develops a discontinuity at the interface
  - The metal next to the interface is hotter than the plastic, but cooler than metal further from the interface
    - The metal densifies towards the interface as it deposits heat into the plastic
  - The opposite happens for the plastic, which is hottest and least dense immediately next to the interface
- The scale lengths of the material on either side of the discontinuity are on order of a micron, and the shape will heavily depend on thermal conductivity

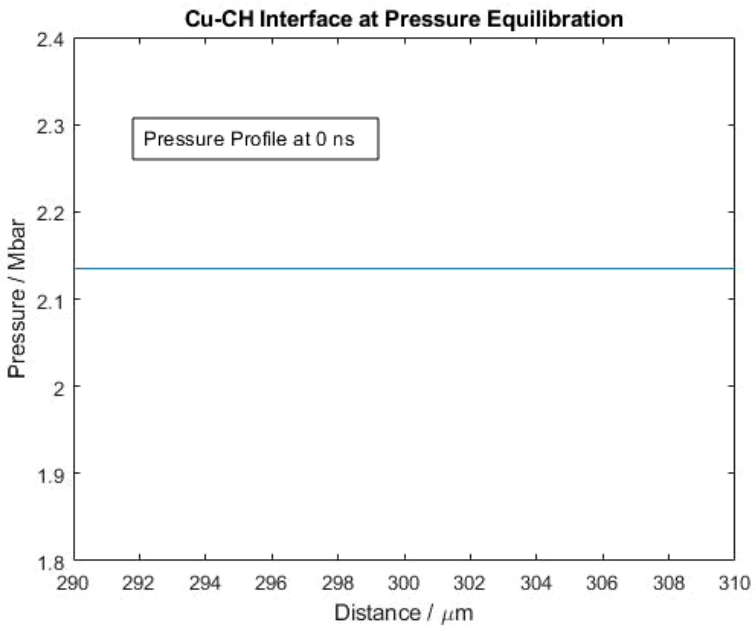

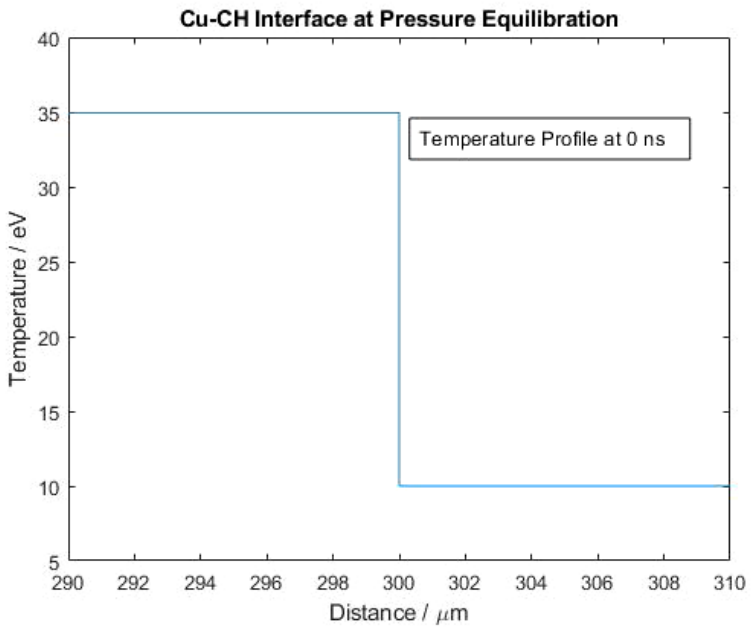

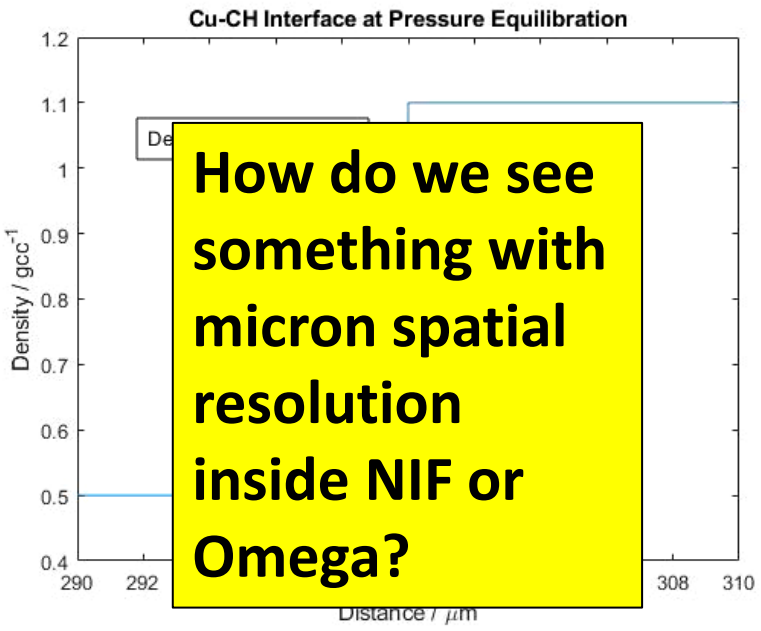

How do we see something with micron spatial resolution inside NIF or Omega?

Thermal conduction will alter density gradients – how much?

- At a pressure – equilibrated interface, the temperature profile is continuous, but the density develops a discontinuity at the interface
  - The metal next to the interface is hotter than the plastic, but cooler than metal further from the interface
    - The metal densifies towards the interface as it deposits heat into the plastic
  - The opposite happens for the plastic, which is hottest and least dense immediately next to the interface
- The scale lengths of the material on either side of the discontinuity are on orSder of a micron, and the shape will heavily depend on thermal conductivity

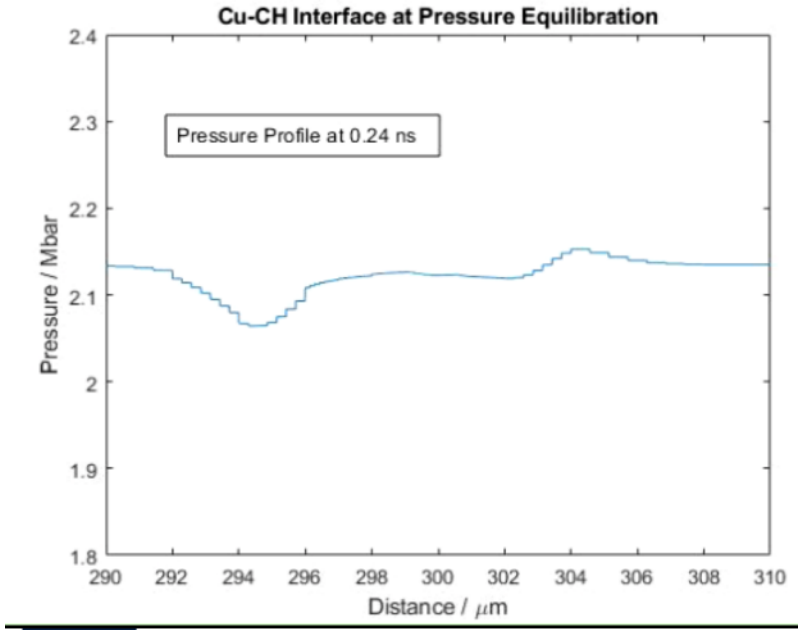

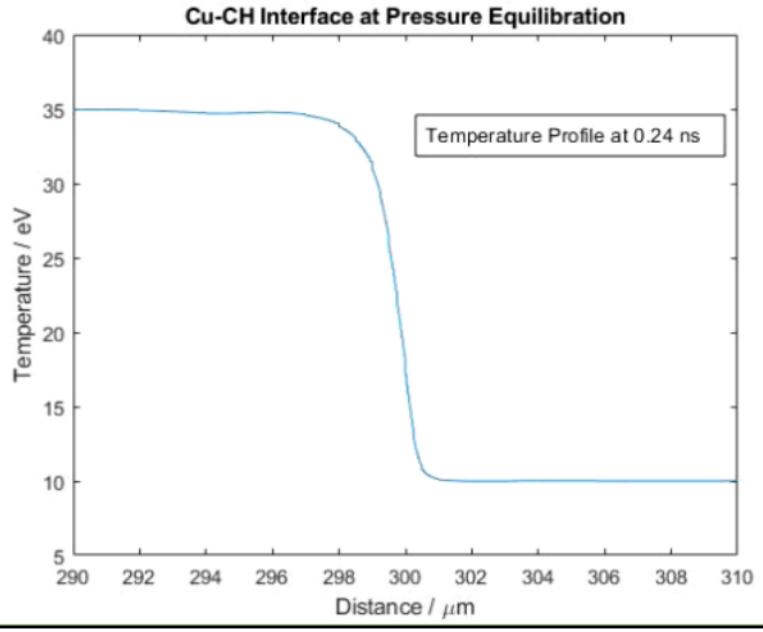

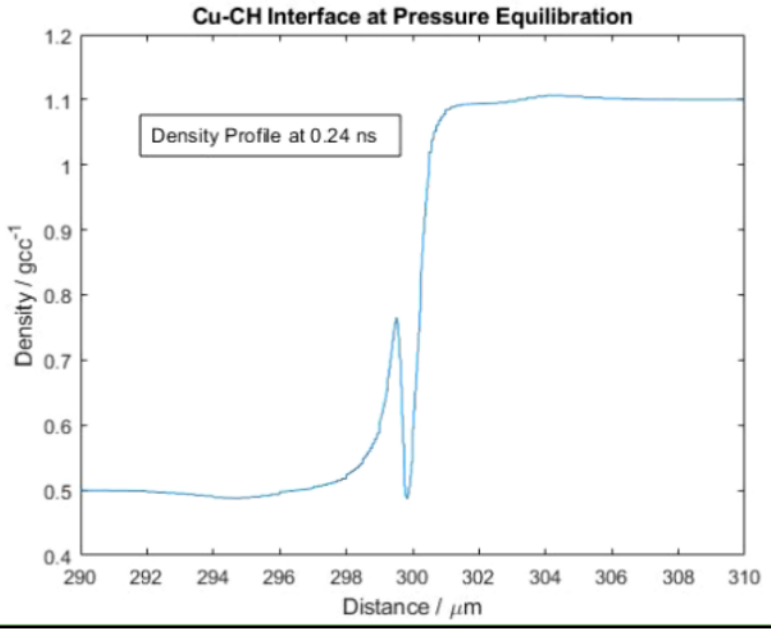

Using a 1 µm wide slit gives a micron-scale source for X-ray radiography

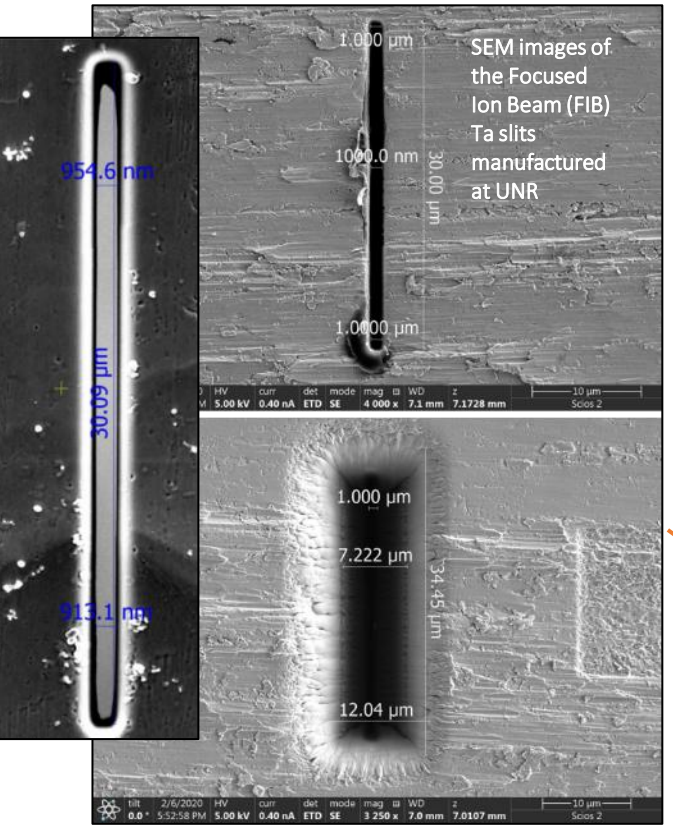

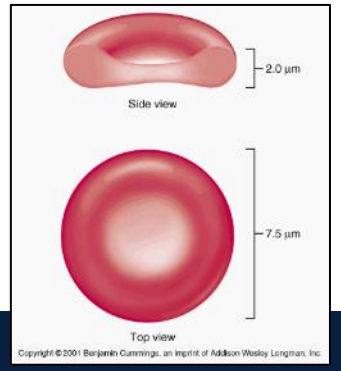

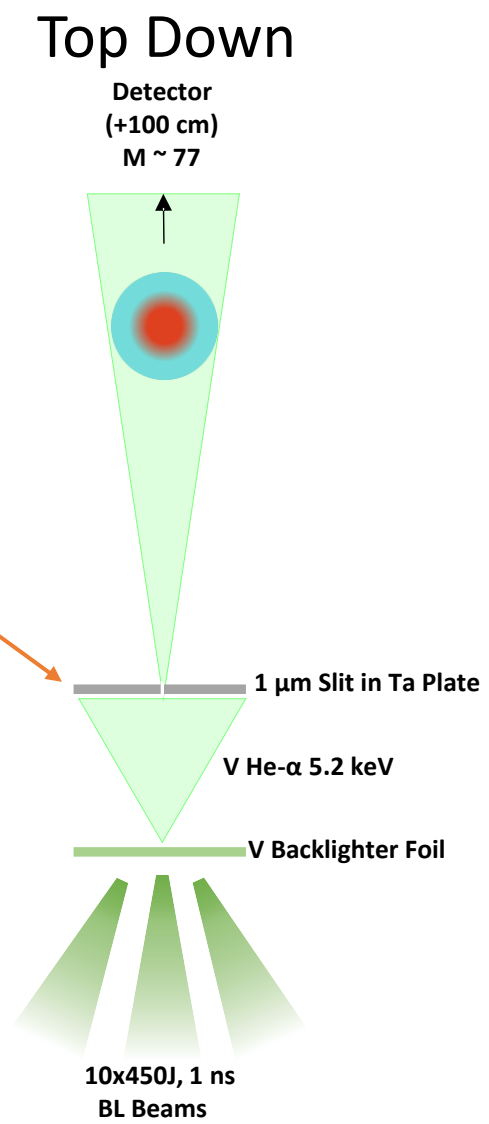

- By placing a micron-wide slit in front of the source, we have the spatial resolution to see micron-scale scale length changes
- A micron-scale source will also have the spatial coherence to be sensitive to interference (refraction, diffraction) effects
- At a sharp boundary between two WDM materials, we will have absorptive, refractive, *and* diffractive effects
  - The combination of these features will be unique to the density profile across the boundary and the imaging geometry
    - From the evolving density profile of a system, we can determine the thermal conductivity for the involved materials
- We call this "Fresnel Diffractive Radiography" (FDR)

The micron-sized source introduces interference effects

- Imaging geometry or source characteristics means that most X-ray imaging is based upon absorption contrast

- For small source sizes and large propagation distances, we move into the phase-contrast imaging (PCI) / **refraction**-enhanced radiography (RER) regime, with improved contrast at weakly absorbing interfaces

- Additionally, **diffraction** fringes occur from material boundaries, but are frequently overshadowed due to larger refraction fringe scales*
  - Diffraction becomes important at Fresnel numbers F ~ 1

$$F = {a^2}/{f\lambda}$$

where f is related to geometry and a is the scale length

"Fresnel Diffraction"

- The major difference between this work and previous RER experiments is **the sensitivity to diffractive effects**

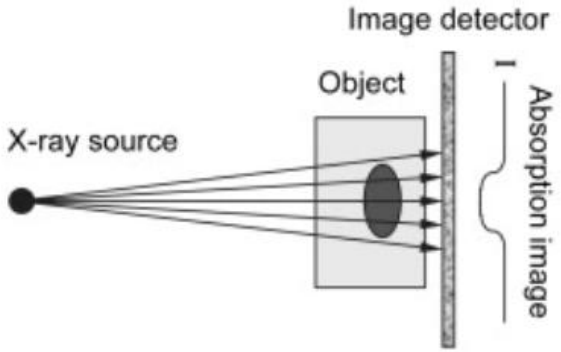

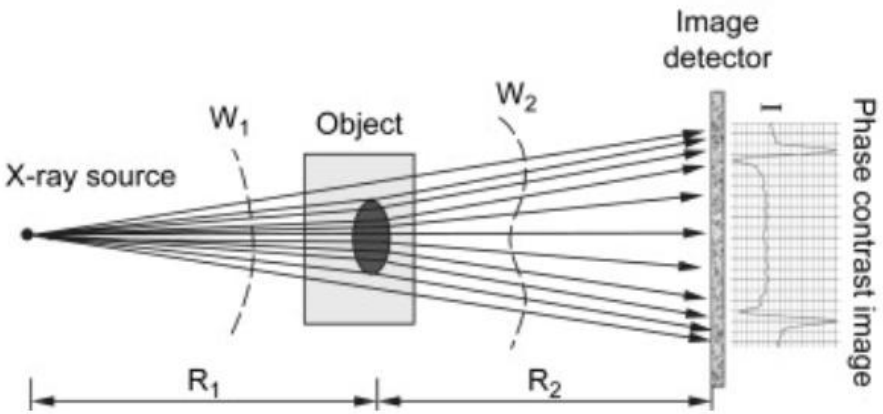

Absorption

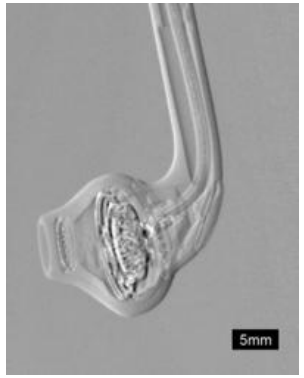

PCI

*J. Koch *et al.* J. Appl. Phys. **105**, 113112 (2009)

Point source X-ray radiography maintains a consistent shape with increasing propagation distance

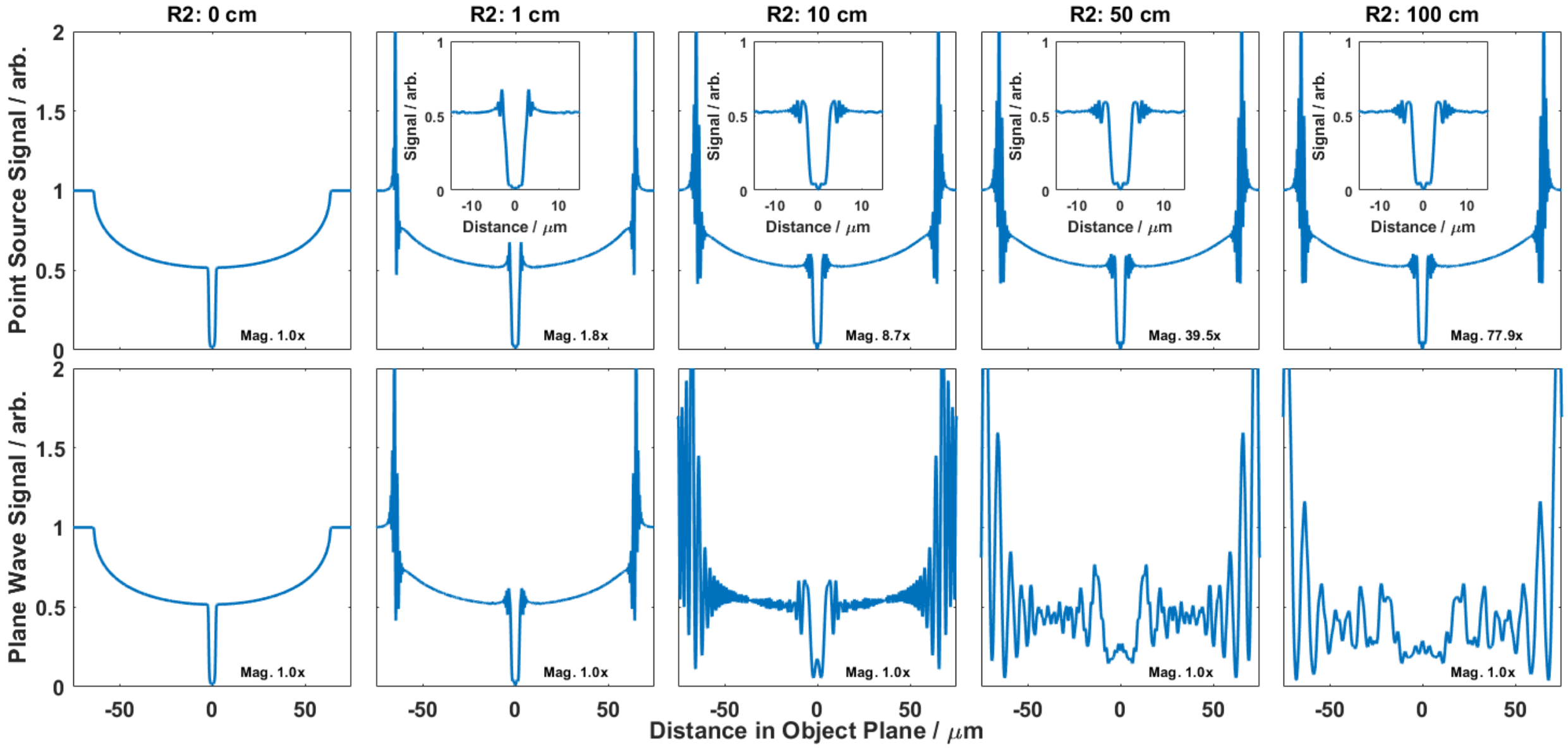

The experiments rely on precise alignment between the slits and the wires

- The initial experimental goal for the Omega shots was to achieve micron-scale spatial resolution with FDR
- The alignment of the wire and the slit is critical to maximize the resolution capabilities of the platform
    - Each degree of relative tilt of with respect to parallel introduces ~ 0.5 µm of source broadening
- We achieve ~ 2 µm source size, due in part to the tapering of the slit

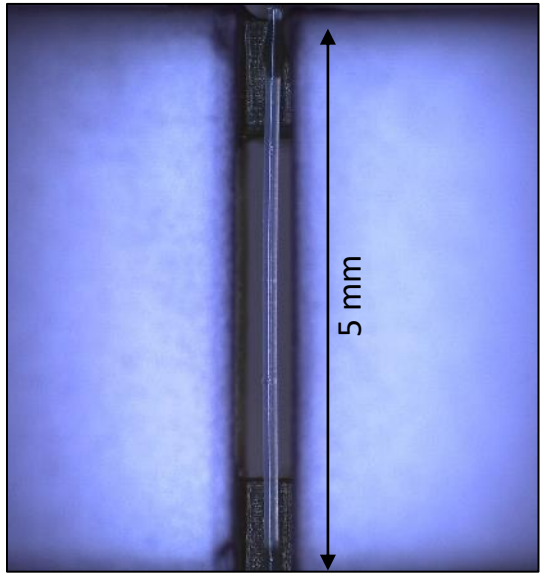

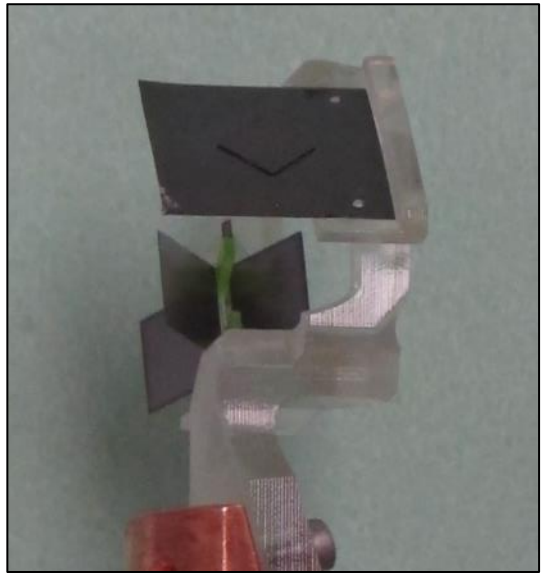

Diffraction enhanced imaging utilizing a laser produced x-ray source

Cite as: Rev. Sci. Instrum. 93, 093502 (2022); https://doi.org/10.1063/5.0091348
Submitted: 14 March 2022 • Accepted: 27 July 2022 • Published Online: 07 September 2022

M. Oliver, C. H. Allen, L. Divol, et al.

Developing a platform for Fresnel diffractive radiography with 1 μm spatial resolution at the National Ignition Facility

Cite as: Rev. Sci. Instrum. 94, 013104 (2023); doi: 10.1063/5.0101890
Submitted: 3 June 2022 • Accepted: 4 January 2023 •
Published Online: 25 January 2023

M. O. Schoelmerich,[1,a] T. Döppner,[1] C. H. Allen,[2] L. Divol,[1] M. Oliver,[2] D. Haden,[2] M. Biener,[1] J. Crippen,[4] J. Delora-Ellefson,[1] B. Ferguson,[1] D. O. Gericke,[2] A. Goldman,[2] A. Haid,[4] C. Heinbockel,[1] D. Kalantar,[1] Z. Karmiol,[2] G. Kemp,[1] J. Kroll,[1] O. L. Landen,[1] N. Masters,[1] Y. Ping,[1] C. Spindloe,[5] W. Theobald,[2] and T. G. White[3]

Research Article — Vol. 61, No. 8 / 10 March 2022 / Applied Optics — 1987

applied optics

Toward an integrated platform for characterizing laser-driven, isochorically heated plasmas with 1 µm spatial resolution

C. H. Allen,[1,*] M. Oliver,[2] L. Divol,[3] O. L. Landen,[3] Y. Ping,[3] M. Schölmerich,[3] R. Wallace,[3] R. Earley,[4] W. Theobald,[4] T. G. White,[1] and T. Döppner[3]

[1]Physics Department, University of Nevada Reno, 1664 N Virginia St, Reno, Nevada 89557, USA
[2]Rutherford Appleton Laboratory, Didcot, OX11 0DE, UK
[3]Lawrence Livermore National Laboratory, L-493, 70000 East Avenue, Livermore, California 94550, USA
[4]Laboratory for Laser Energetics, 250 E River Rd, Rochester, New York 14623, USA
*Corresponding author: challen@unr.edu

Received 18 October 2021; revised 4 February 2022; accepted 15 February 2022; posted 15 February 2022; published 3 March 2022

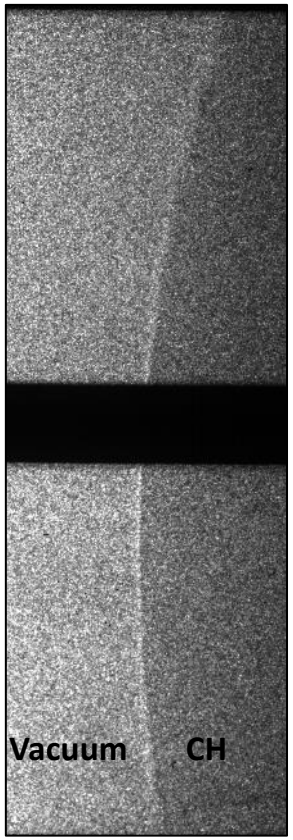

Preliminary data from Schölmerich/ Döppner March 2023

Imaging a sphere with a slit demonstrates that the alignment between the slit and the interface is important

Diffraction patterns are very useful for measuring small objects

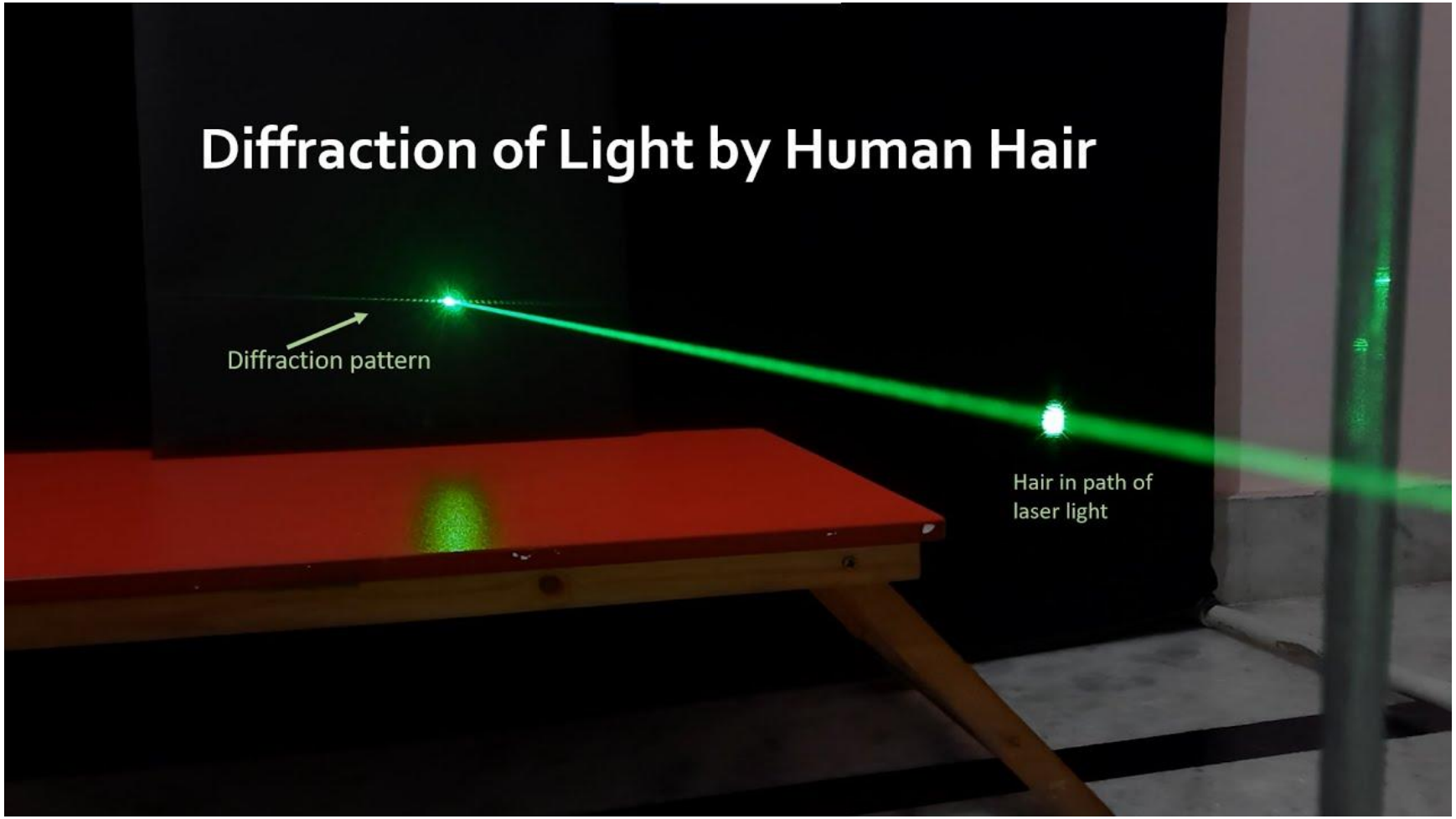

Human Hair: ~100 µm diameter
Optical wavelength: 532 nm
We perform the same experiment, but at 1000x smaller scale

We use FDR to image an isochorically heated buried wire

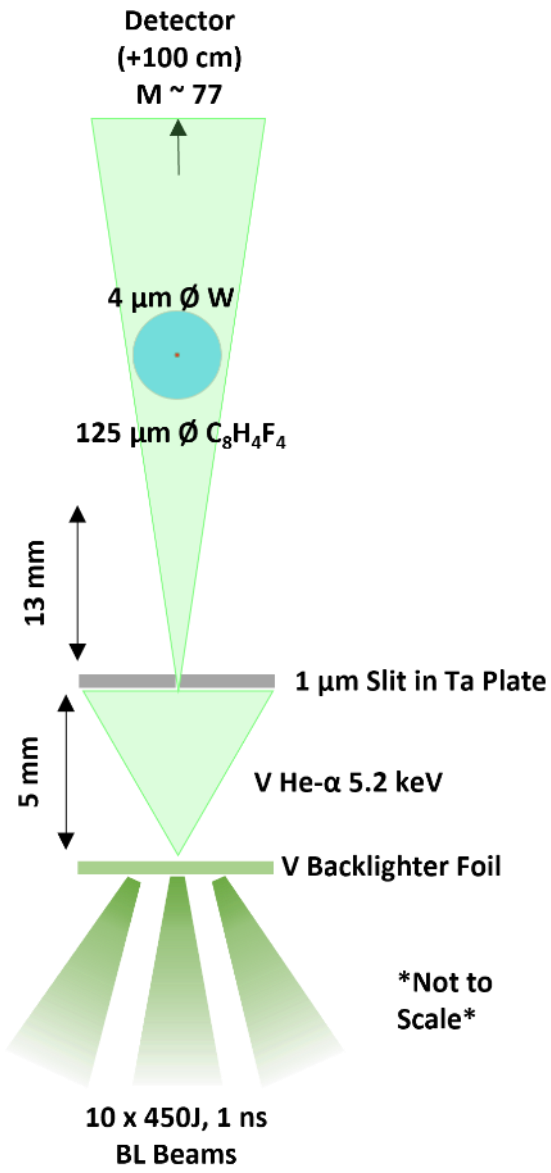

We use FDR to image an isochorically heated buried wire

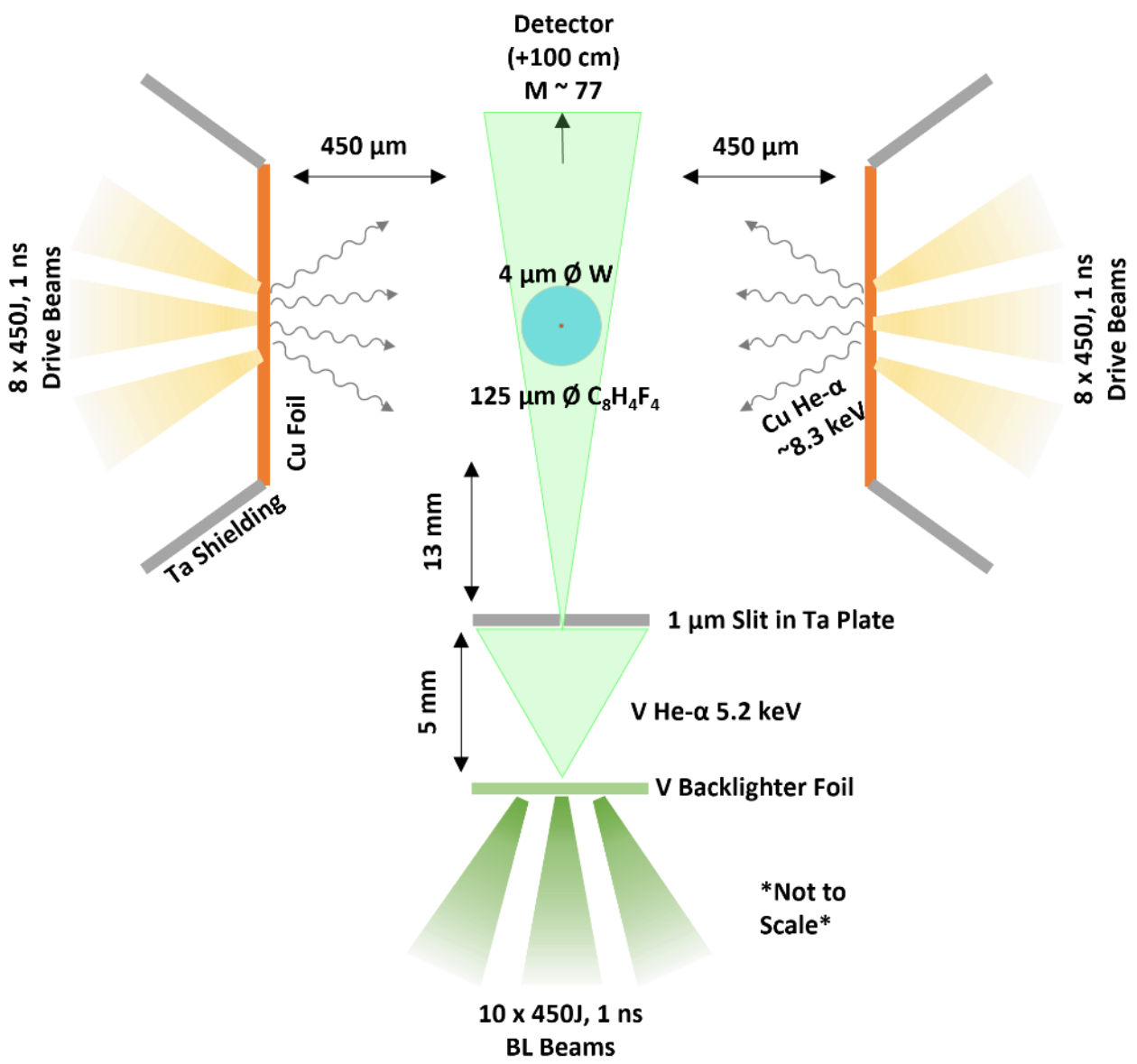

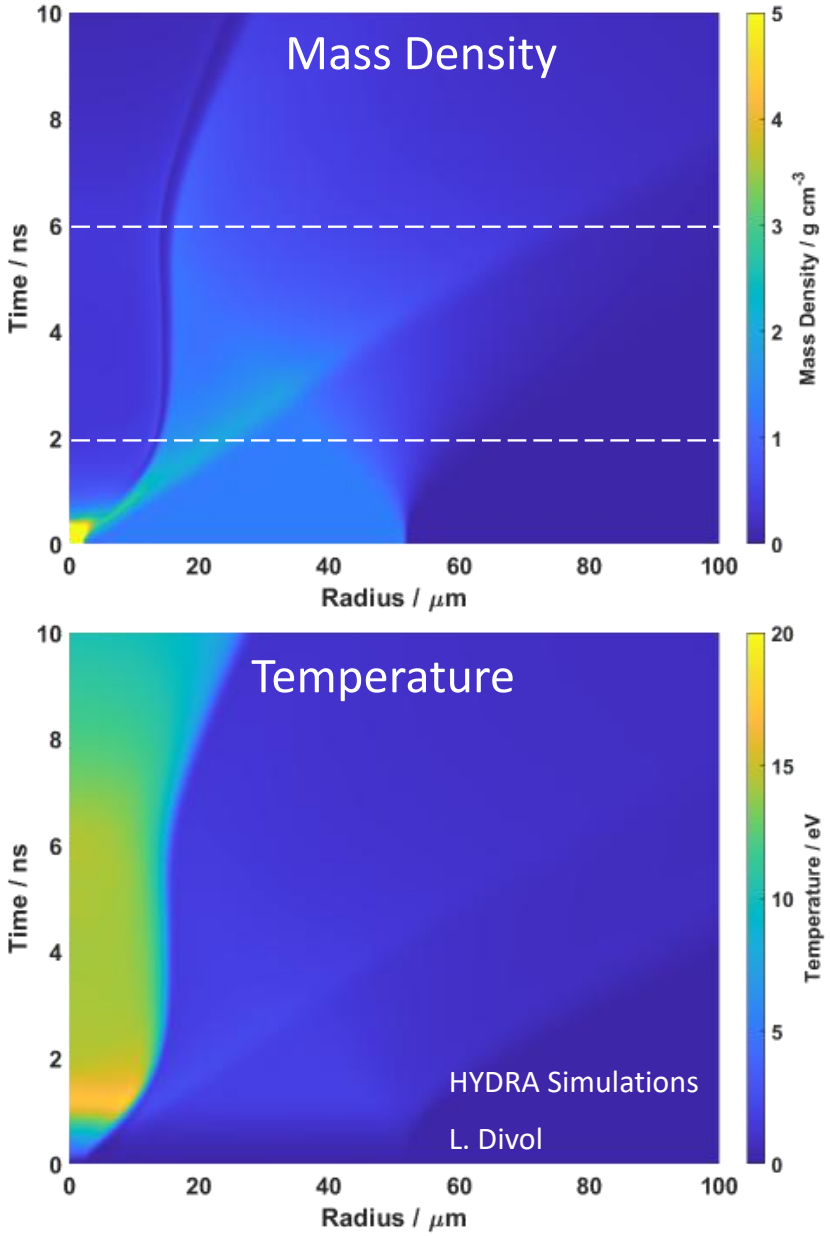

The FDR platform has achieved amazing results

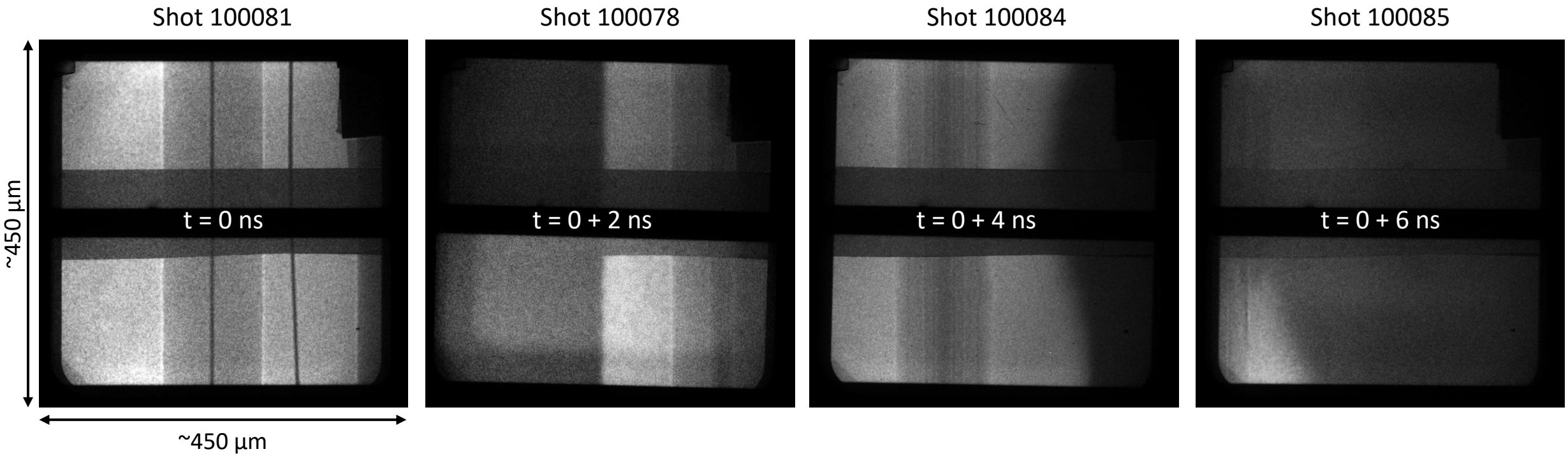

- The primary XRFC diagnostic recorded excellent data, allowing for a time sequence over multiple shots/targets
- Target positioning on the detector sometimes left data on the edge (as in 100085) – more recent target designs have improved fiducials allowing for much more repeatable placement

Target alignment has been improved greatly with 3d printed target frames

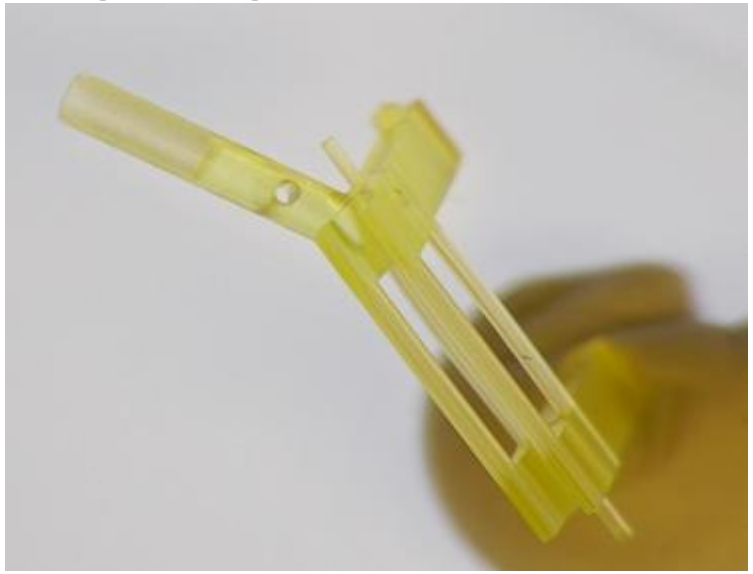

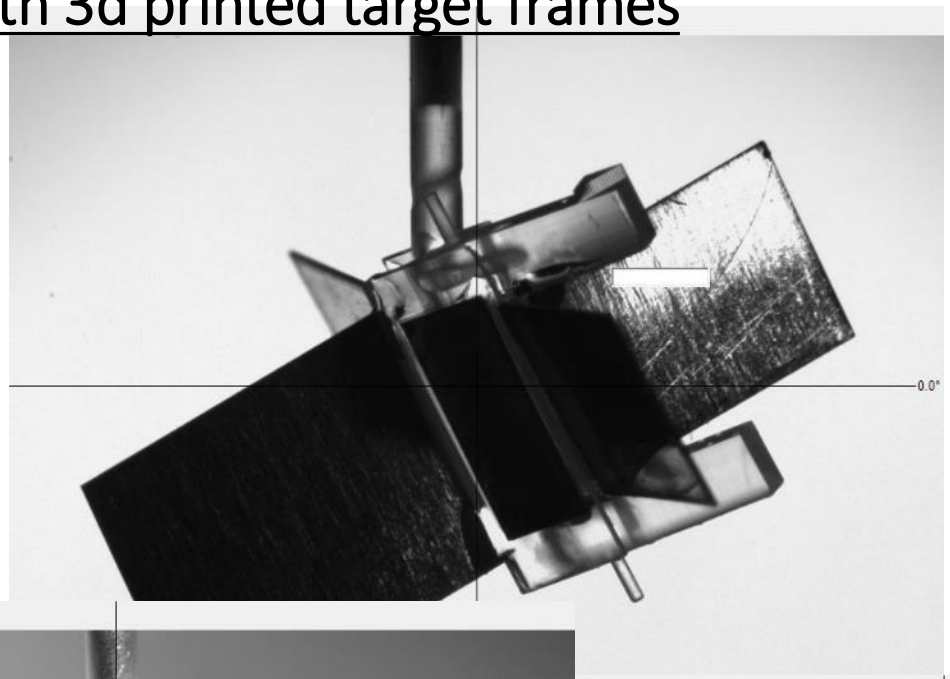

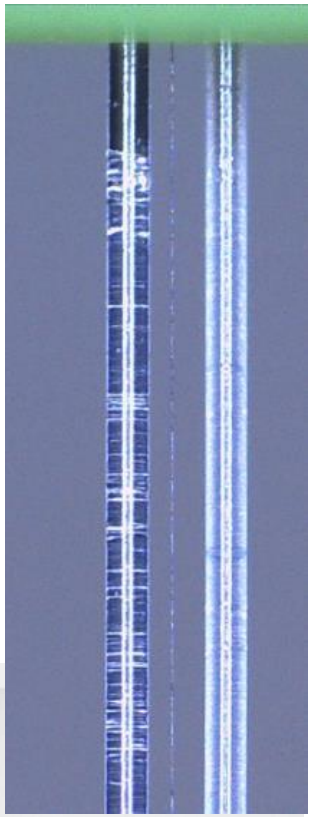

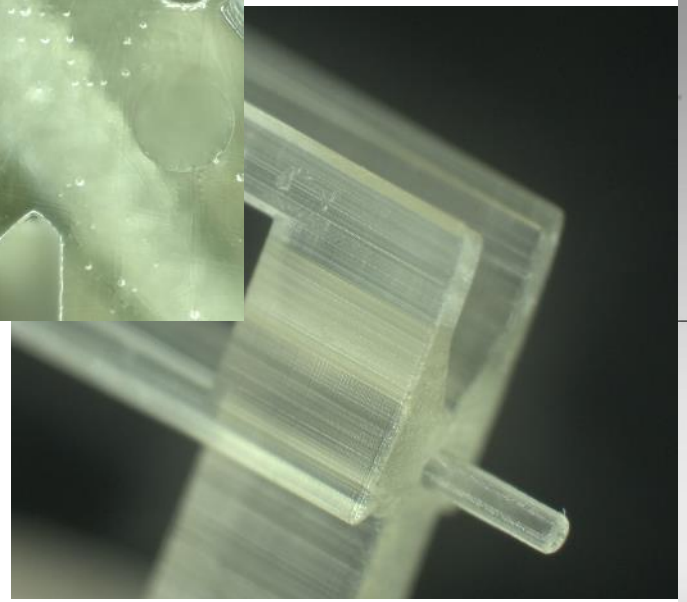

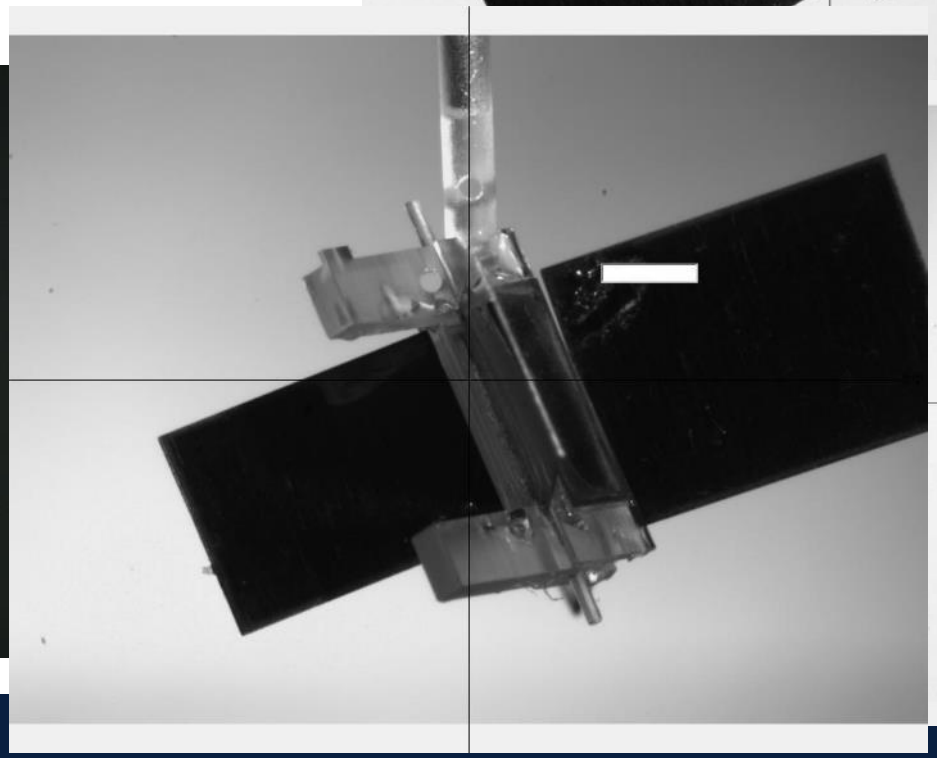

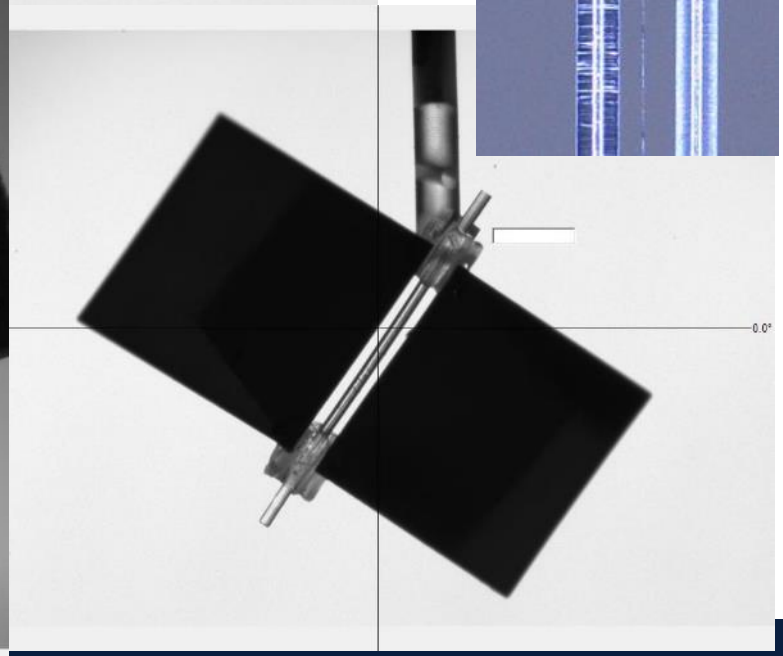

The evolving system and its features can tell us about the properties of the materials

- The notable features in the expanded system include:
  - W wire expansion (~4 µm → ~20 µm)
  - Outgoing shock waves
  - Rarefaction features from expanded outside edge

- The data is *extremely* symmetric, especially around the interface region we are interested in

- By taking data at different times, we can track the evolution of the interface changing over time
  - Goal is to determine the shape of the interface to determine thermal conductivity

Shot Image

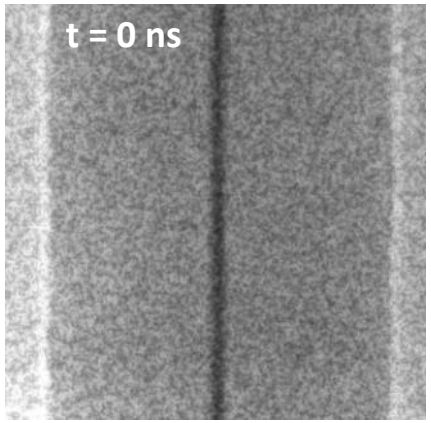

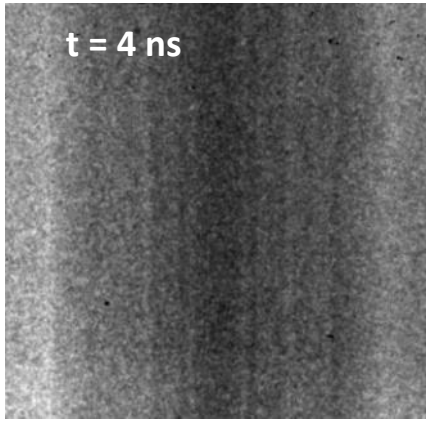

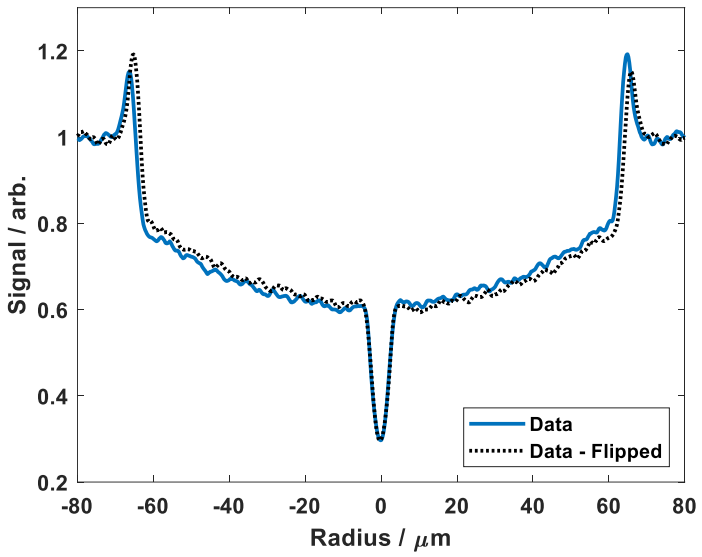

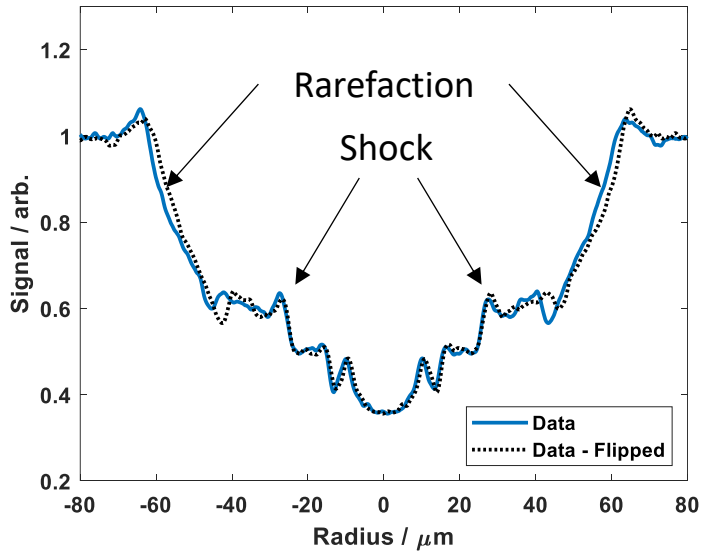

The key piece of analysis is forward modeling of the diffraction-refraction patterns

- We have developed a code that solves the Fresnel-Kirchoff Equation* for a parameterized density profile, calculating both refractive and diffractive effects
- The cold data gives us excellent agreement with a known step-like density profile and a <2 um source size

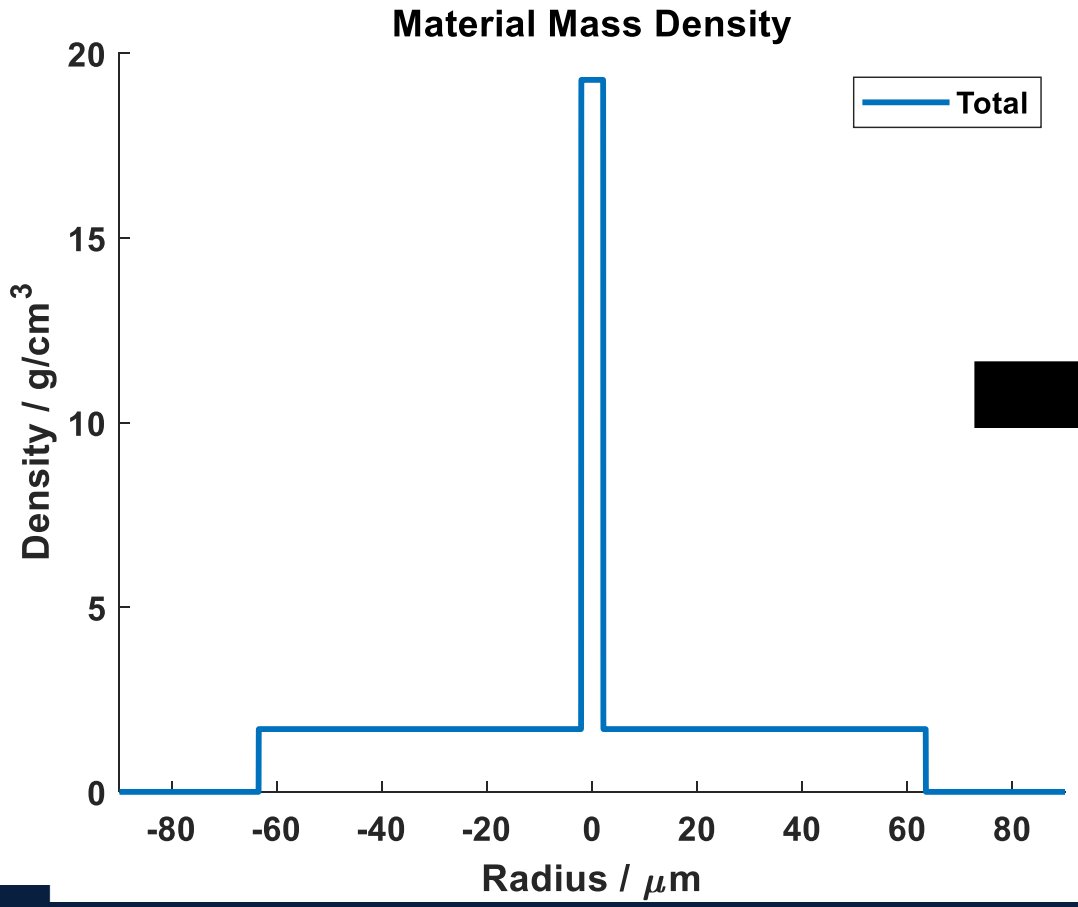

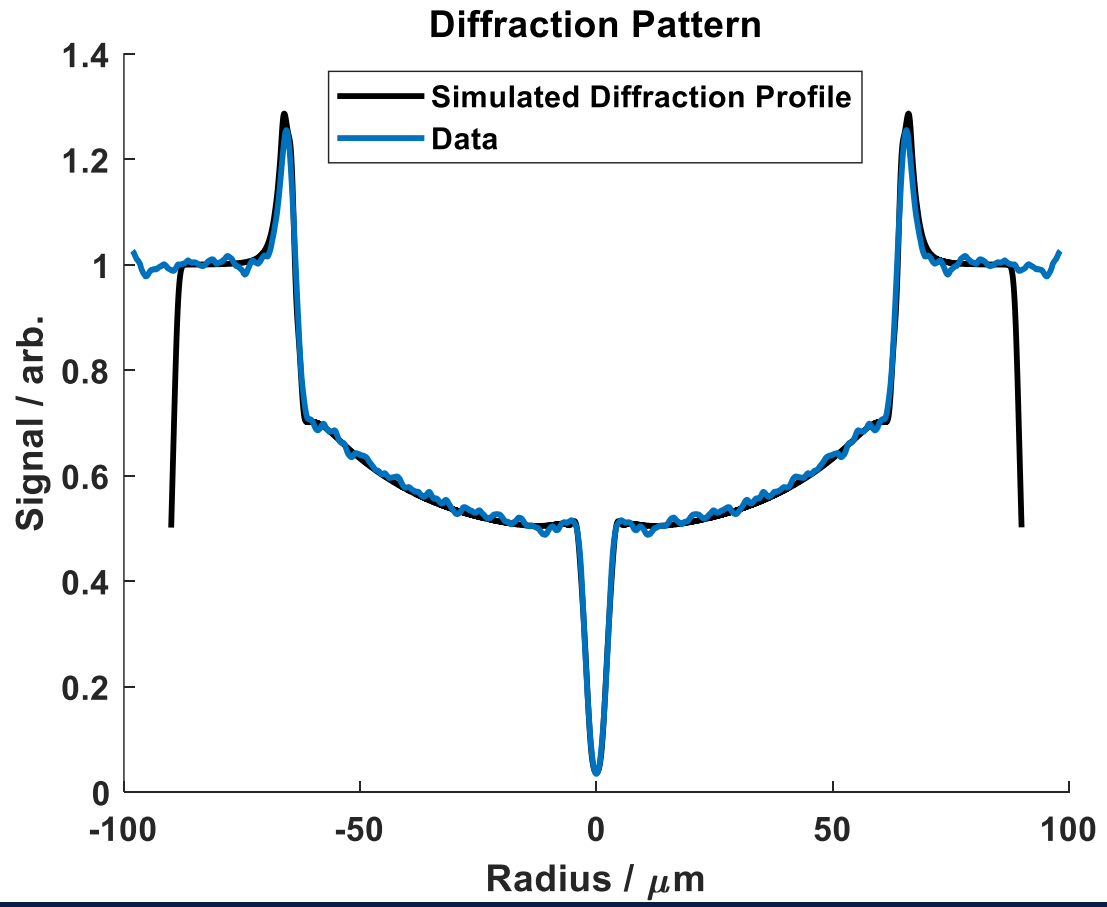

* A. Pogany *et al.* Rev. Sci. Inst. **68** 2774 (1997)

For the hot data, we utilized parameterized density profiles at the interface

- We created parameterized density profiles and simulated the diffraction patterns to match the data
- Requires material and density as functions of radius
- Going from outside in to be self-consistent:
  - Use the plastic data to determine the radial density profile for the target up to the shock wave
  - Parameterize the W-CHF interface to include a discontinuity, expanded W radius, and CHF density after the shock
- Initial material parameters need to be the consistent for all shots – the coated wires were made at the same time
  - Similar W radius, similar CHF radius

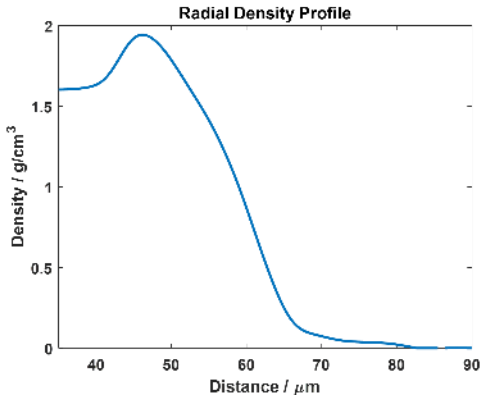

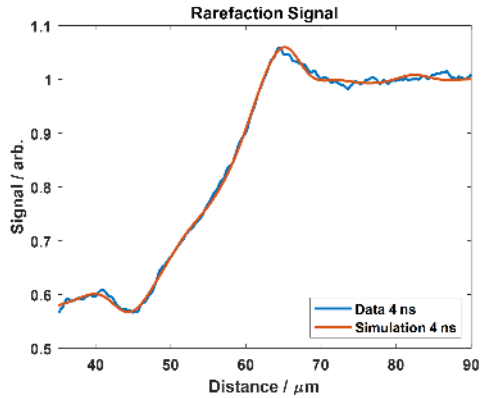

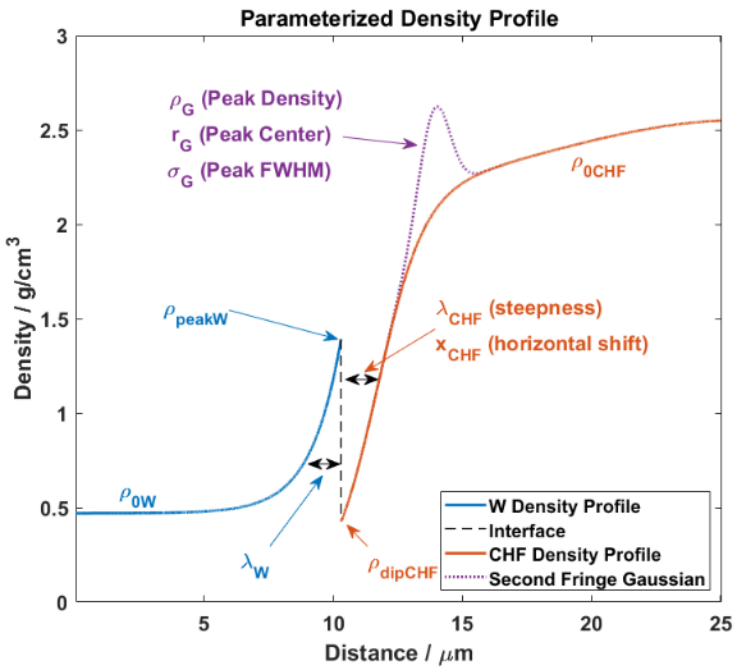

These parameterized density profiles have been fantastically successful

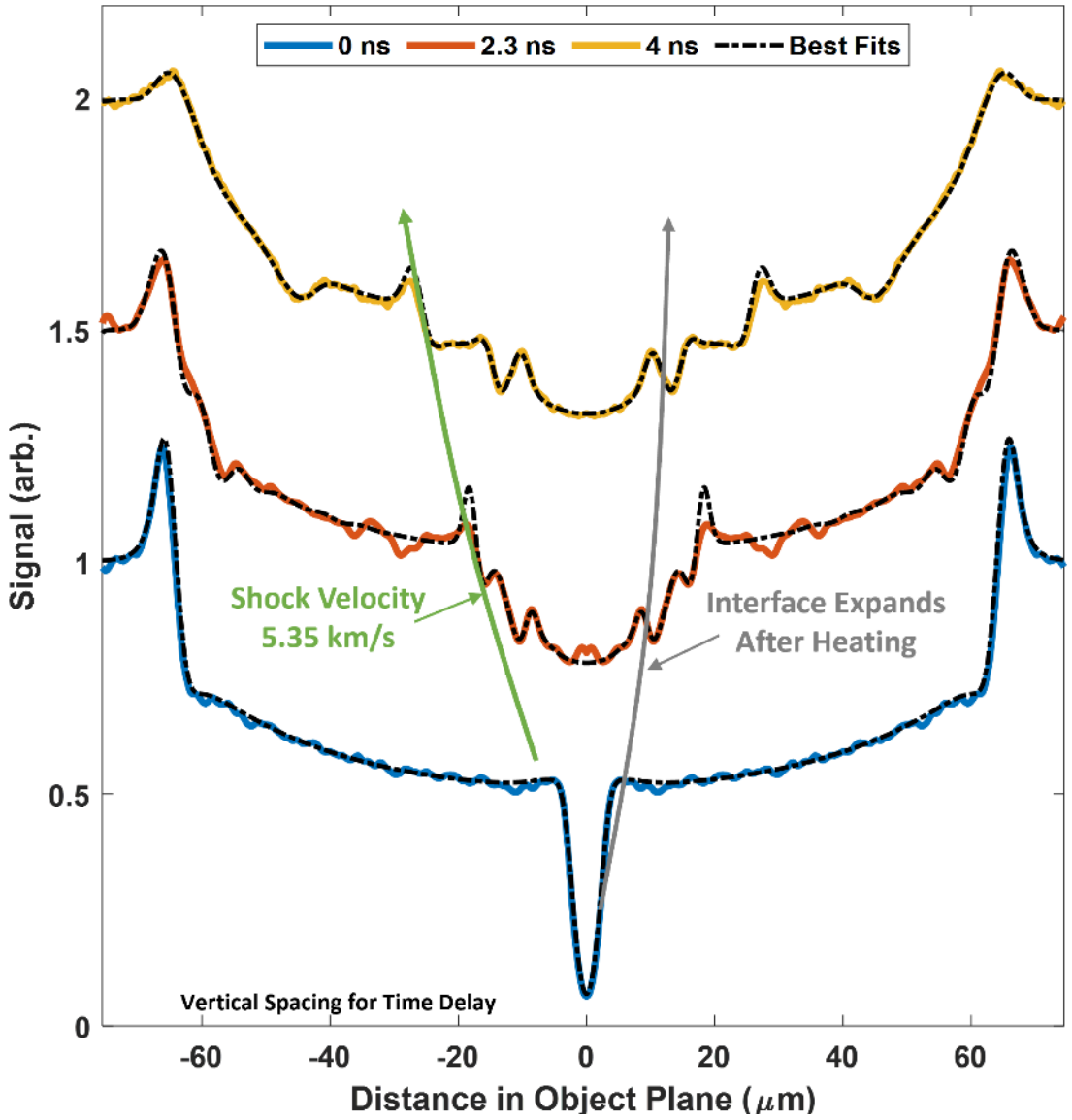

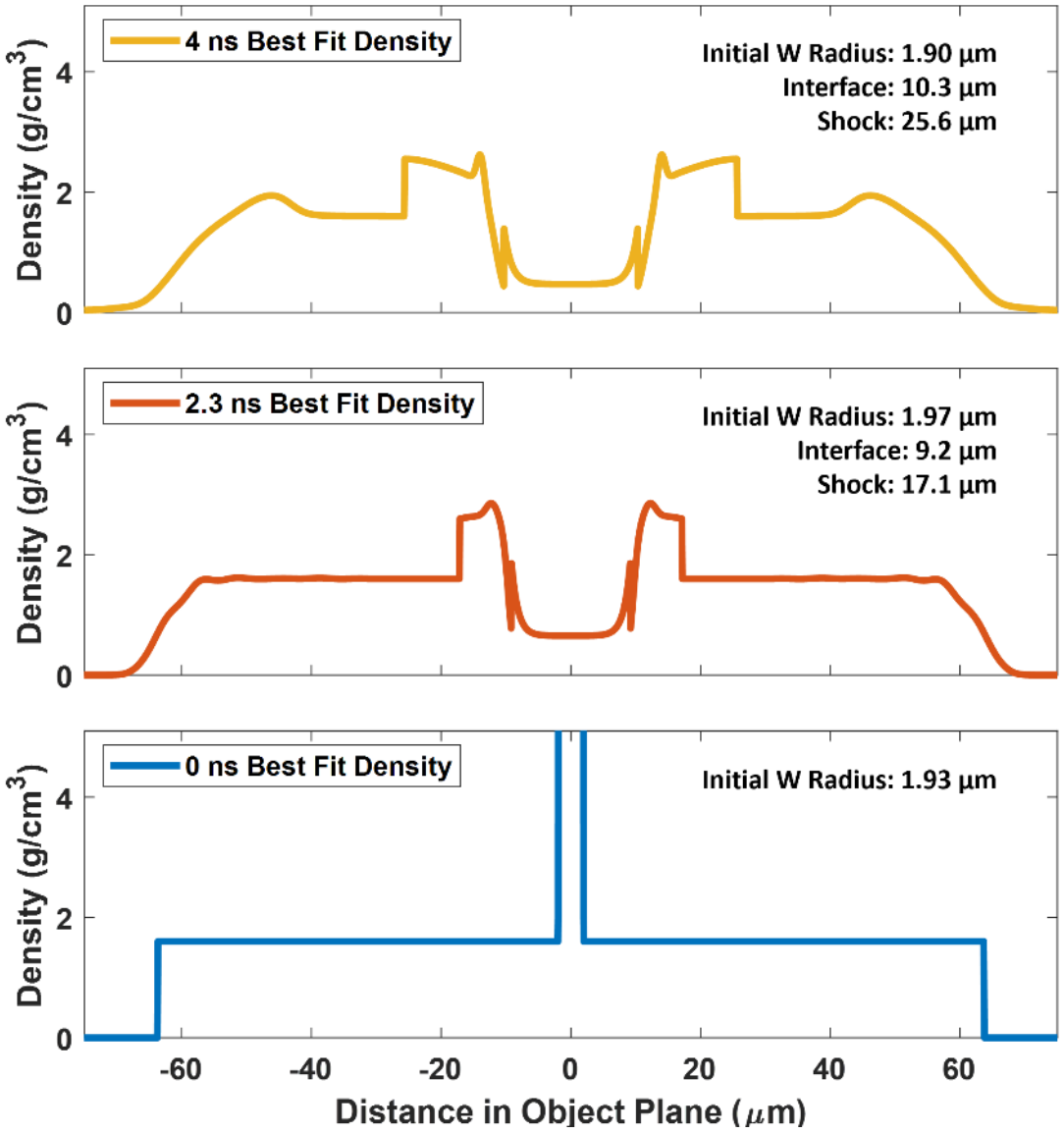

Use of Bayesian Inference to Determine Uniqueness

- To help determine the accuracy of our density profiles, we use Bayesian inference / MCMC in the style of Kasim *et al.** to sample phase space for the parameterized interface and provide error estimates

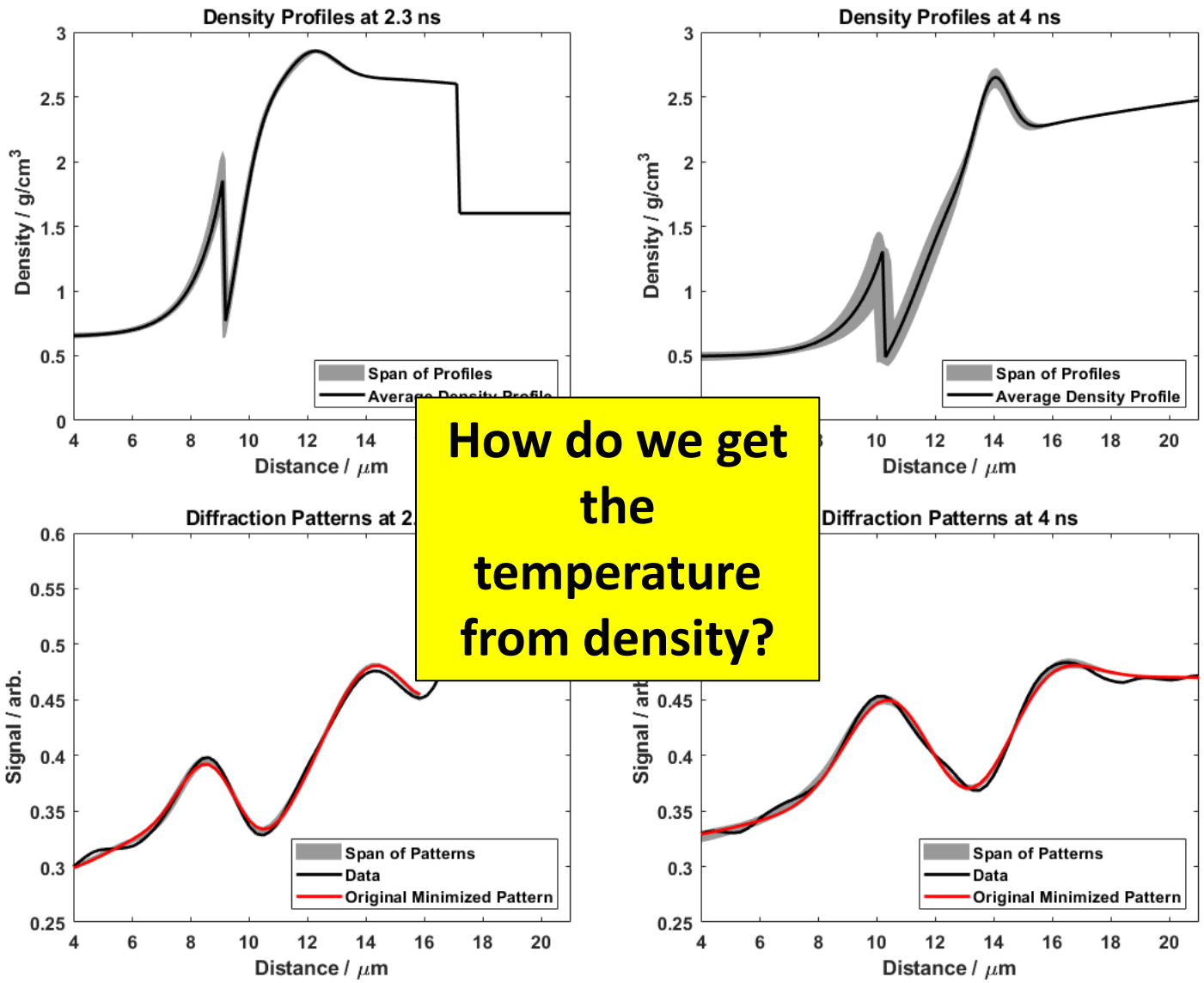

How do we get the temperature from density?

*M. F. Kasim *et al.* Phys. Plasmas **26**, 112706 (2019)

Capturing the shock in our data allows us to find a temperature

- **The plan:** If we have a density and a pressure, we can calculate a temperature

- Using FEOS tables for both the W and CHF, we can determine the matching pressure across the interface
  - Both the W and CHF should be subjected to the same X-ray flux – cross-over point is the equilibrium pressure

- The outward travelling shock in the CHF can be used to determine the pressure after the shock and near the interface from a form of Hugoniot Relations:

$$\Delta P = u_s^2 \left(\rho_1 - {\rho_1^2}/{\rho_2}\right)$$

- The three data points (0, 2.3, 4 ns) are used to estimate the shock velocity at the 2.3 ns
  - This ends up being $r \propto t^{0.8}$ from previous wire explosion work on pulsed power machines

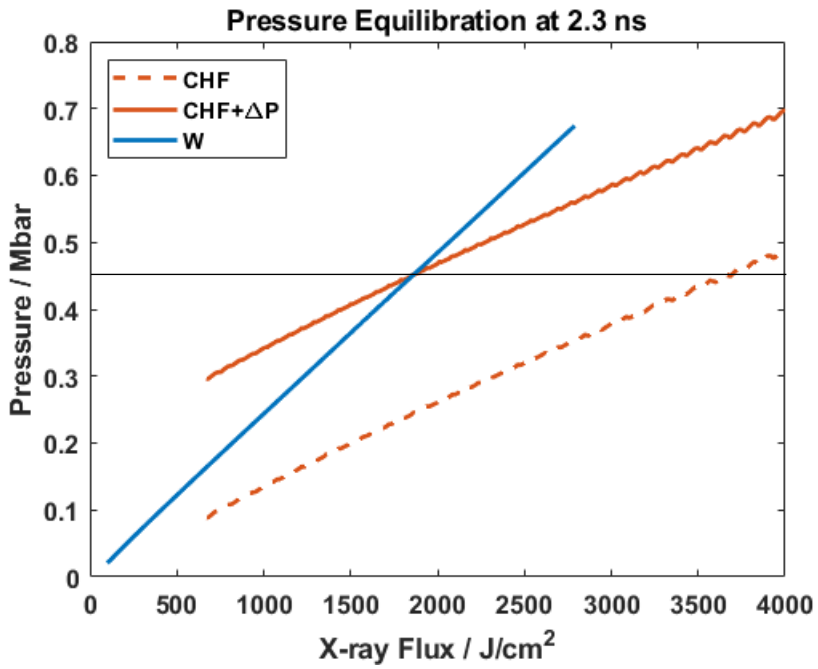

The temperature profile features a discontinuity at the interface

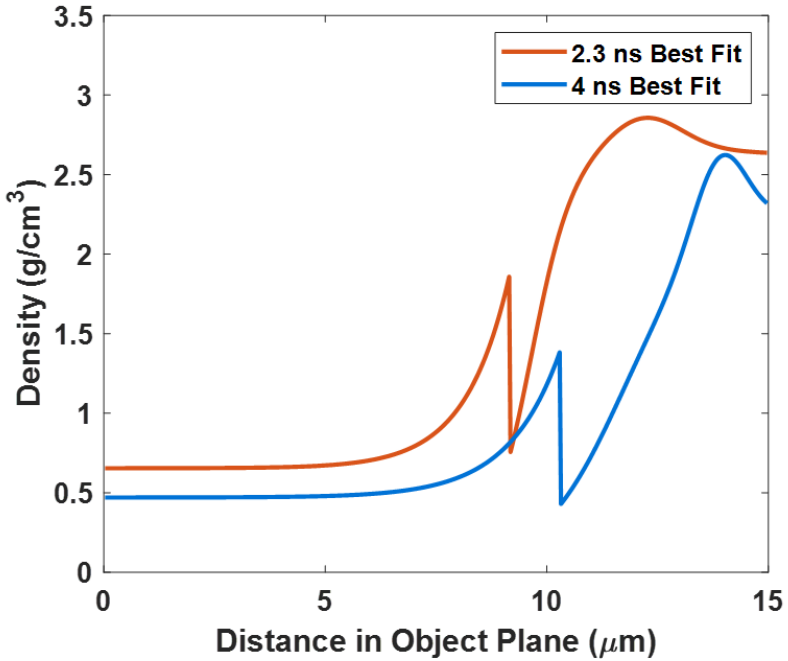

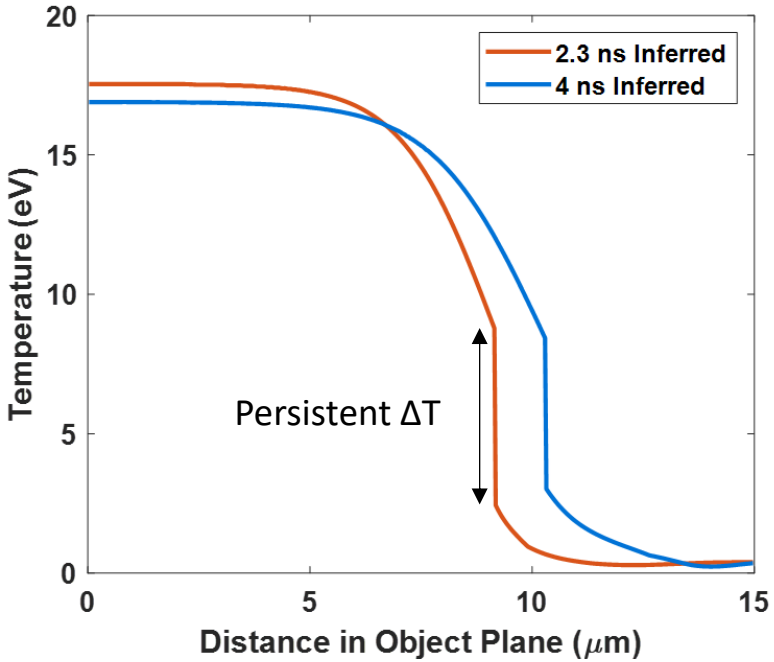

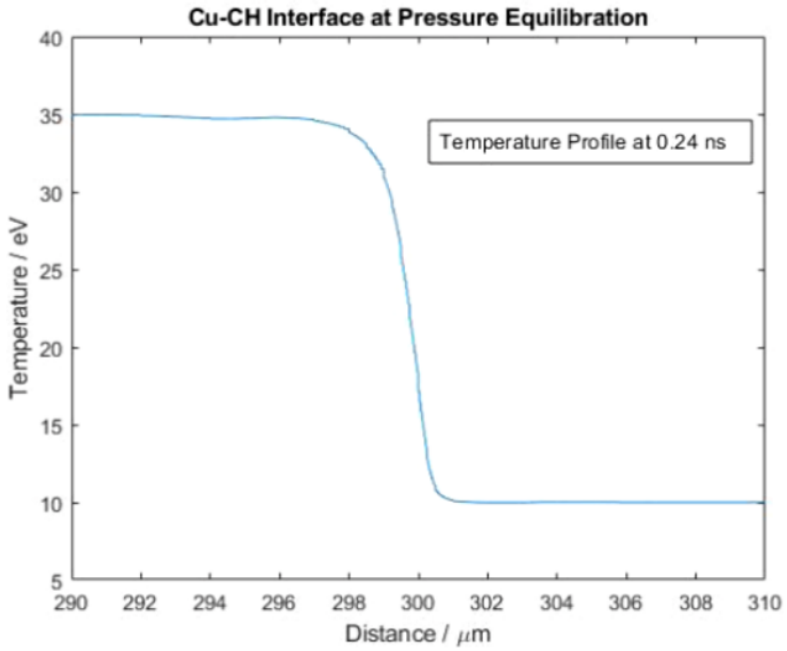

The temperature profile features a discontinuity at the interface

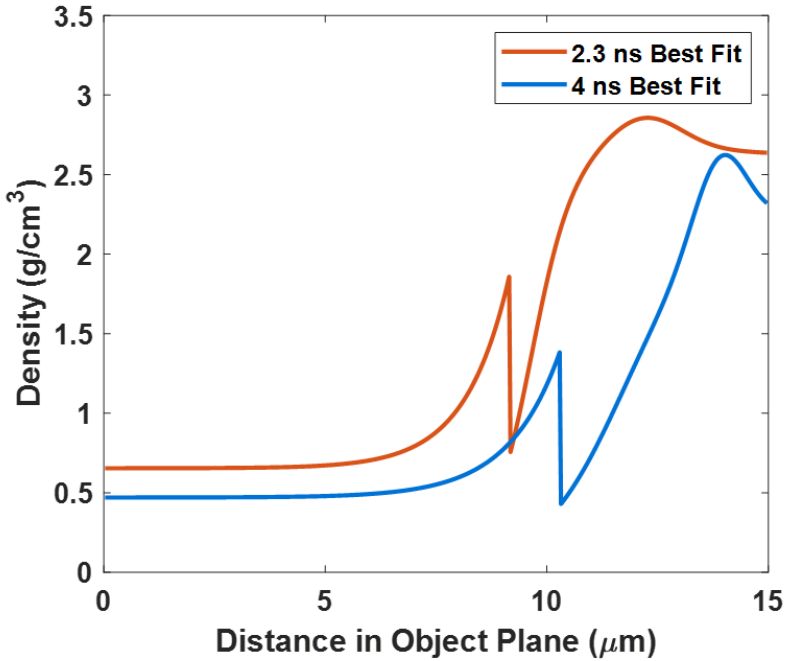

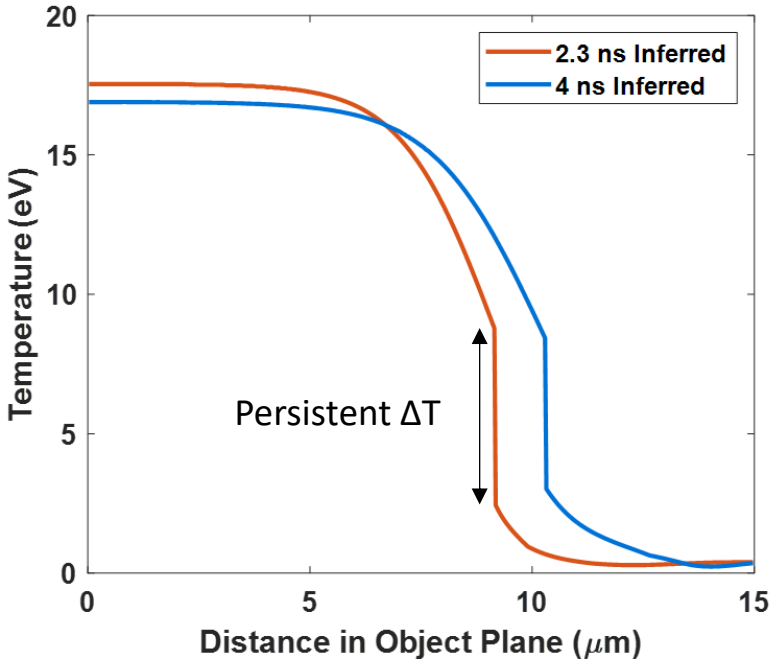

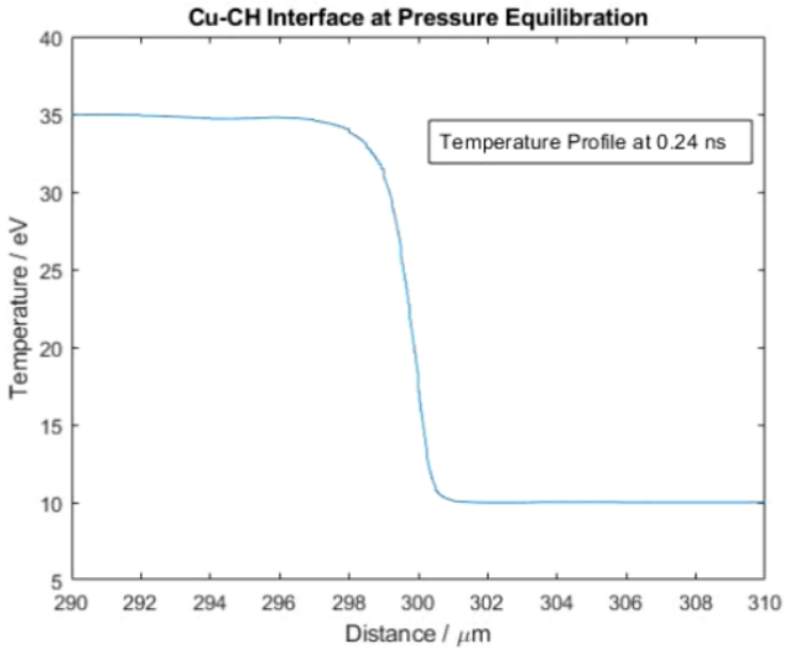

"Why isn't the heat diffusing through the interface??!!!!"

Thermal contact conductance

3 languages

Article Talk Read Edit View history Tools

From Wikipedia, the free encyclopedia

In physics, **thermal contact conductance** is the study of heat conduction between solid or liquid bodies in thermal contact. The **thermal contact conductance coefficient**, h_c, is a property indicating the thermal conductivity, or ability to conduct heat, between two bodies in contact. The inverse of this property is termed **thermal contact resistance**.

Definition [edit]

When two solid bodies come in contact, such as A and B in Figure 1, heat flows from the hotter body to the colder body. From experience, the temperature profile along the two bodies varies, approximately, as shown in the figure. A temperature drop is observed at the interface between the two surfaces in contact. This phenomenon is said to be a result of a *thermal contact resistance* existing between the contacting surfaces. Thermal contact resistance is defined as the ratio between this temperature drop and the average heat flow across the interface.[1]

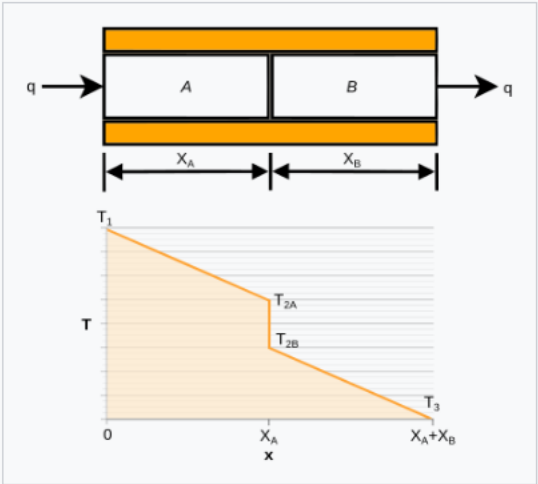

Fig. 1: Heat flow between two solids in contact and the temperature distribution.

According to **Fourier's law**, the heat flow between the bodies is found by the relation:

$$q = -kA\frac{dT}{dx} \tag{1}$$

where q is the heat flow, k is the thermal conductivity, A is the cross sectional area and dT/dx is the temperature gradient in the direction of flow.

From considerations of energy conservation, the heat flow between the two bodies in contact, bodies A and B, is found as:

$$q = \frac{T_1 - T_3}{X_A/(k_A A) + 1/(h_c A) + X_B/(k_B A)} \tag{2}$$

One may observe that the heat flow is directly related to the thermal conductivities of the bodies in contact, k_A and k_B, the contact area A, and the thermal contact resistance, $1/h_c$, which, as previously noted, is the inverse of the thermal conductance coefficient, h_c.

Interfacial thermal resistance

4 languages

Article Talk Read Edit View history Tools

From Wikipedia, the free encyclopedia

The article's lead section **may need to be rewritten**. Please help improve the lead and read the lead layout guide. *(December 2019)* *(Learn how and when to remove this template message)*

Interfacial thermal resistance, also known as **thermal boundary resistance**, or **Kapitza resistance**, is a measure of resistance to thermal flow at the interface between two materials. While these terms may be used interchangeably, **Kapitza resistance** technically refers to an atomically perfect, flat interface whereas **thermal boundary resistance** is a more broad term.[1] This thermal resistance differs from contact resistance (not to be confused with electrical contact resistance) because it exists even at atomically perfect interfaces. Owing to differences in electronic and vibrational properties in different materials, when an energy carrier (phonon or electron, depending on the material) attempts to traverse the interface, it will scatter at the interface. The probability of transmission after scattering will depend on the available energy states on side 1 and side 2 of the interface.

Assuming a constant thermal flux is applied across an interface, this interfacial thermal resistance will lead to a finite temperature discontinuity at the interface. From an extension of Fourier's law, we can write

$$Q = \frac{\Delta T}{R} = G\Delta T$$

where Q is the applied flux, ΔT is the observed temperature drop, R is the thermal boundary resistance, and G is its inverse, or thermal boundary conductance.

Understanding the thermal resistance at the interface between two materials is of primary significance in the study of its thermal properties. Interfaces often contribute significantly to the observed properties of the materials. This is even more critical for nanoscale systems where interfaces could significantly affect the properties relative to bulk materials.

Low thermal resistance at interfaces is technologically important for applications where very high heat dissipation is necessary. This is of particular concern to the development of microelectronic semiconductor devices as defined by the International Technology Roadmap for Semiconductors in 2004 where an 8 nm feature size device is projected to generate up to 100000 W/cm^2 and would need efficient heat dissipation of an anticipated die level heat flux of 1000 W/cm^2 which is an order of magnitude higher than current devices.[2] On the other hand, applications requiring good thermal isolation such as jet engine turbines would benefit from interfaces with high thermal resistance. This would also require material interfaces which are stable at very high temperature. Examples are metal-ceramic composites which are currently used for these applications. High thermal resistance can also be achieved with multilayer systems.

As stated above, thermal boundary resistance is due to carrier scattering at an interface. The type of carrier scattered will depend on the materials governing the interfaces. For example, at a metal-metal interface, electron scattering effects will dominate thermal boundary resistance, as electrons are the primary thermal energy carriers in metals.

Two widely used predictive models are the acoustic mismatch model (AMM) and the diffuse mismatch model (DMM). The AMM assumes a geometrically perfect interface and phonon transport across it is entirely elastic, treating phonons as waves in a continuum. On the other hand, the DMM assumes scattering at the interface is diffusive, which is accurate for interfaces with characteristic roughness at elevated temperatures.

Molecular dynamics (MD) simulations are a powerful tool to investigate interfacial thermal resistance. Recent MD studies have demonstrated that the solid-liquid interfacial thermal resistance is reduced on nanostructured solid surfaces by enhancing the solid-liquid interaction energy per unit area, and reducing the difference in vibrational density of states between solid and liquid.[3]

REVIEWS OF MODERN PHYSICS, VOLUME 94, APRIL–JUNE 2022

Interfacial thermal resistance: Past, present, and future

Jie Chen* and Xiangfan Xu†

Center for Phononics and Thermal Energy Science, China–EU Joint Lab for Nanophononics, MOE Key Laboratory of Advanced Micro-structured Materials, School of Physics Science and Engineering, Tongji University, Shanghai 200092, China

Jun Zhou‡

Phonon Engineering Research Center of Jiangsu Province, Center for Quantum Transport and Thermal Energy Science, Institute of Physics Frontiers and Interdisciplinary Sciences, School of Physics and Technology, Nanjing Normal University, Nanjing 210023, China

Baowen Li§

Department of Material Science and Engineering, Department of Physics, Shenzhen Institute for Quantum Science and Engineering, Southern University of Science and Technology, Shenzhen 518055, China and Paul M. Rady Department of Mechanical Engineering and Department of Physics, University of Colorado, Boulder, Colorado 80305-0427, USA

This problem has attracted the attention of scientists for centuries. The first recorded discussion was from Fourier (1822) in the early 19th century. Fourier recognized that the quantity of heat that the solid bodies lose to their surrounding gas through the surface obeys the same principle. He used the term "external conducibility" to characterize the quantity of heat through surface per unit time per unit area per unit temperature drop. This definition is exactly the same as the modern term interfacial thermal conductance (ITC). Later Poisson (1835) started his study with the following continuity of the heat flux at the interface:

$$J = \kappa_1 |\nabla T|_1 = \kappa_2 |\nabla T|_2 = h_I \Delta T. \qquad (1)$$

This is not a new phenomena!

The temperature profile features a discontinuity at the interface

- We infer the radial temperature profile of our system from the FEOS* tables, and find a discontinuous temperature jump at the interface
- This is a temperature discontinuity resulting from *interfacial thermal resistance* (ITR)**
  - Due to differences in heat carriers between materials
  - Experimentally measured for solid-solid[1], solid-liquid[2], and solid-gas[3] interfaces; MD simulations for liquid-liquid[4]
  - To our knowledge, it has not been explored for WDM or dense plasmas

1. E. T. Schwartz & R. O. Pohl. App. Phys. Let. **51**, 2200 (1987)
2. G. L. Pollack. Rev. Mod. Phys. **41**, 48-81 (1969)
3. M. S. de Smolan. Phil. Mag. **46**, 279 (1898)
4. H. A. Patel *et al*. Nano Let. **5**, 2225 (2005)

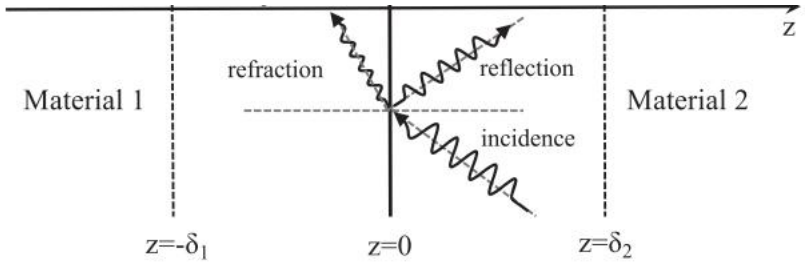

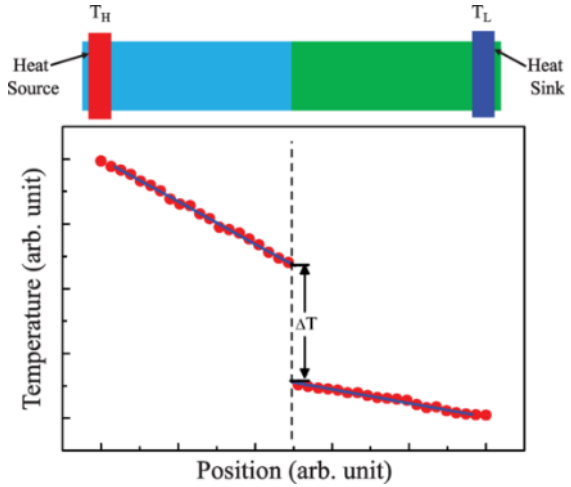

Schematic Diagram of interfacial thermal resistance.
J. Chen *et al.* Review of Modern Physics 94, 025002 (2022)

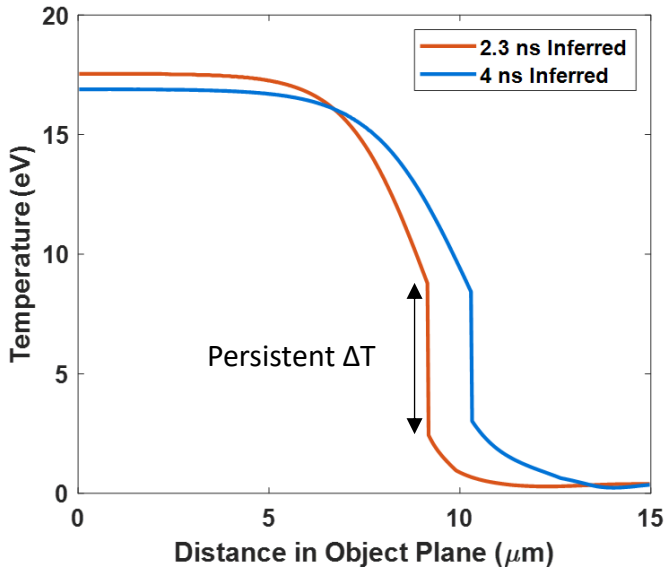

The data at 2.3 ns can be evolved to match the data at 4 ns

- To extract quantitative numbers, we evolve one time step to the

$$q(r,t) = \kappa\nabla$$

- We get a quantitative is comparable to prev insulator systems at r
  - $R_{Int} \approx 3.7\text{x}10^{-9}$ K
  - $G_{Int} = 1/R_{Int} \approx 2$

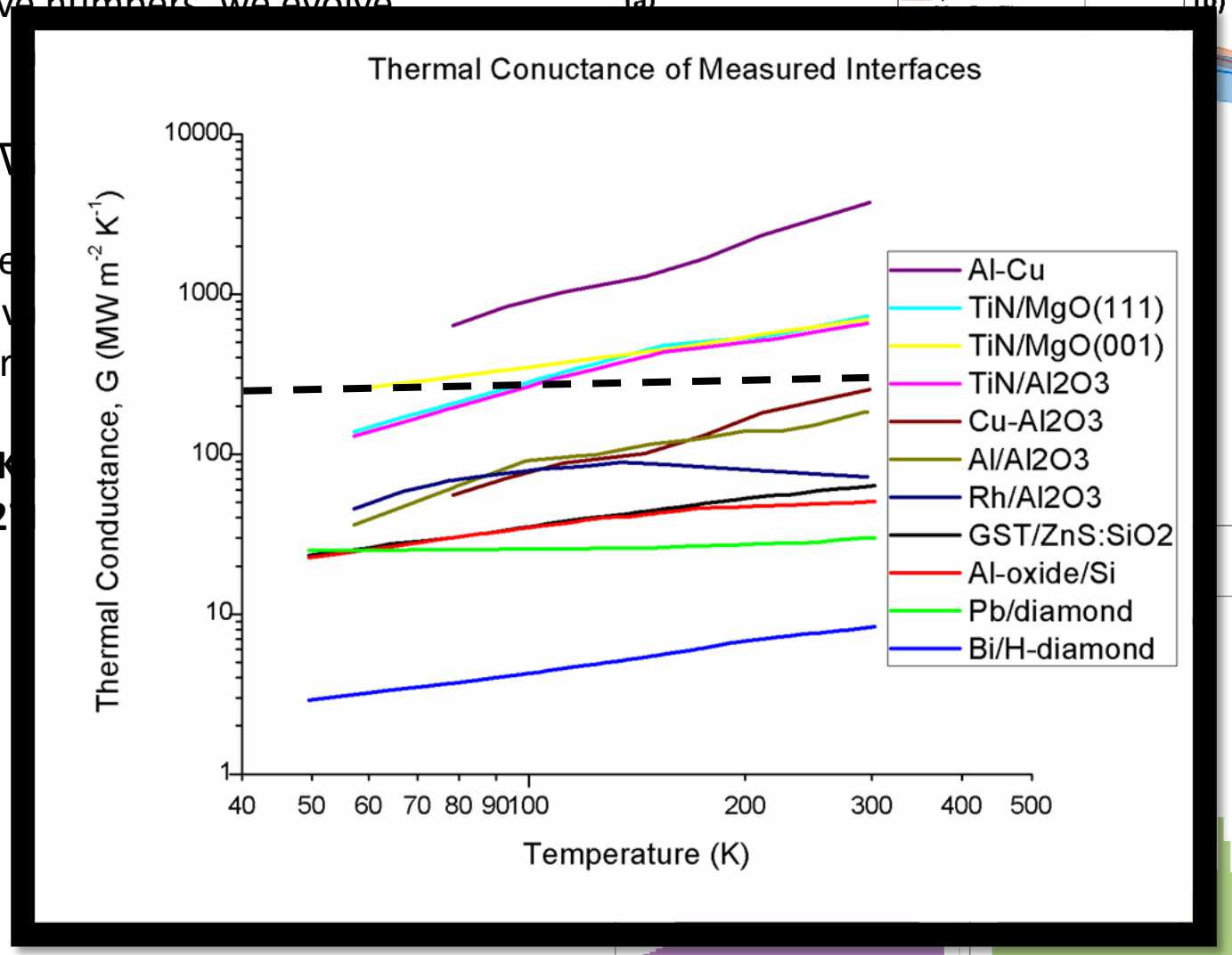

*J. Chen *et al*. Rev. Mod. Phys. **94**, 025002 (2022)

The data at 2.3 ns can be evolved to match the data at 4 ns

- To extract quantitative numbers, we evolve one time step to the next using Fourier's Law:

$$q(r,t) = \kappa \nabla T = \frac{\Delta T}{R}\left[\frac{J}{m^2 s}\right]$$

- We get a quantitative number for the ITR that is comparable to previously measured metal-insulator systems at room temperatures*:
  - **$R_{Int} \approx 3.7\times10^{-9}$ K m²/W**
  - **$G_{Int} = 1/R_{Int} \approx 270$ MW/m²/K**

We expect similar effects at many interfaces in the HED regime, however the theory is still a work in process. For e⁻-e⁻ scattering:

$$h_{I,e} = \frac{1}{4}\int_0^\infty (\varepsilon - \varepsilon_{F,1}) D_1(\varepsilon) \frac{\partial f_1(\varepsilon)}{\partial T} v_{e,1} \zeta_{e,1\to2}(\varepsilon) d\varepsilon,$$

$$\zeta_{e,1\to2}(\varepsilon) = \frac{D_2(\varepsilon)[1-f_2(\varepsilon)]v_2(\varepsilon)}{D_1(\varepsilon)f_1(\varepsilon)v_1(\varepsilon) + D_2(\varepsilon)[1-f_2(\varepsilon)]v_2(\varepsilon)}.$$

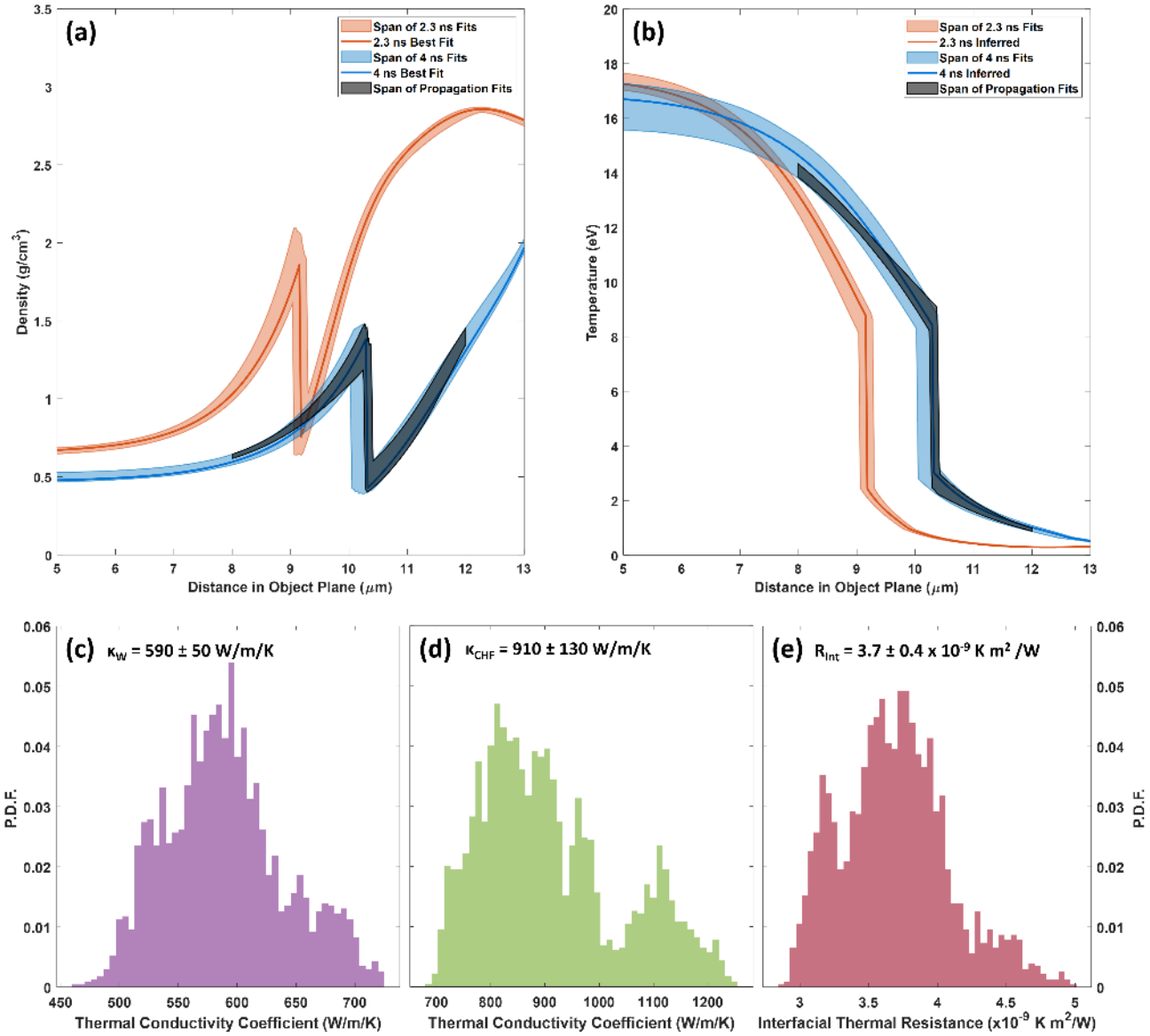

*J. Chen *et al*. Rev. Mod. Phys. **94**, 025002 (2022)

Discussion topics

- Heat transport across warm dense matter interfaces
  - Observation of *Interfacial Thermal Resistance* at Extreme Conditions
- **Direct ion temperature measurements at free electron lasers**
  - **Bond strength in non-equilibrium gold**
  - Electron ion equilibration in warm dense matter
  - Superheating beyond the entropy catastrophe
- Forward Scattering
  - Sound speed in warm dense methane
  - Phonon dispersion and temperature through detailed balance

Travis Griffin
5th year GRA

Short pulse (fs) laser induced warm dense matter (WDM) creates highly non-equilibrium state

- Non-equilibrium refers to Local Thermodynamic Equilibrium (LTE)

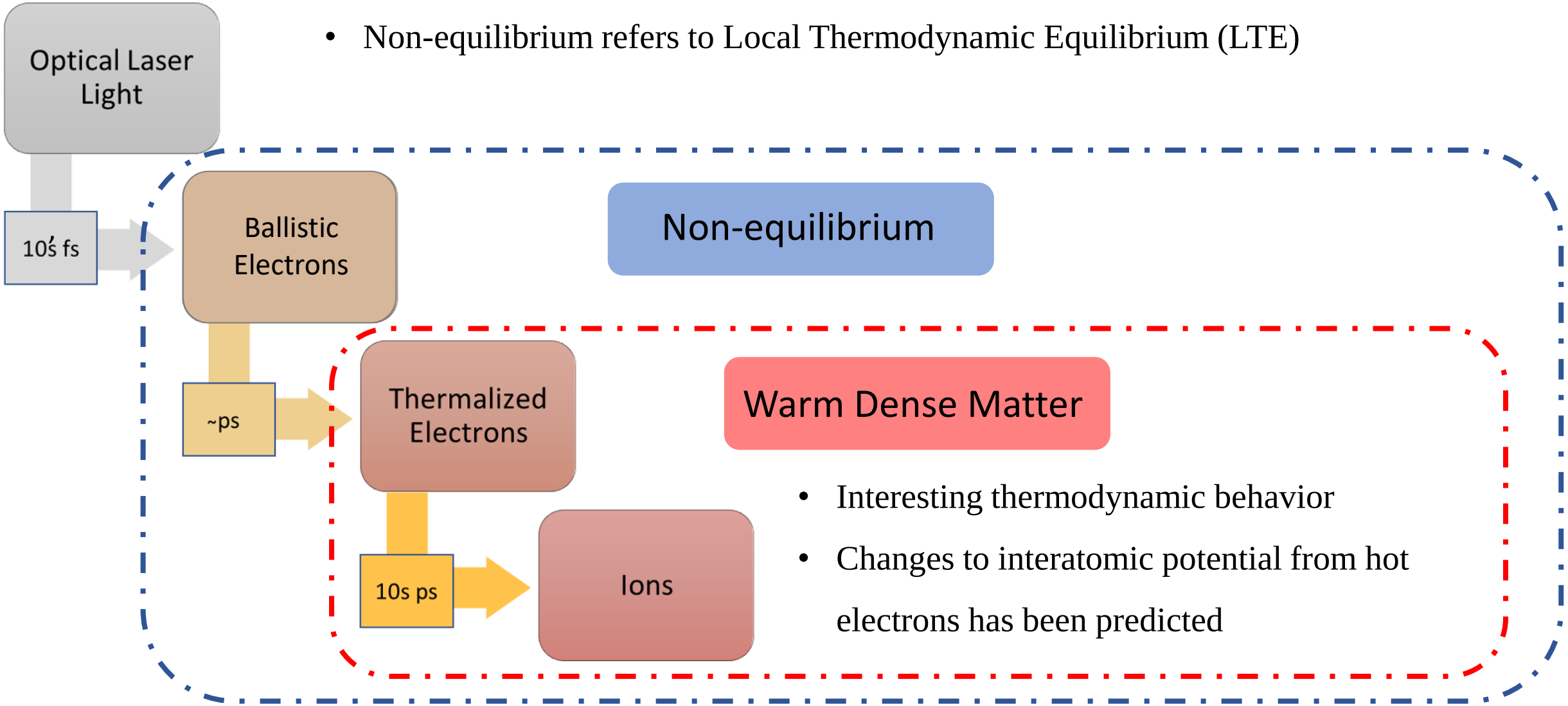

- Interesting thermodynamic behavior
- Changes to interatomic potential from hot electrons has been predicted

Ab initio calculations indicate changes to bond strength in nonequilibrium gold WDM

- Debye temperature (θ_D) acts as a proxy for interatomic bond strength
- Recoules *et al.*[1] ab initio calculations show increase in θ_D as a function of electron temperature (i.e. bond 'hardening')
- Simulations confirm θ_D at ambient conditions for bulk single-crystal gold sample[2]

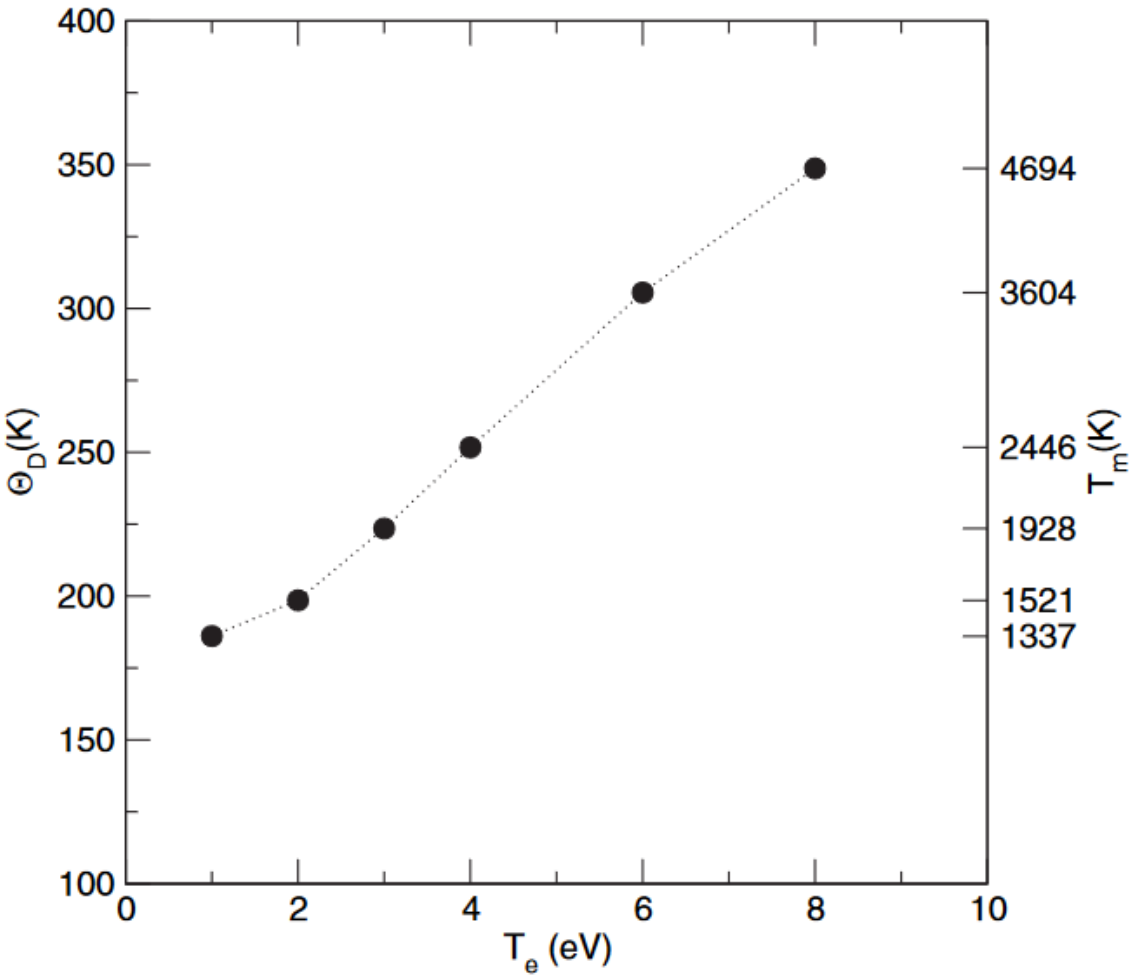

Figure used Recoules *et al.* [1]

[1]V. Recoules et al. Phys. Rev. Lett. 96, 055503 (2006)
[2]V. Synecek et al. Acta Cryst. A26, 108-113 (1970)

Ab initio calculations indicate changes to bond strength in nonequilibrium gold WDM

- Debye temperature (θ_D) acts as a proxy for interatomic bond strength
- Recoules *et al.*[1] ab initio calculations show increase in θ_D as a function of electron temperature (i.e. bond 'hardening')
- Simulations confirm θ_D at ambient conditions for bulk single-crystal gold sample[2]

$$\langle u^2 \rangle = \frac{9h^2}{4\pi^2 M k_B \theta_D}\left[\frac{1}{4} + \left(\frac{T_i}{\theta_D}\right)^2 \int_0^{\theta_D/T_i} \frac{x}{\exp(x) - 1}\,dx\right]$$

- θ_D and mean squared displacement ($\langle u^2 \rangle$) of the ions have an inverse relationship

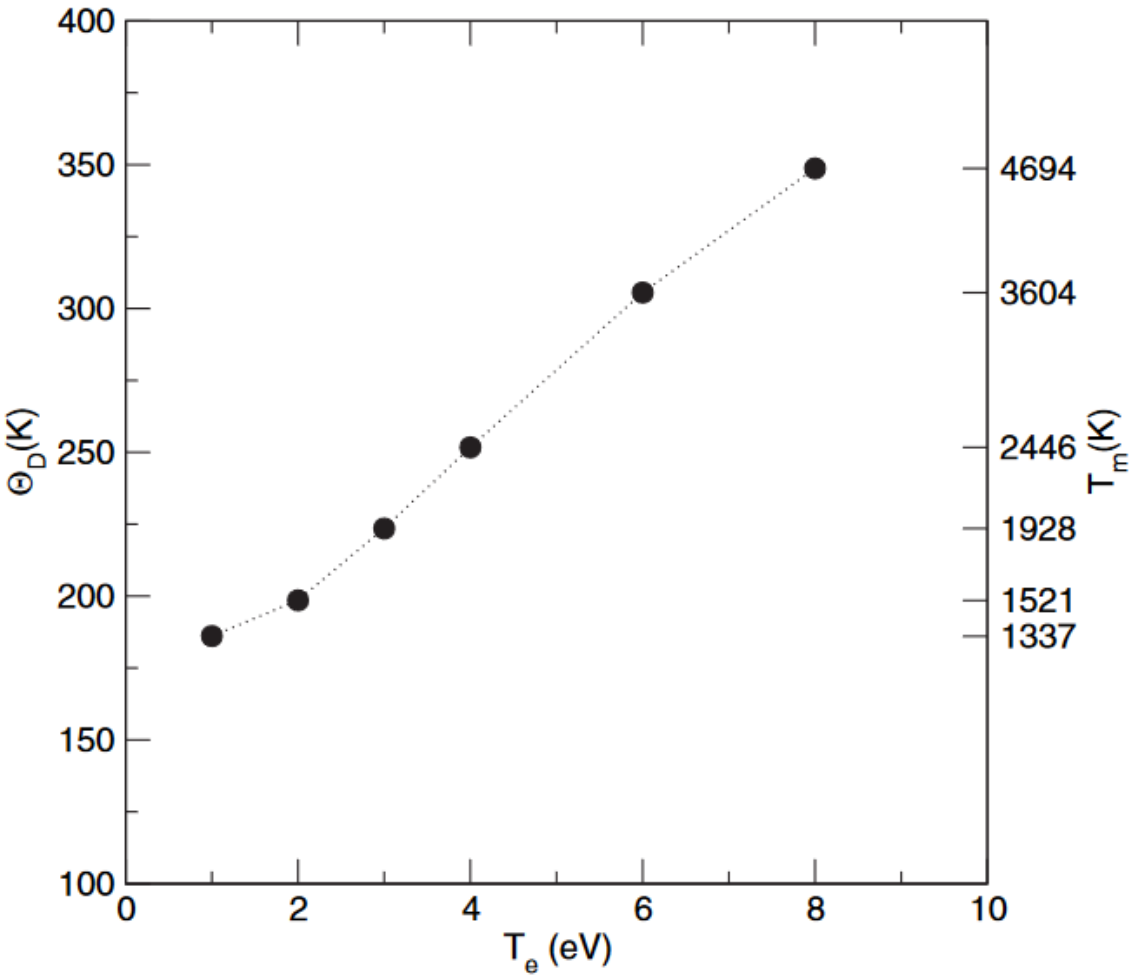

Figure used Recoules *et al.* [1]

[1]V. Recoules et al. Phys. Rev. Lett. 96, 055503 (2006)
[2]V. Synecek et al. Acta Cryst. A26, 108-113 (1970)

Decades old controversy over bond strength of WDM gold

PRL 96, 055503 (2006) PHYSICAL REVIEW LETTERS week ending 10 FEBRUARY 2006

Effect of Intense Laser Irradiation on the Lattice Stability of Semiconductors and Metals

V. Recoules,[1,*] J. Clérouin,[1] G. Zérah,[1] P. M. Anglade,[2] and S. Mazevet[3]

www.sciencemag.org SCIENCE VOL 323 20 FEBRUARY 2009

The Formation of Warm Dense Matter: Experimental Evidence for Electronic Bond Hardening in Gold

Ralph Ernstorfer,* Maher Harb, Christoph T. Hebeisen, Germán Sciaini, Thibault Dartigalongue, R. J. Dwayne Miller†

- Recoules (2006): Bond-hardening
- Ernstorfer (2009): Bond-hardening

PHYSICAL REVIEW B 88, 184101 (2013)

Structural dynamics of laser-irradiated gold nanofilms

Szymon L. Daraszewicz,[1] Yvelin Giret,[1,2] Nobuyasu Naruse,[2] Yoshie Murooka,[2] Jinfeng Yang,[2] Dorothy M. Duffy,[1] Alexander L. Shluger,[1] and Katsumi Tanimura[2]

- Daraszewicz (2013): Bond-softening

SCIENCE • 29 Jun 2018 • Vol 360, Issue 6396 • pp. 1451-1455

Heterogeneous to homogeneous melting transition visualized with ultrafast electron diffraction

M. Z. Mo[1*†], Z. Chen[1†], R. K. Li[2], M. Dunning[3], B. B. L. White[1,4], J. K. Baldwin[4], L. B. Fletcher[5], J. B. Kim[5], A. Ng[6], R. Redmer[7], A. H. Reid[8], P. Shekhar[9], X. Z. Shen[1], M. Shen[9], K. Sokolowski-Tinten[10], Y. Y. Tsui[6], Y. Q. Wang[8], Q. Zheng[8], X. J. Wang[8], S. H. Glenzer[5*]

- Mo (2018): neither Bond-hardening nor Bond-softening

SCIENCE ADVANCES | RESEARCH ARTICLE

PHYSICS

Evidence for phonon hardening in laser-excited gold using x-ray diffraction at a hard x-ray free electron laser

Adrien Descamps[1,2,3*], Benjamin K. Ofori-Okai[1,4], Oliviero Bistoni[5,6], Zhijiang Chen[1], Eric Cunningham[1], Luke B. Fletcher[1], Nicholas J. Hartley[1], Jerome B. Hastings[1], Dimitri Khaghani[1], Mianzhen Mo[1,4], Bob Nagler[1], Vanina Recoules[5,6], Ronald Redmer[7], Maximilian Schörner[7], Debbie G. Senesky[2], Peihao Sun[1]†, Hai-En Tsai[1], Thomas G. White[8], Siegfried H. Glenzer[1], Emma E. McBride[1,3,4*]

- Descamps (2023): Reasserts Bond-hardening

Debye temperature determined by combining ion temperatures with Bragg peak diffraction

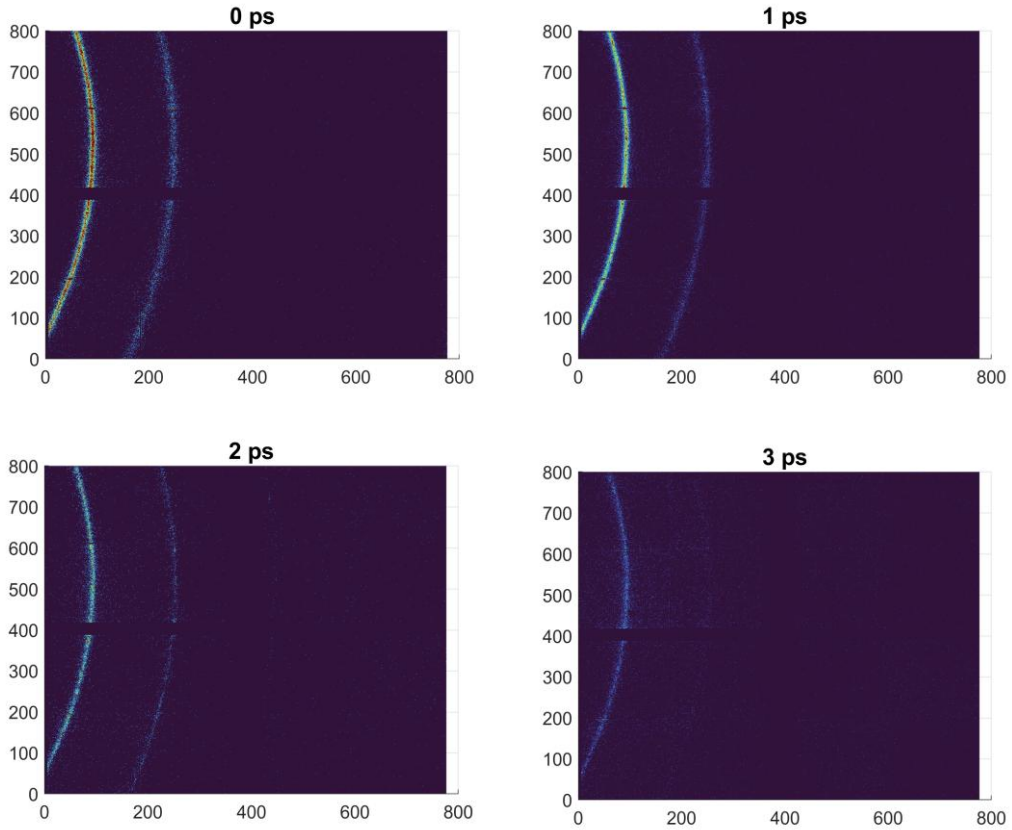

$$\langle u^2 \rangle = \frac{9h^2}{4\pi^2 M k_B \theta_D}\left[\frac{1}{4} + \left(\frac{T_i}{\theta_D}\right)^2 \int_0^{\theta_D/T_i} \frac{x}{\exp(x) - 1}\, dx\right]$$

- $\langle u^2 \rangle$ can be determined using Bragg peak diffraction ratios

$$I_{200}/I_{111} = \exp\left\{-\frac{1}{3}\langle u^2 \rangle(t)[k_{200}^2 - k_{111}^2]\right\}$$

- Where $\langle u_0^2 \rangle$ is the mean square displacement at room temperature

Debye temperature determined by combining ion temperatures with Bragg peak diffraction

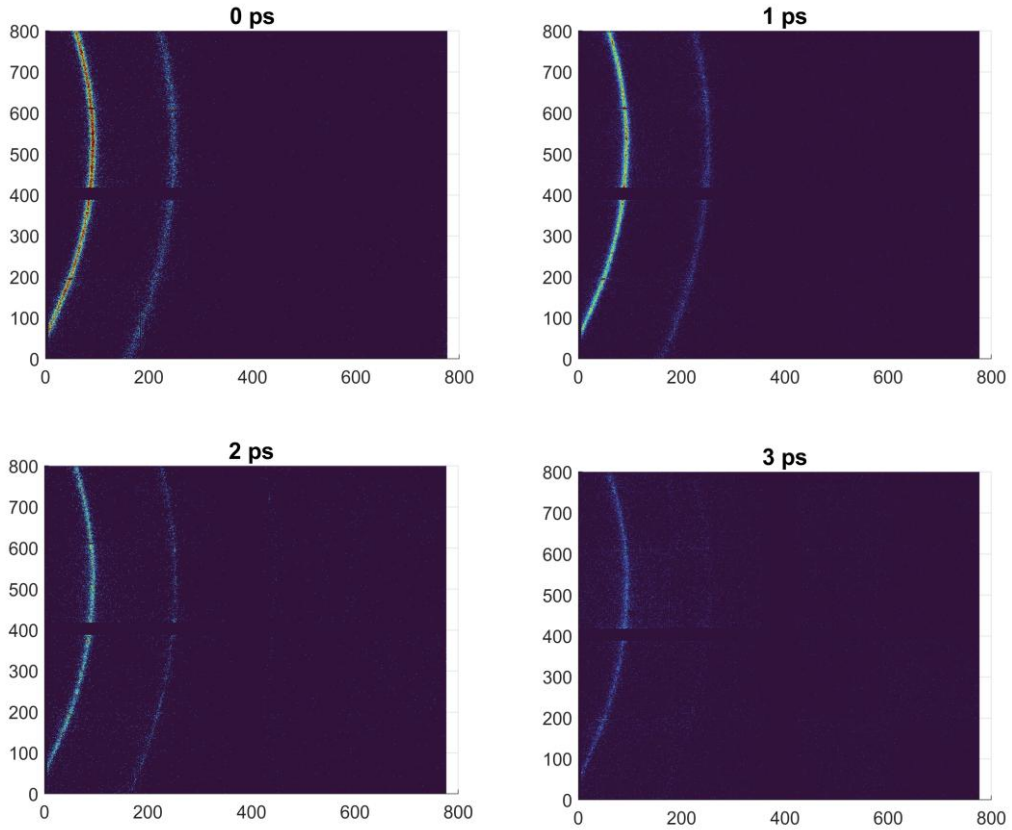

Measure diffraction peak intensity

$$\langle u^2 \rangle = \frac{9h^2}{4\pi^2 M k_B \theta_D}\left[\frac{1}{4} + \left(\frac{T_i}{\theta_D}\right)^2 \int_0^{\theta_D/T_i} \frac{x}{\exp(x) - 1}\,dx\right]$$

- $\langle u^2 \rangle$ can be determined using Bragg peak diffraction ratios

$$I_{200}/I_{111} = \exp\left\{-\frac{1}{3}\langle u^2 \rangle(t)\left[k_{200}^2 - k_{111}^2\right]\right\}$$

- Where $\langle u_0^2 \rangle$ is the mean square displacement at room temperature

Debye temperature determined by combining ion temperatures with Bragg peak diffraction

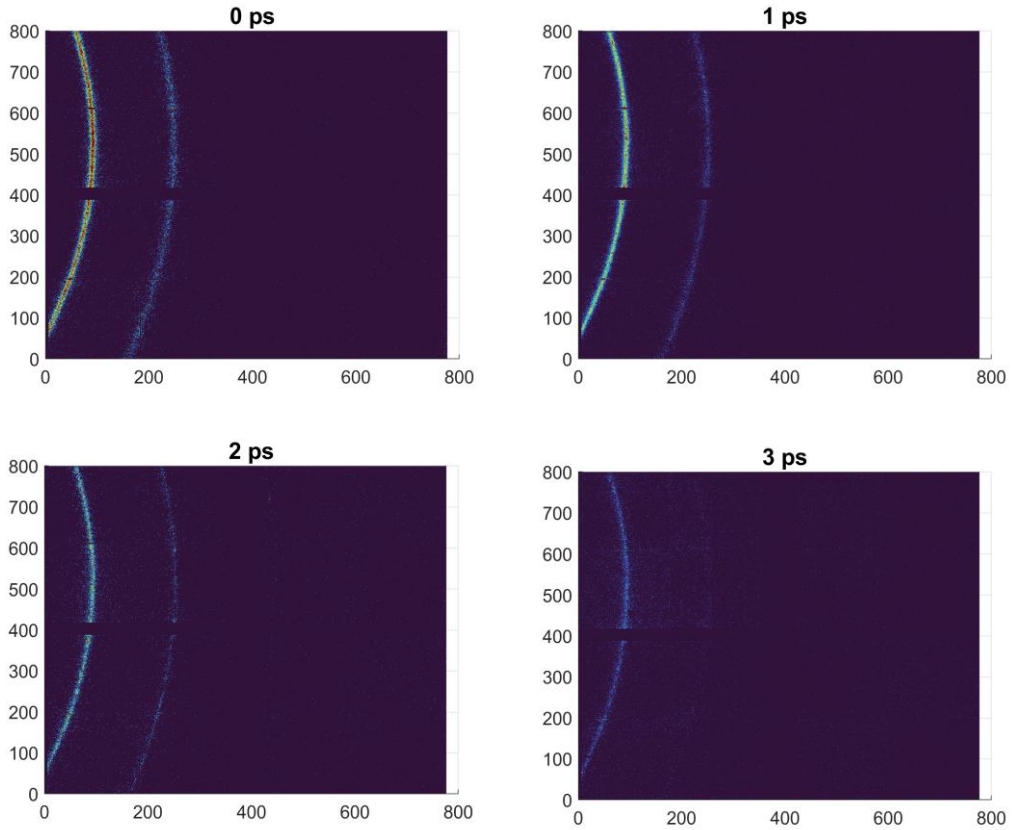

Measure diffraction peak intensity

$$\langle u^2 \rangle = \frac{9h^2}{4\pi^2 M k_B \theta_D}\left[\frac{1}{4} + \left(\frac{T_i}{\theta_D}\right)^2 \int_0^{\theta_D/T_i} \frac{x}{\exp(x) - 1}\,dx\right]$$

- $\langle u^2 \rangle$ can be determined using Bragg peak diffraction ratios

$$I_{200}/I_{111} = \exp\left\{-\frac{1}{3}\langle u^2 \rangle(t)\left[k_{200}^2 - k_{111}^2\right]\right\}$$

- Where $\langle u_0^2 \rangle$ is the mean square displacement at room temperature

Determine ratio ion-temperature and Debye temperature

Debye temperature determined by combining ion temperatures with Bragg peak diffraction

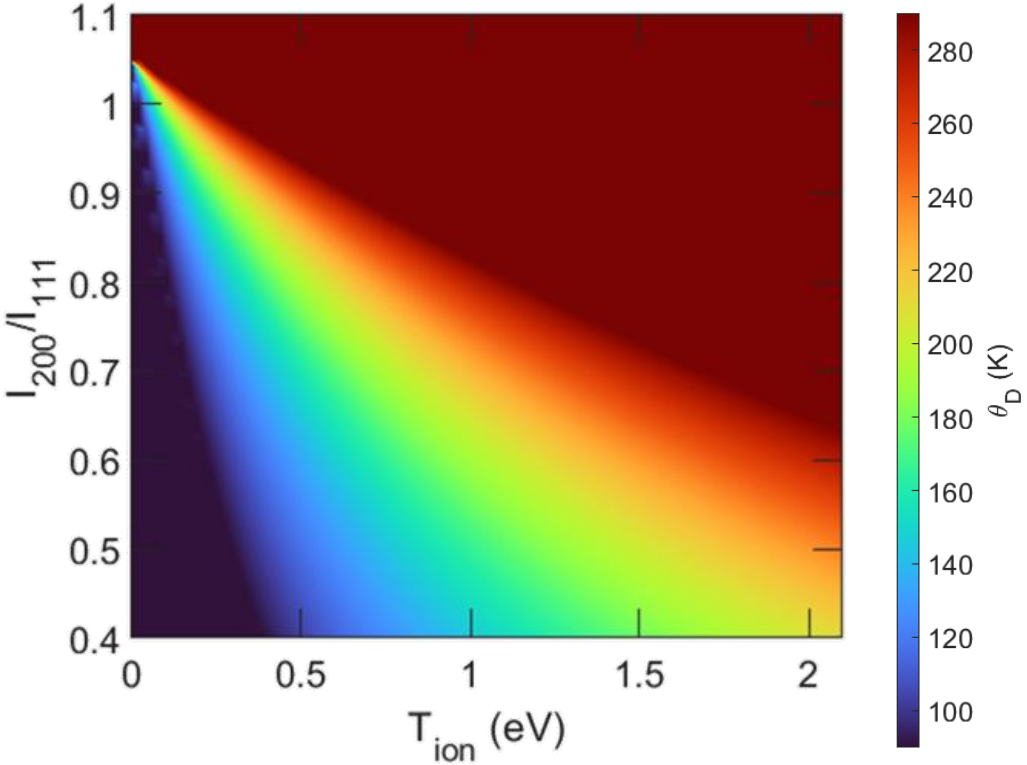

Measure diffraction peak intensity

$$\langle u^2 \rangle = \frac{9h^2}{4\pi^2 M k_B \theta_D}\left[\frac{1}{4} + \left(\frac{T_i}{\theta_D}\right)^2 \int_0^{\theta_D/T_i} \frac{x}{\exp(x)-1}\,dx\right]$$

- $\langle u^2 \rangle$ can be determined using Bragg peak diffraction ratios

$$I_{200}/I_{111} = \exp\left\{-\frac{1}{3}\langle u^2 \rangle(t)\left[k_{200}^2 - k_{111}^2\right]\right\}$$

- Where $\langle u_0^2 \rangle$ is the mean square displacement at room temperature

Determine ratio ion-temperature and Debye temperature

Debye temperature determined by combining ion temperatures with Bragg peak diffraction

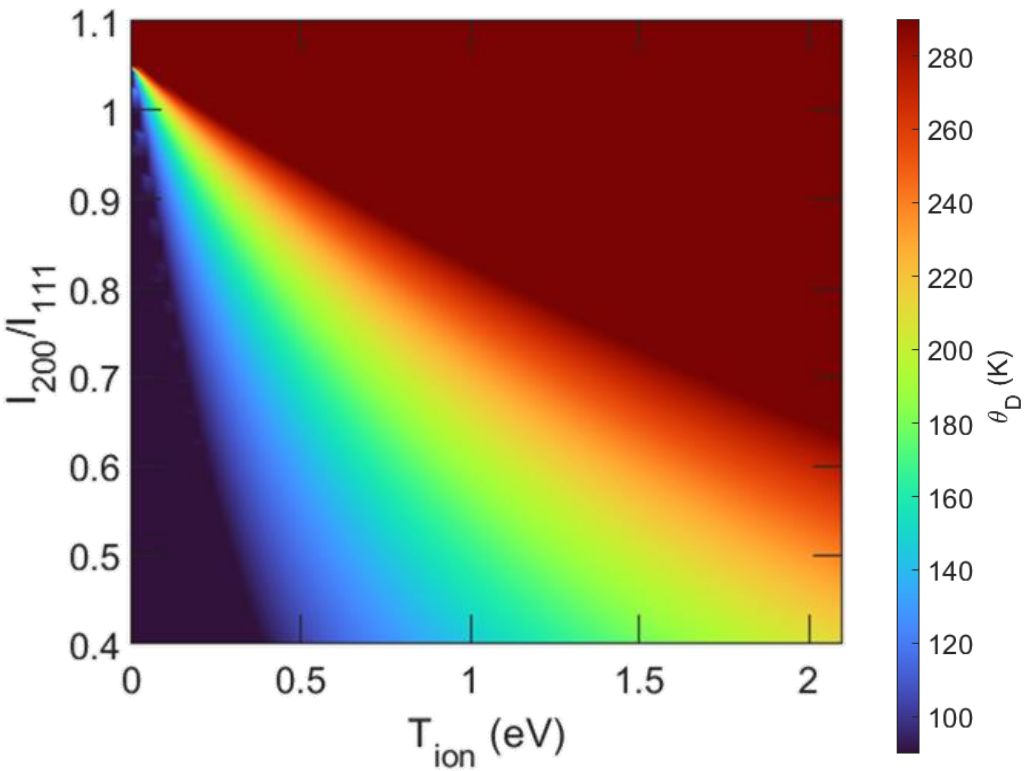

Measure diffraction peak intensity

Ion-temperature inferred from models

$$\langle u^2 \rangle = \frac{9h^2}{4\pi^2 M k_B \theta_D}\left[\frac{1}{4} + \left(\frac{T_i}{\theta_D}\right)^2 \int_0^{\theta_D/T_i} \frac{x}{\exp(x) - 1}\,dx\right]$$

- $\langle u^2 \rangle$ can be determined using Bragg peak diffraction ratios

$$I_{200}/I_{111} = \exp\left\{-\frac{1}{3}\langle u^2 \rangle(t)\left[k_{200}^2 - k_{111}^2\right]\right\}$$

- Where $\langle u_0^2 \rangle$ is the mean square displacement at room temperature

Determine ratio ion-temperature and Debye temperature

Model dependent ion-temperatures are the reason we have this 'goldilocks' problem in bond hardening

Debye temperature determined by combining ion temperatures with Bragg peak diffraction

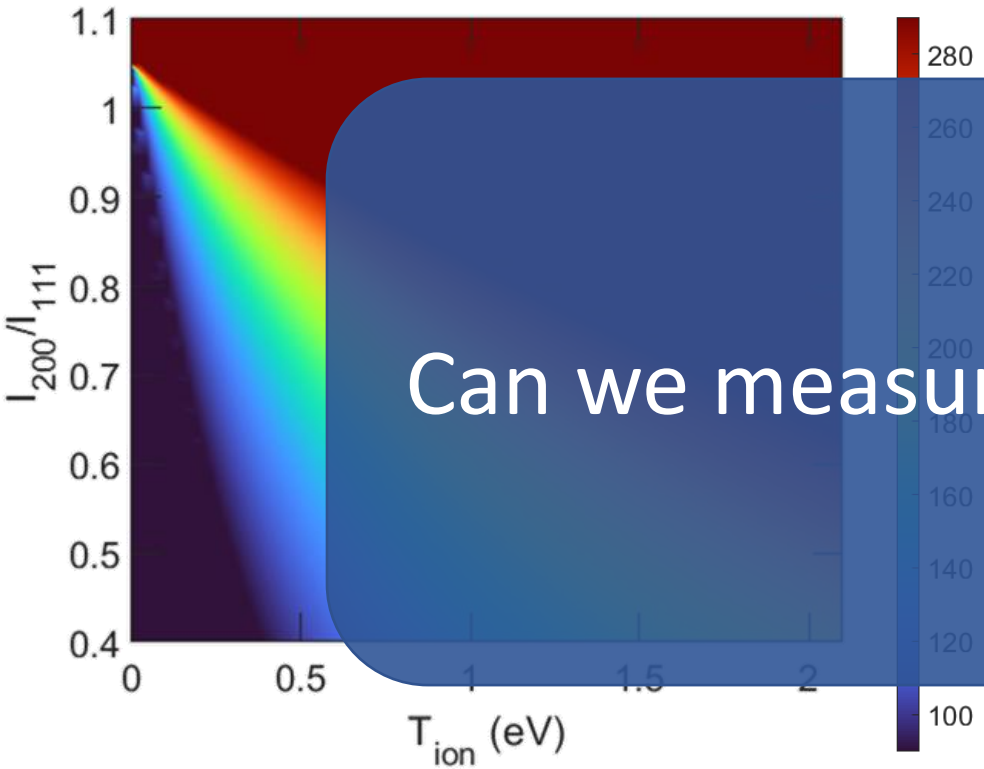

Measure diffraction peak intensity

Ion-temperature inferred from models

$$\langle u^2 \rangle = \frac{9h^2}{4\pi^2 M k_B \theta_D}\left[\frac{1}{4} + \left(\frac{T_i}{\theta_D}\right)^2 \int_0^{\theta_D/T_i} \frac{x}{\exp(x) - 1}\,dx\right]$$

- $\langle u^2 \rangle$ can be determined using Bragg peak diffraction ratios

$$I_{200}/I_{111} = \exp\left\{-\frac{2}{3}\langle u^2 \rangle (\theta)[k_{200}^2 - k_{111}^2]\right\}$$

- Where $\langle u_0^2 \rangle$ is the mean square displacement at room temperature

Determine ratio ion-temperature and Debye temperature

Can we measure ion-temperature directly?

Model dependent ion-temperatures rely variety of input parameters that differ from group to group.

Ultra-high resolution inelastic X-ray Scattering is a Direct Measure of the Ion Temperature in a Plasma

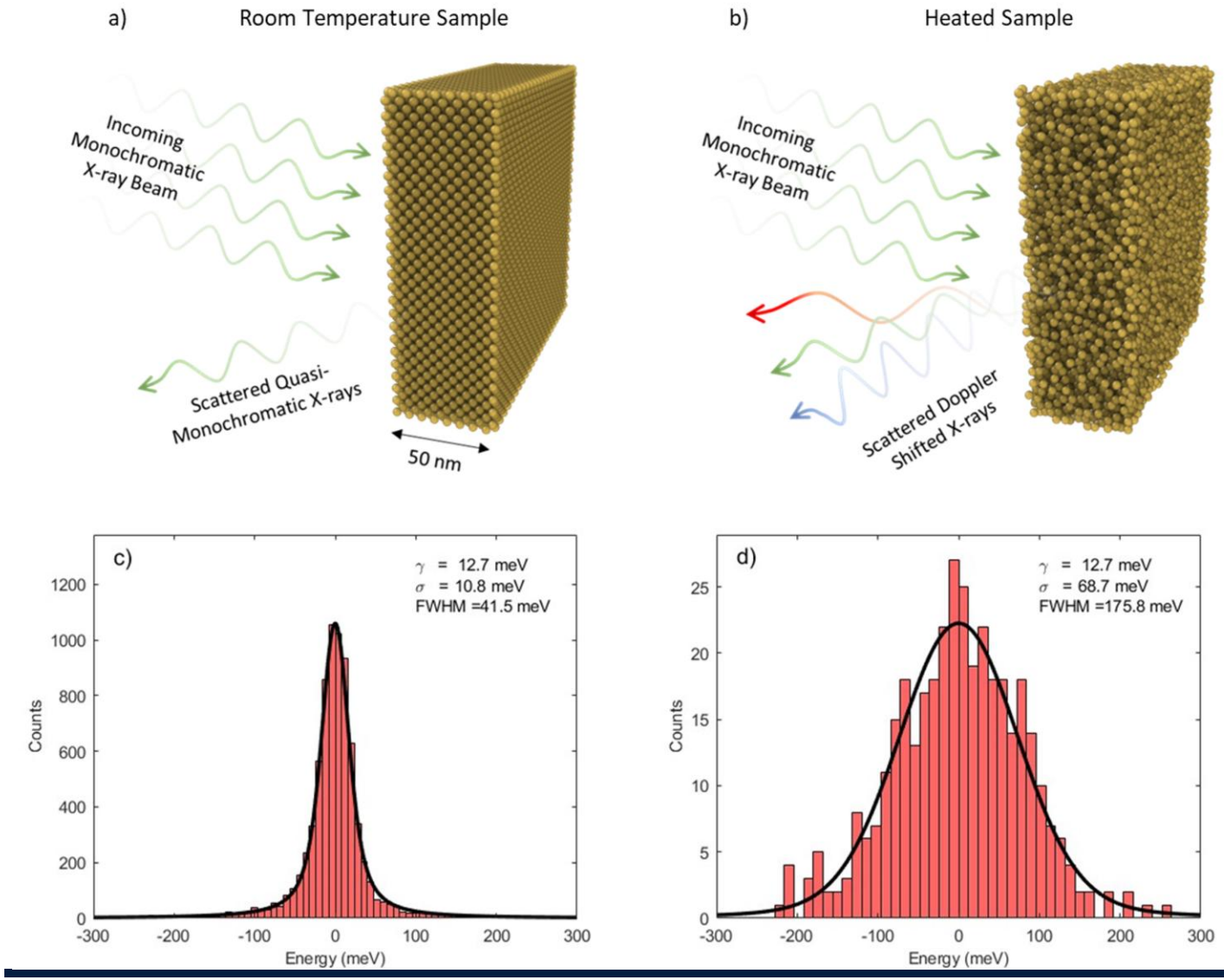

X-ray Scattering Overview

Assuming 7.5 keV scattering at 170° the dimensionless scattering parameter α is:

$$\alpha = \frac{1}{ka} = \frac{1}{(7.6\ \text{Å}^{-1})\times(1.6\ \text{Å})} = 0.1 << 1$$

In this free-particle limit, the dynamic structure factor is well-described by a single Gaussian (the quasi-elastic Rayleigh peak):

$$S(k,\omega) \propto e^{-\frac{m\omega^2}{2T_i k^2}}$$

The width of this Gaussian can then be related to the temperature of the ions.

$$T_i = \frac{1}{4}\frac{m_i c^2}{8\ln 2}\left(\frac{\Delta E}{E_0}\right)^2$$

T_i ~ 1 eV corresponds to ~**100 meV broadening**

High-resolution achievable at LCLS free-electron laser

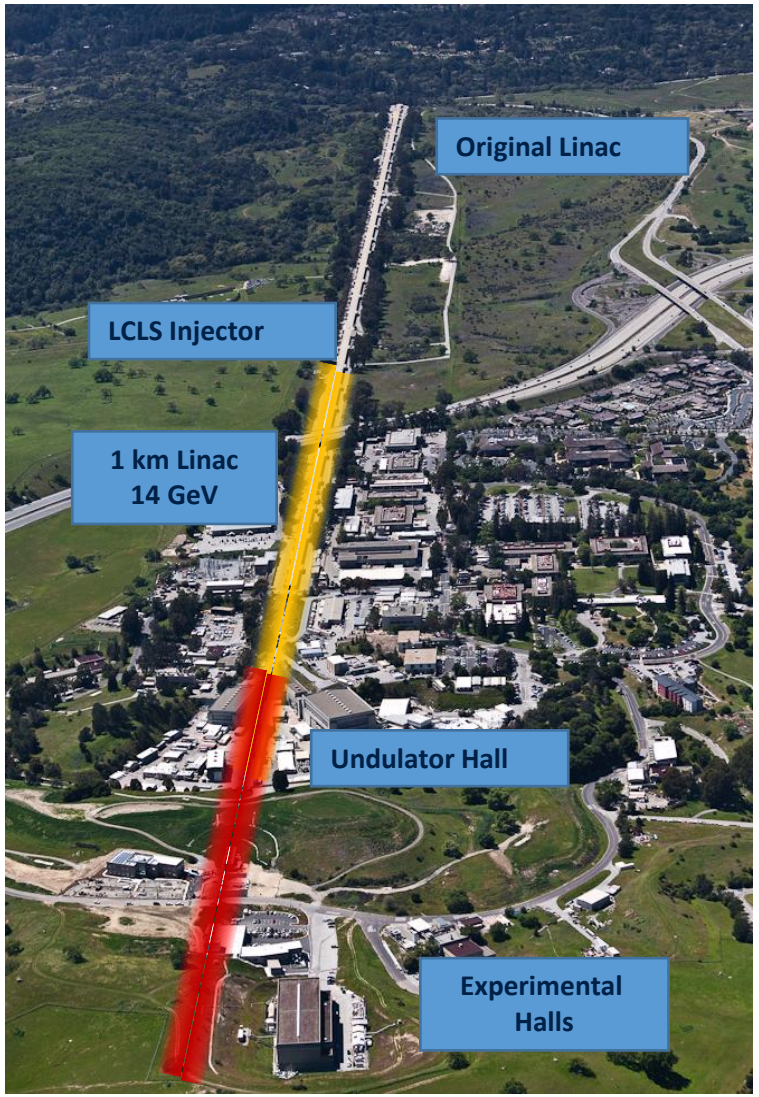

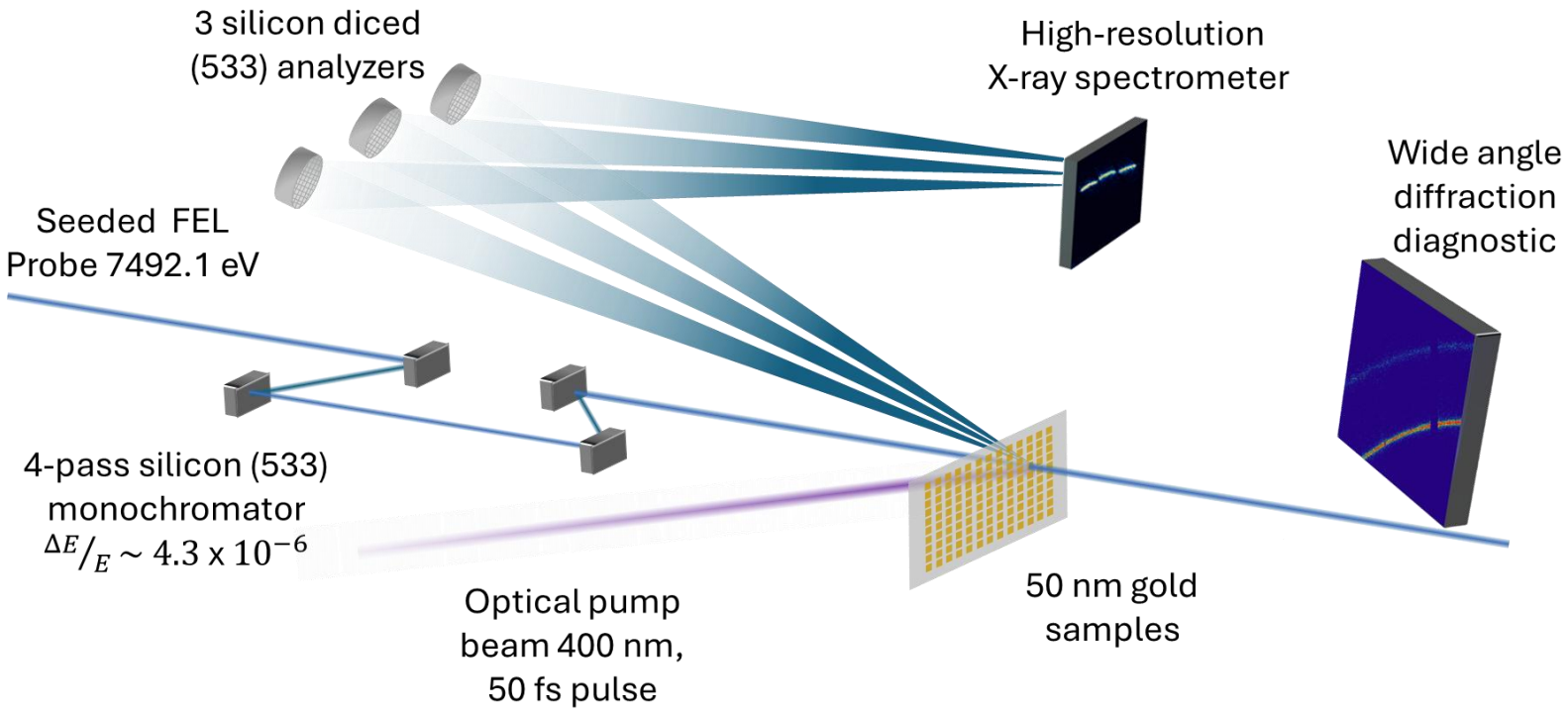

- Experimental setup provides resolution of ~50 meV
- Setups allows for simultaneous ion temperature and X-ray diffraction measurements

See B. Nagler September 18, 15:00: "Direct Measurement of temperature and Electron-Ion Equilibration Rates in Warm Dense Gold" for further discussion

Resolving the dynamic ion-ion structure factor requires meV resolution

University of Nevada, Reno

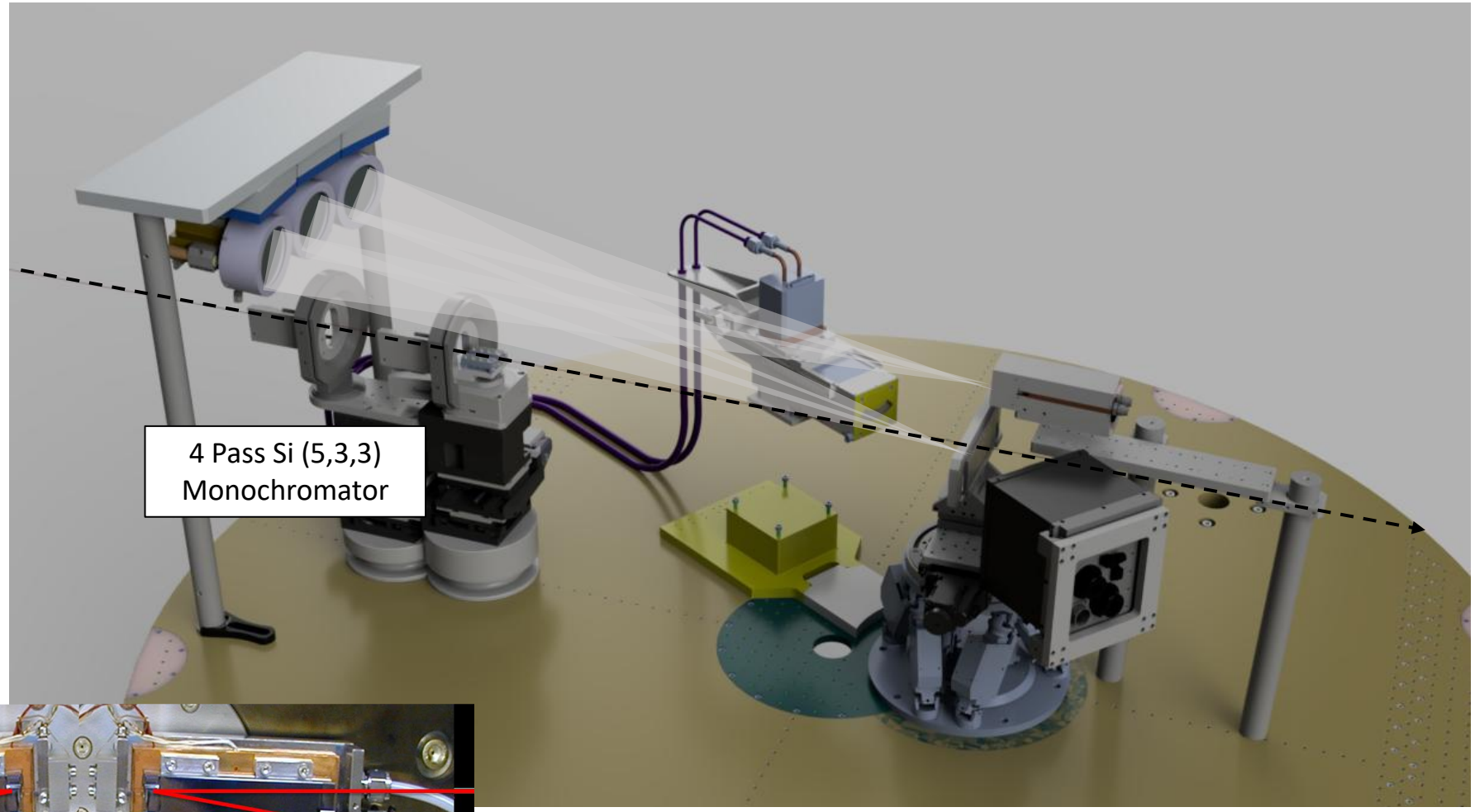

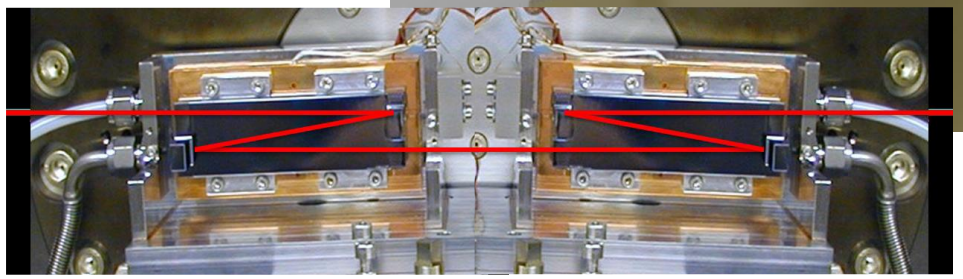

E. E. McBride, T. G. White, A. Descamps et al. Rev. Sci. Inst. 89(10), 10F104 (2018)

Resolving the dynamic ion-ion structure factor requires meV resolution

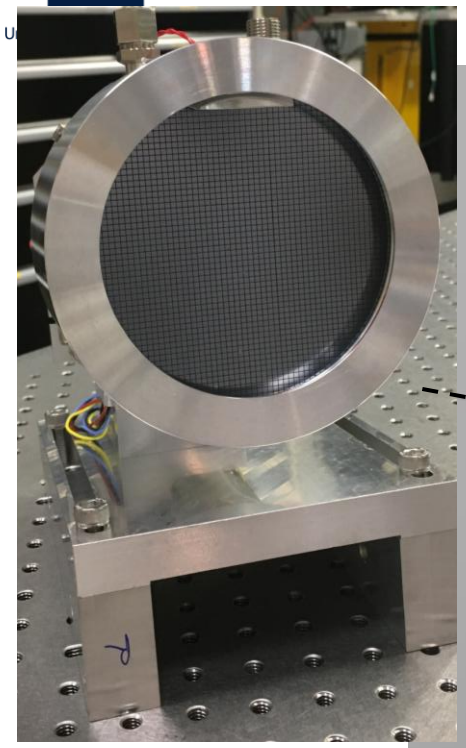

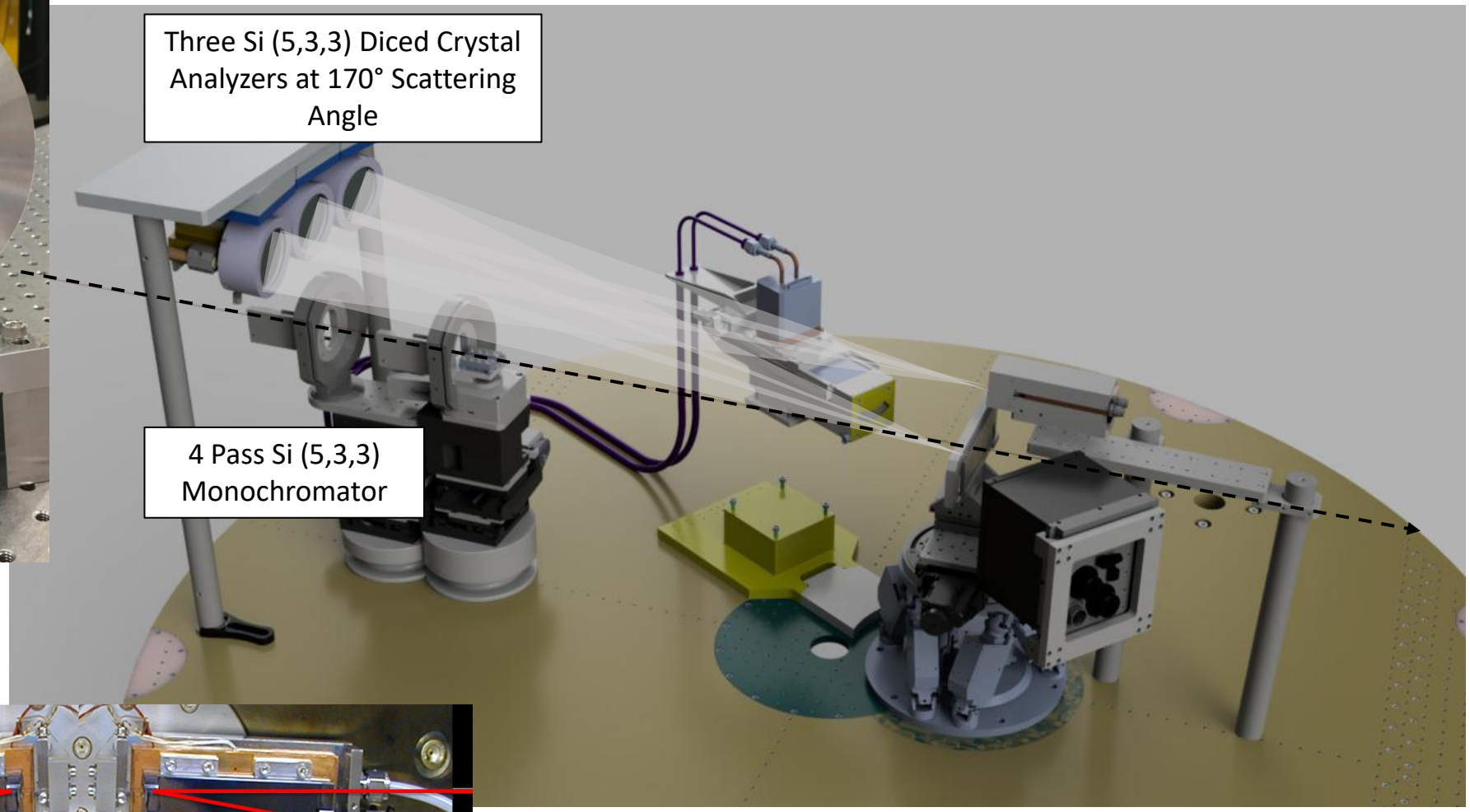

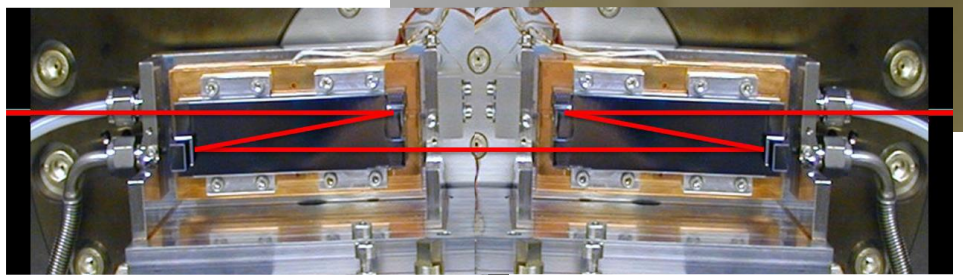

E. E. McBride, T. G. White, A. Descamps et al. Rev. Sci. Inst. 89(10), 10F104 (2018)

Resolving the dynamic ion-ion structure factor requires meV resolution

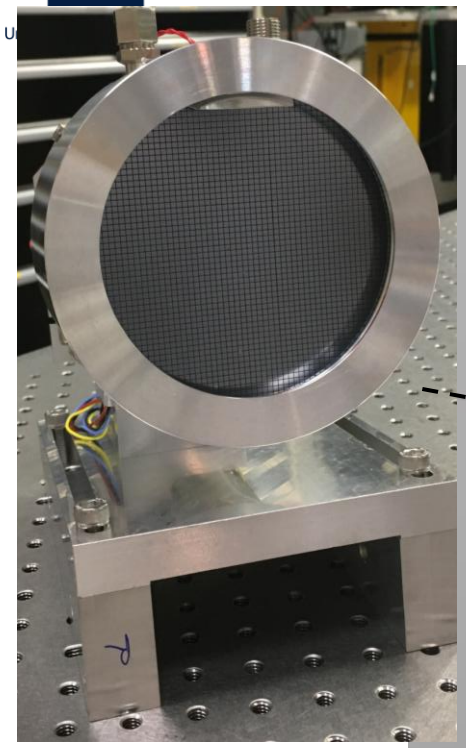

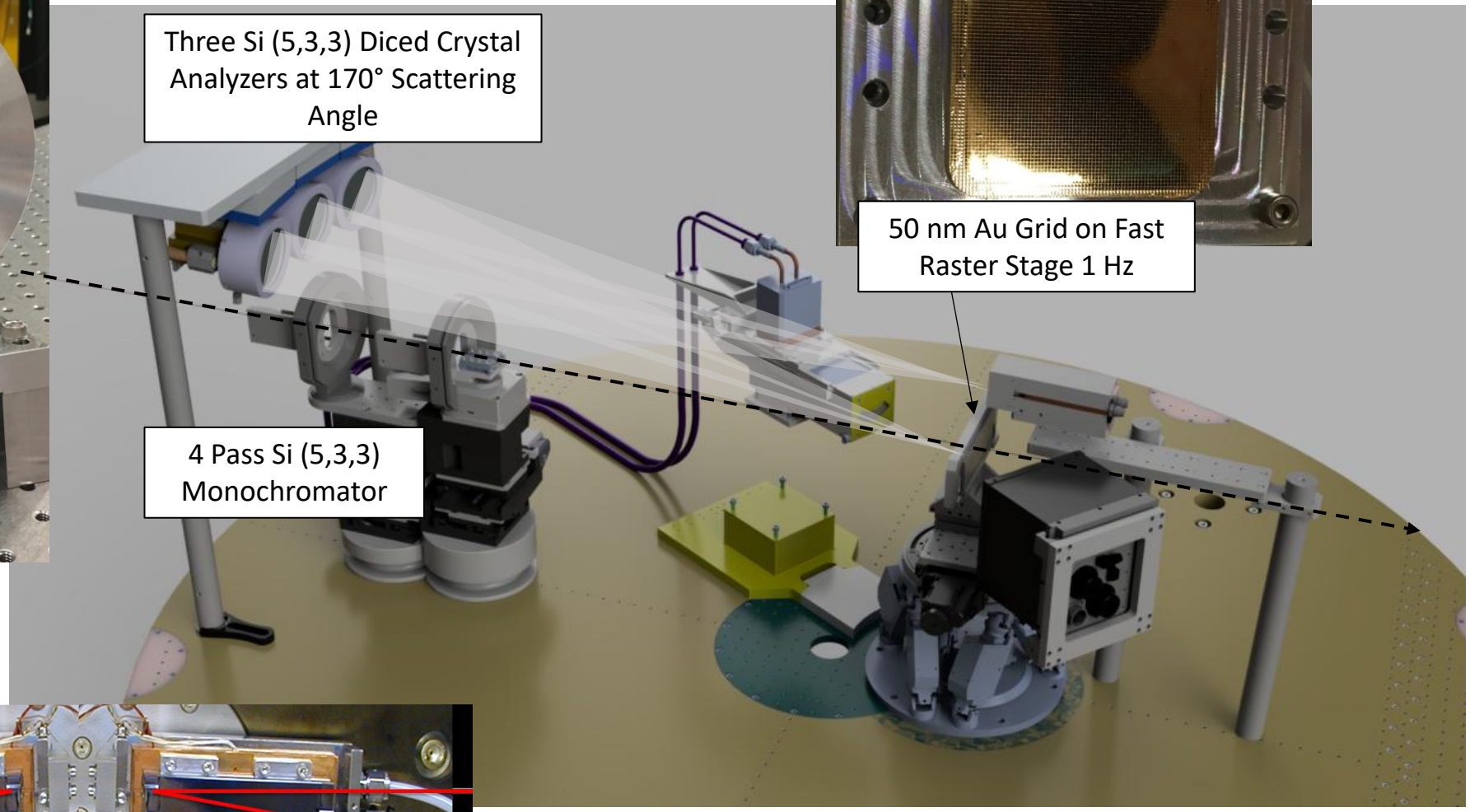

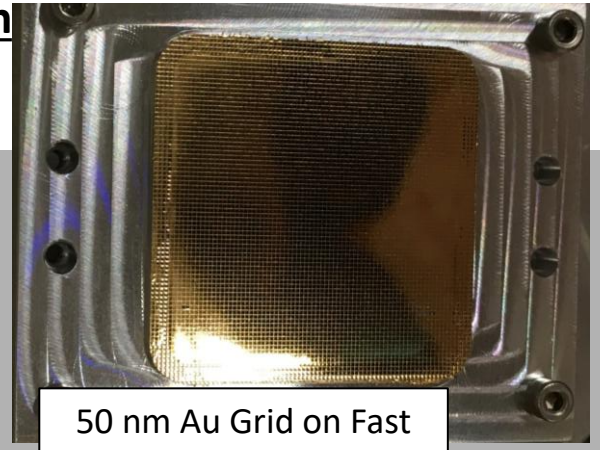

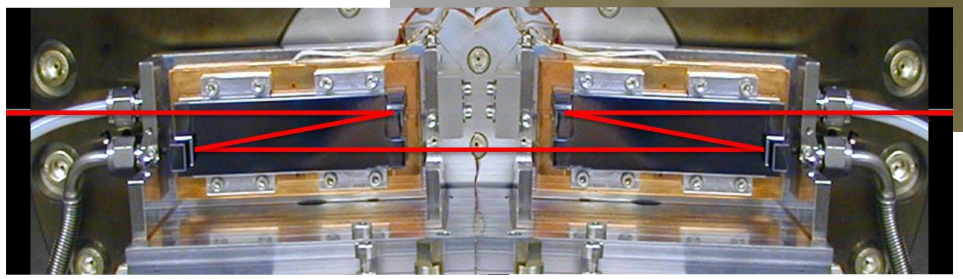

E. E. McBride, T. G. White, A. Descamps et al. Rev. Sci. Inst. 89(10), 10F104 (2018)

Resolving the dynamic ion-ion structure factor requires meV resolution

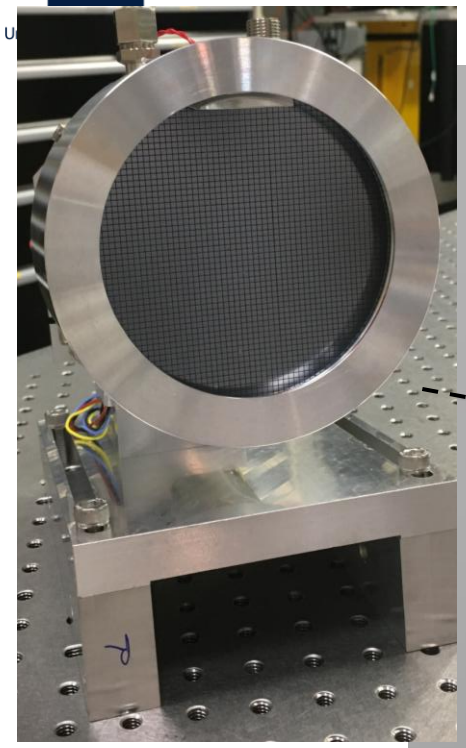

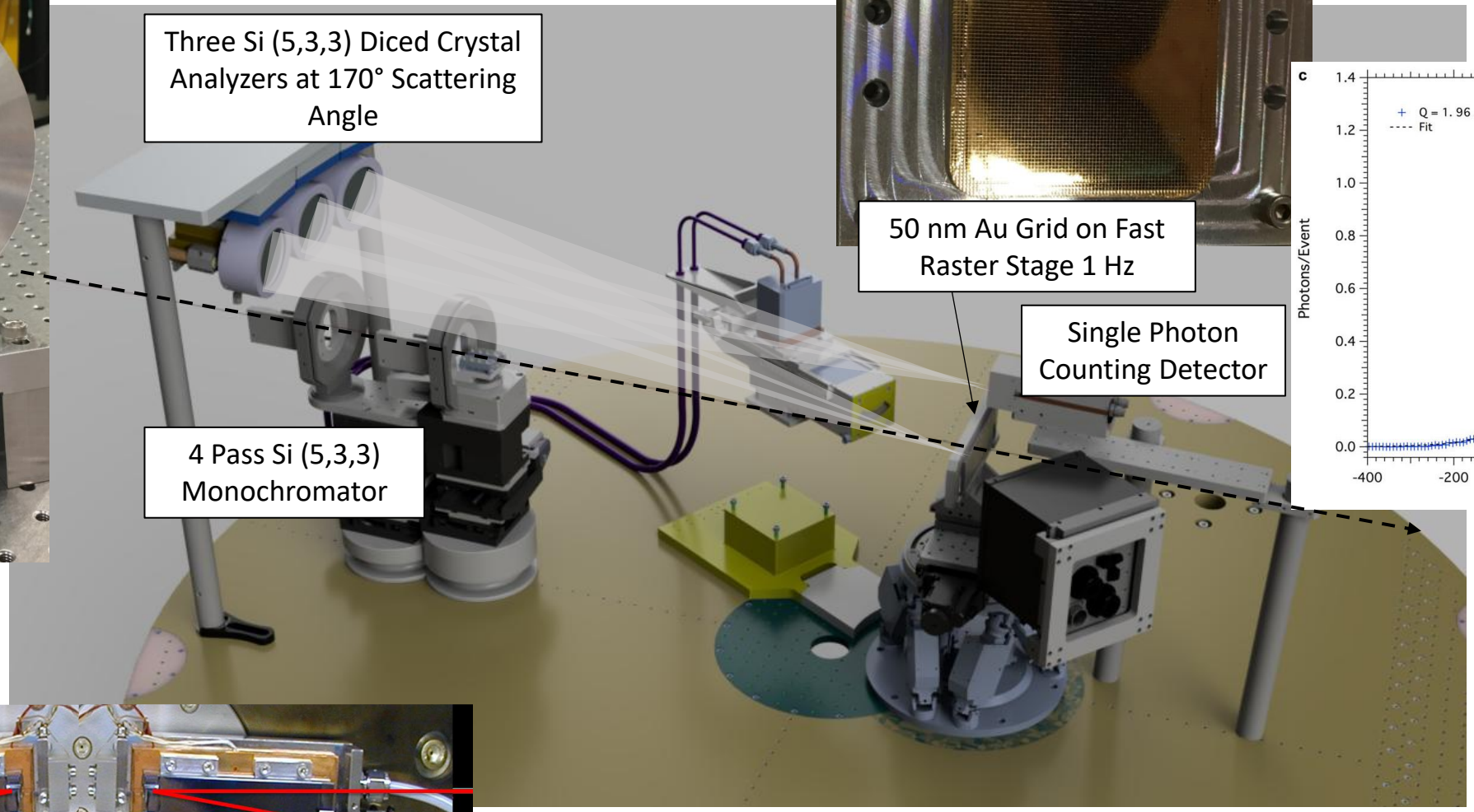

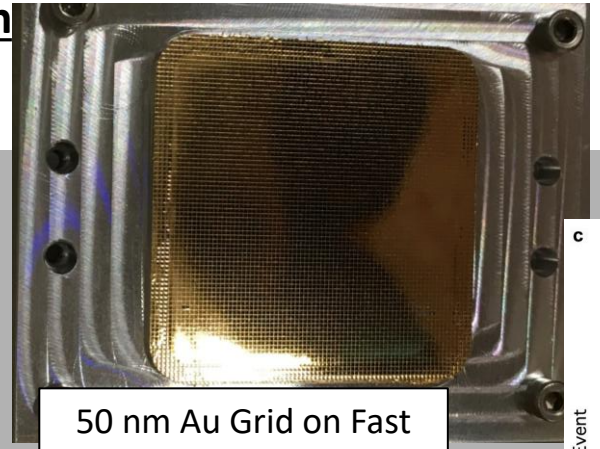

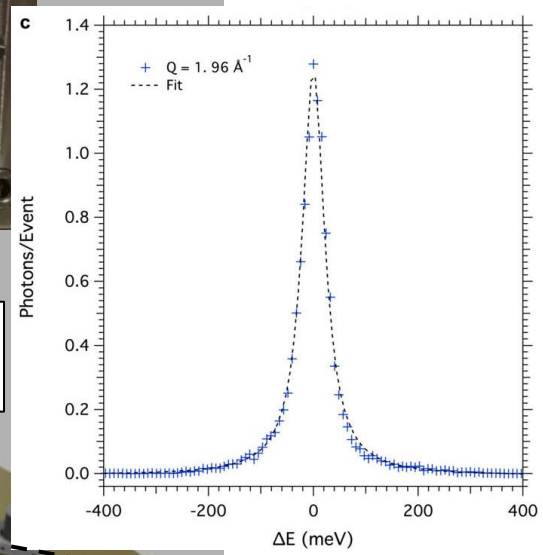

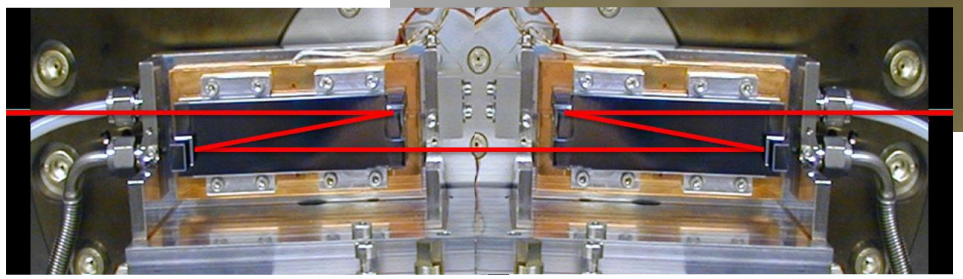

E. E. McBride, T. G. White, A. Descamps et al. Rev. Sci. Inst. 89(10), 10F104 (2018)

Resolving the dynamic ion-ion structure factor requires meV resolution

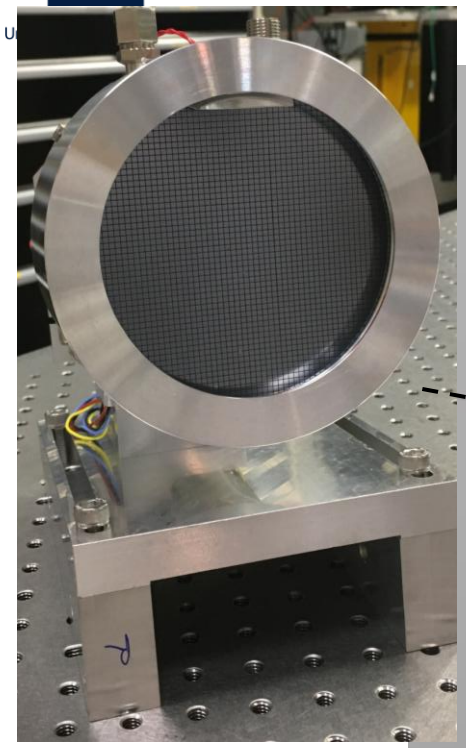

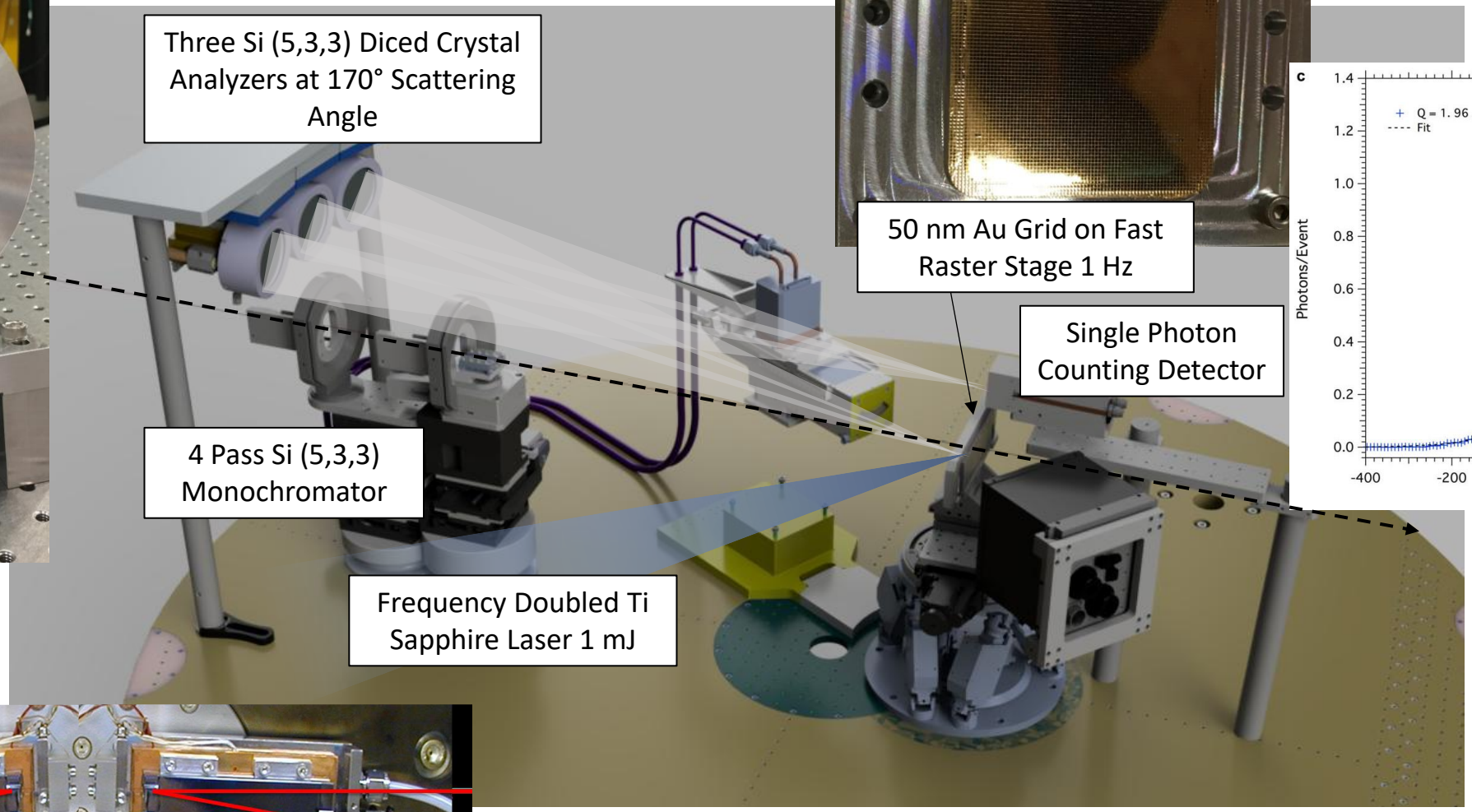

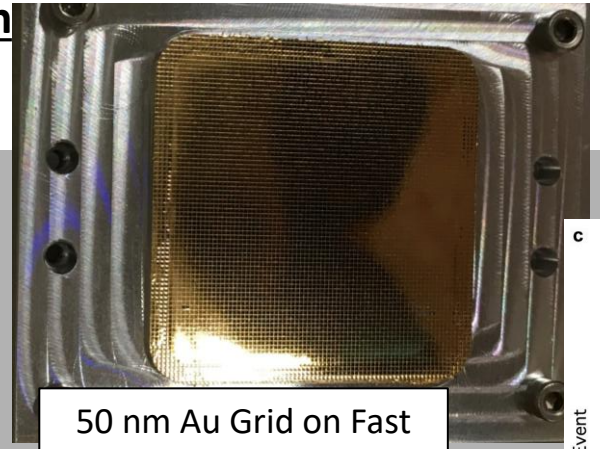

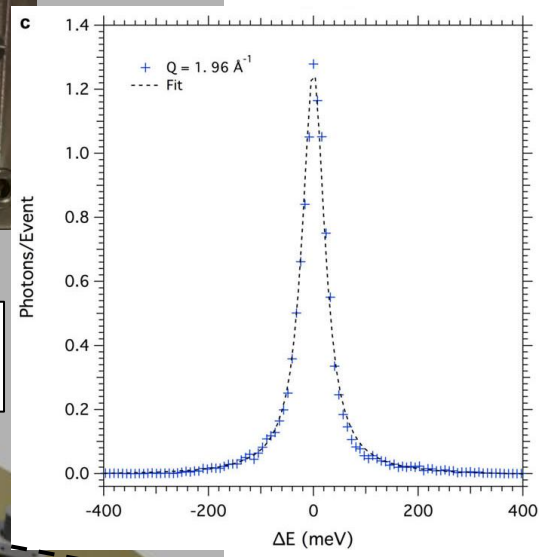

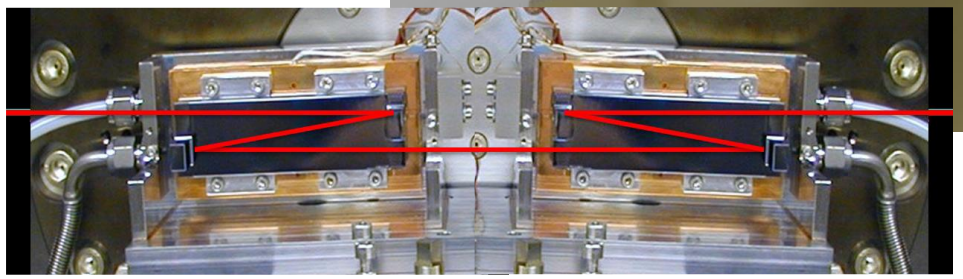

E. E. McBride, T. G. White, A. Descamps et al. Rev. Sci. Inst. 89(10), 10F104 (2018)

Resolving the dynamic ion-ion structure factor requires meV resolution

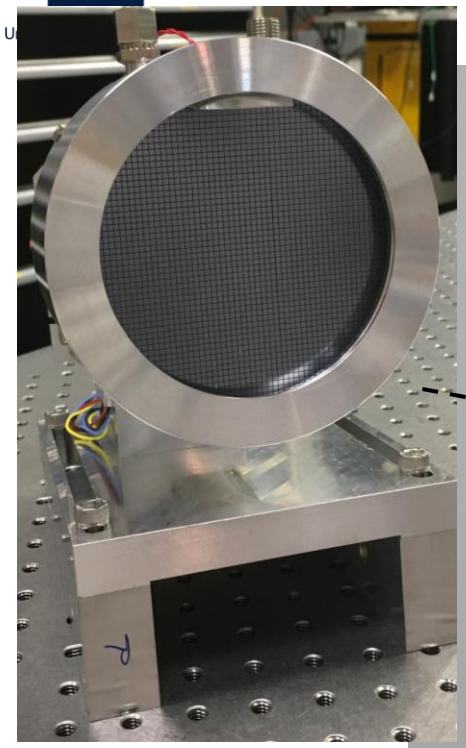

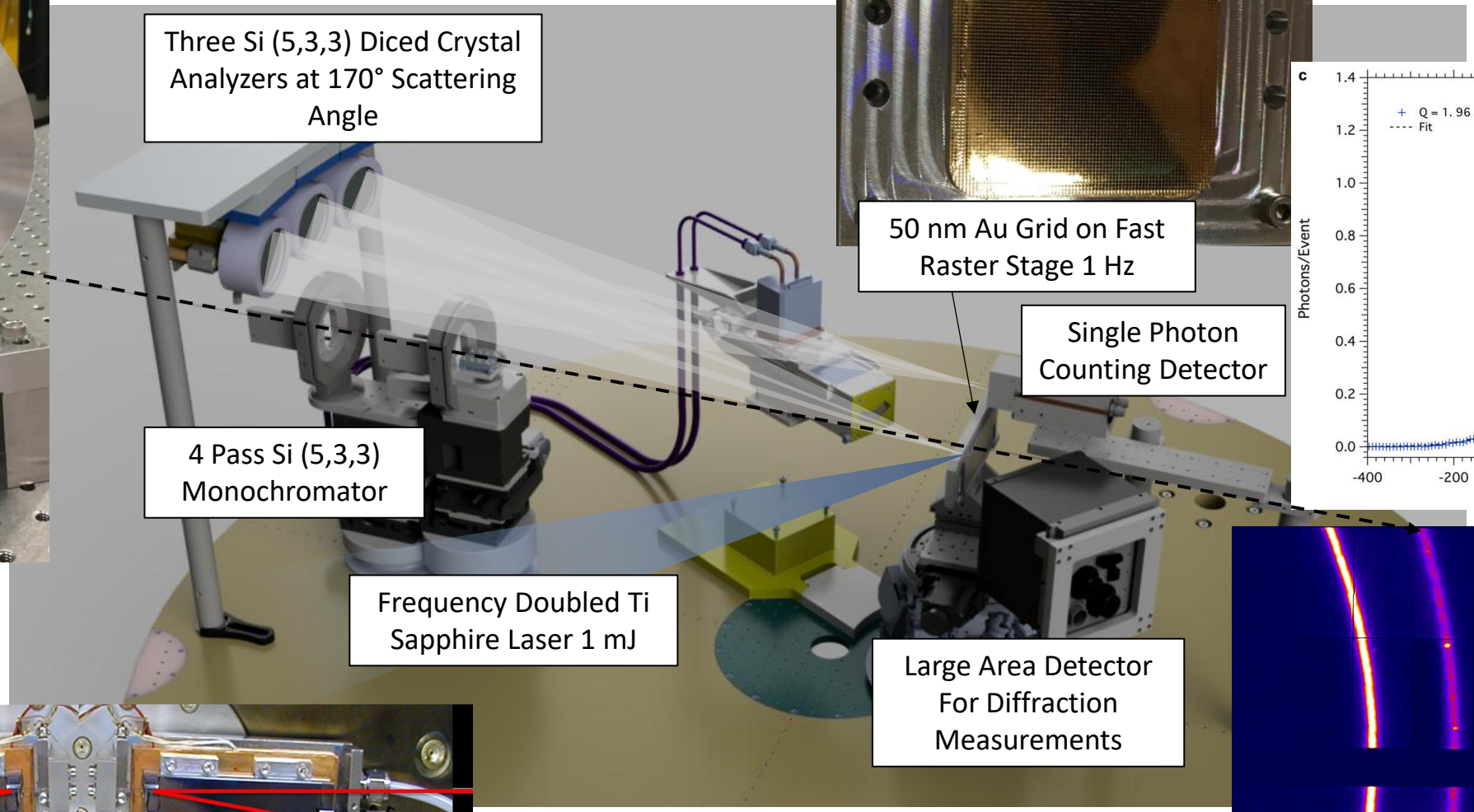

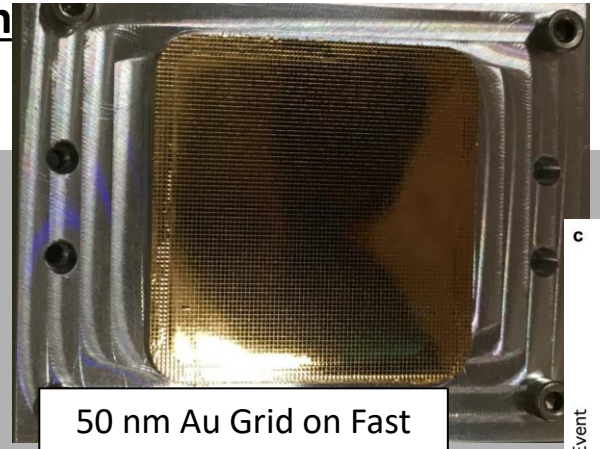

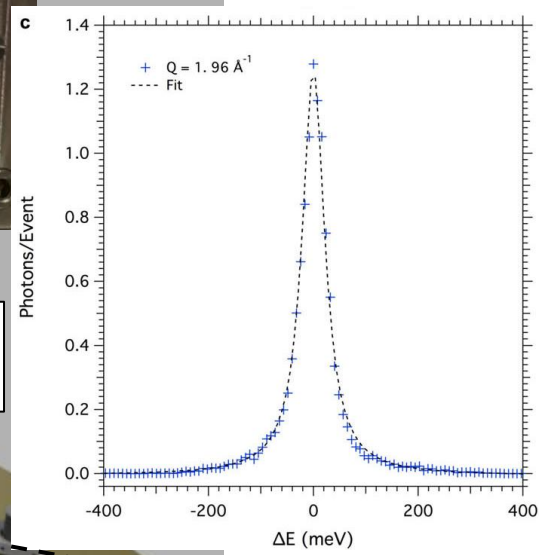

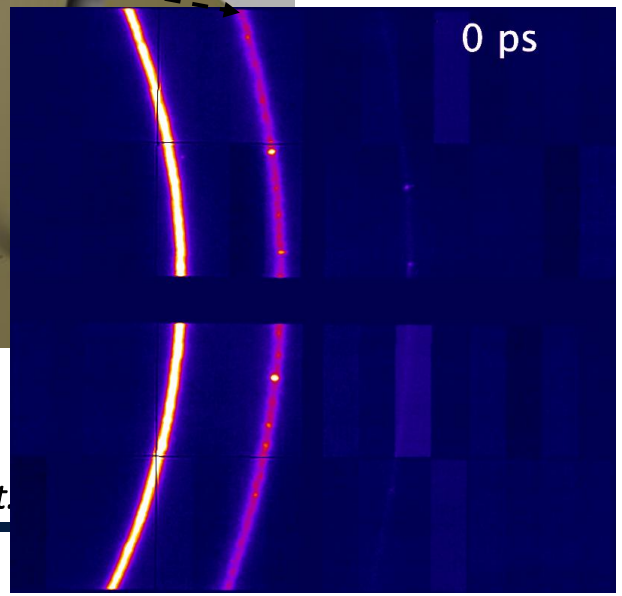

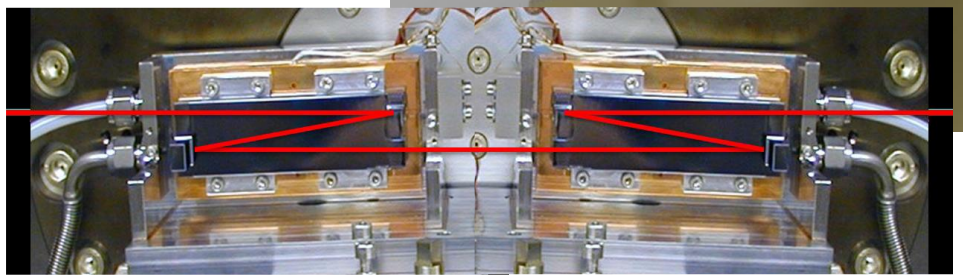

E. E. McBride, T. G. White, A. Descamps et al. Rev. Sci. Inst.

Ion temperature profiles fit using a two-temperature model to calculate electron temperatures

Laser Fluence:
1.0 ± 0.25 J/cm^2

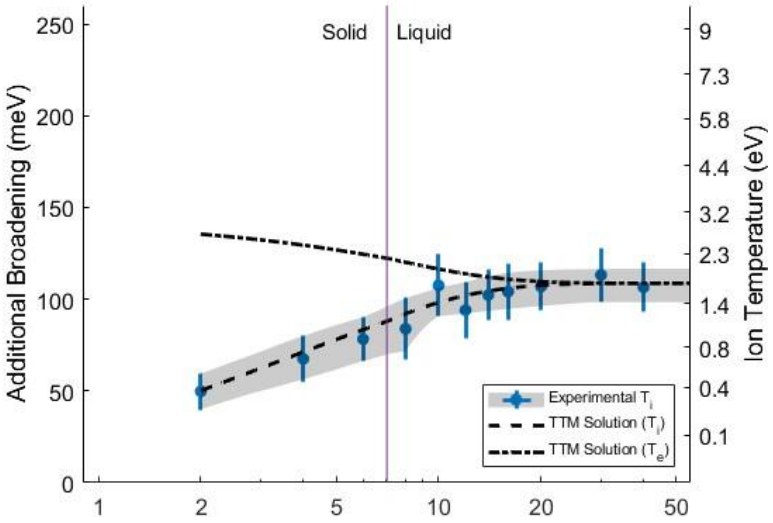

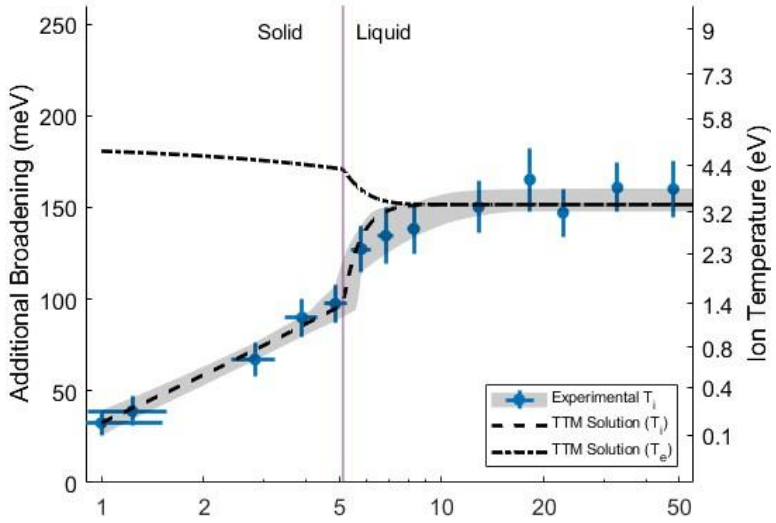

Laser Fluence:
1.9 ± 0.5 J/cm^2

Laser Fluence:
2.0 ± 0.35 J/cm^2

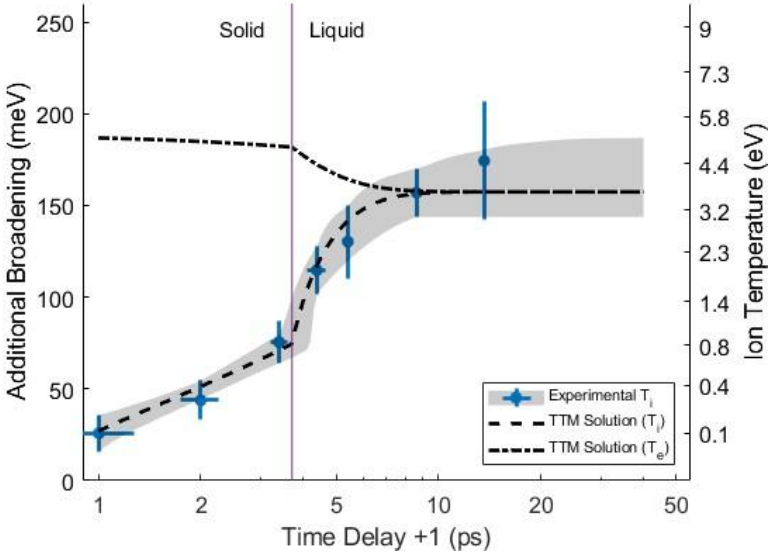

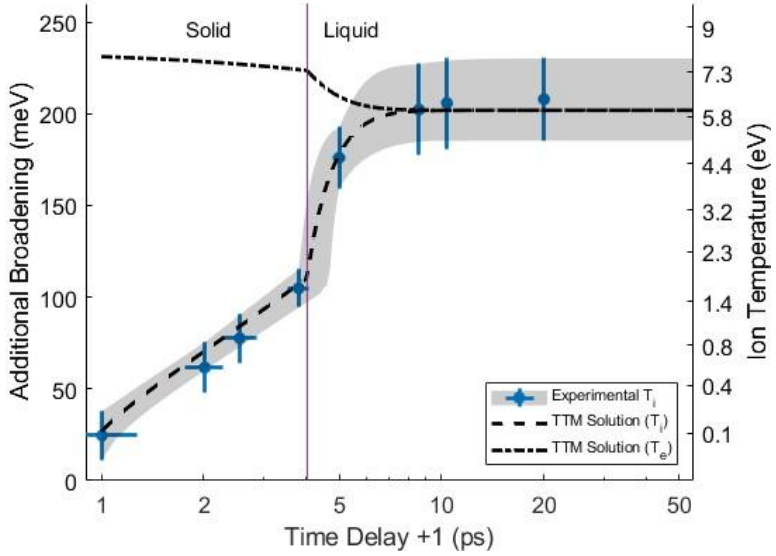

Laser Fluence:
4.95 ± 0.75 J/cm^2

See B. Nagler September 18, 15:00: “Direct Measurement of temperature and Electron-Ion Equilibration Rates in Warm Dense Gold” for further discussion

Ion temperature profiles fit using a two-temperature model to calculate electron temperatures

Laser Fluence:
1.0 ± 0.25 J/cm^2

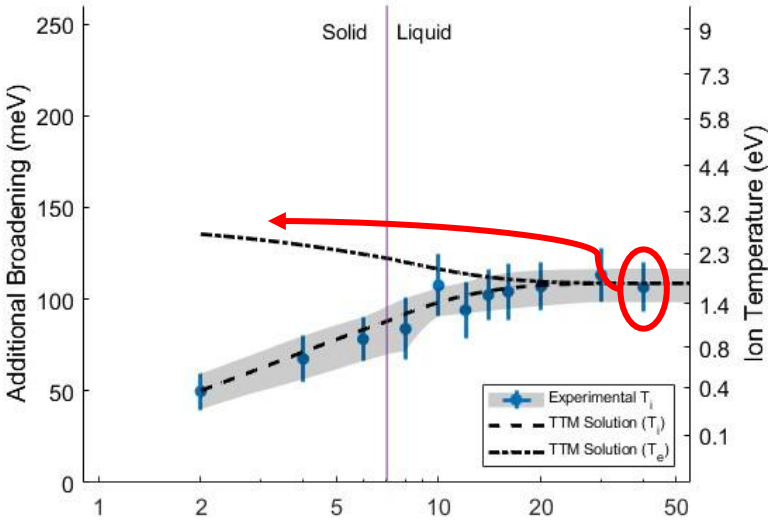

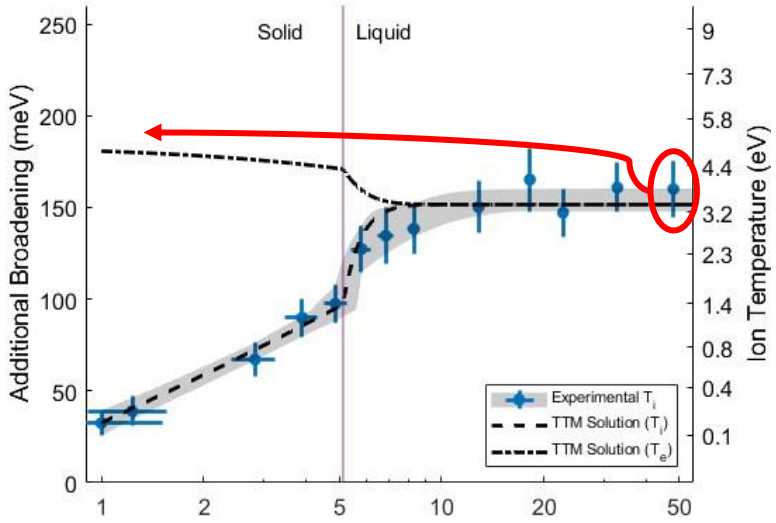

Laser Fluence:
1.9 ± 0.5 J/cm^2

Laser Fluence:
2.0 ± 0.35 J/cm^2

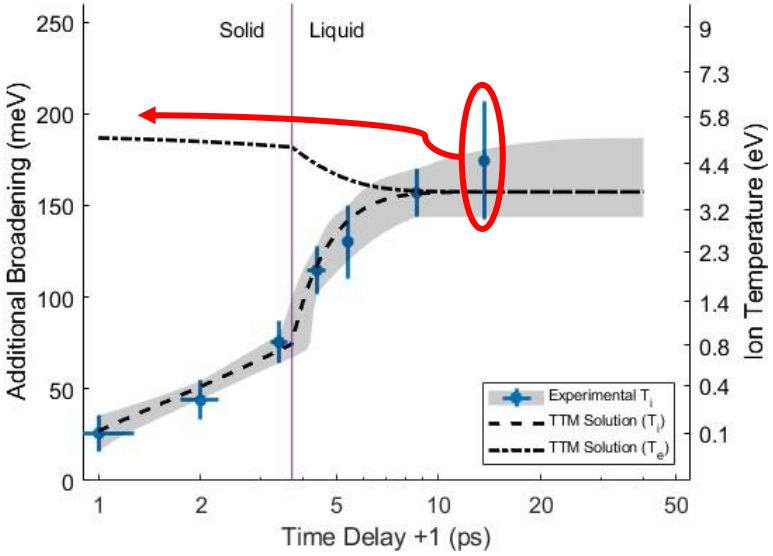

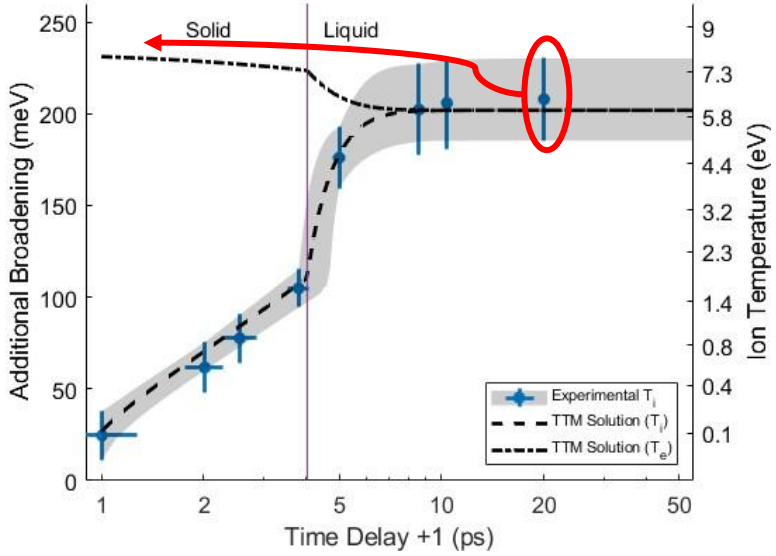

Laser Fluence:
4.95 ± 0.75 J/cm^2

Bounds on Debye temperature can be determined using the Debye Waller equations

- Experimental data can be plotted onto the Debye Waller phase space.
- Dashed lines indicated bounds on the experimental data.
- Only the final data point is used as this differences in θ_D are easier to recognize.

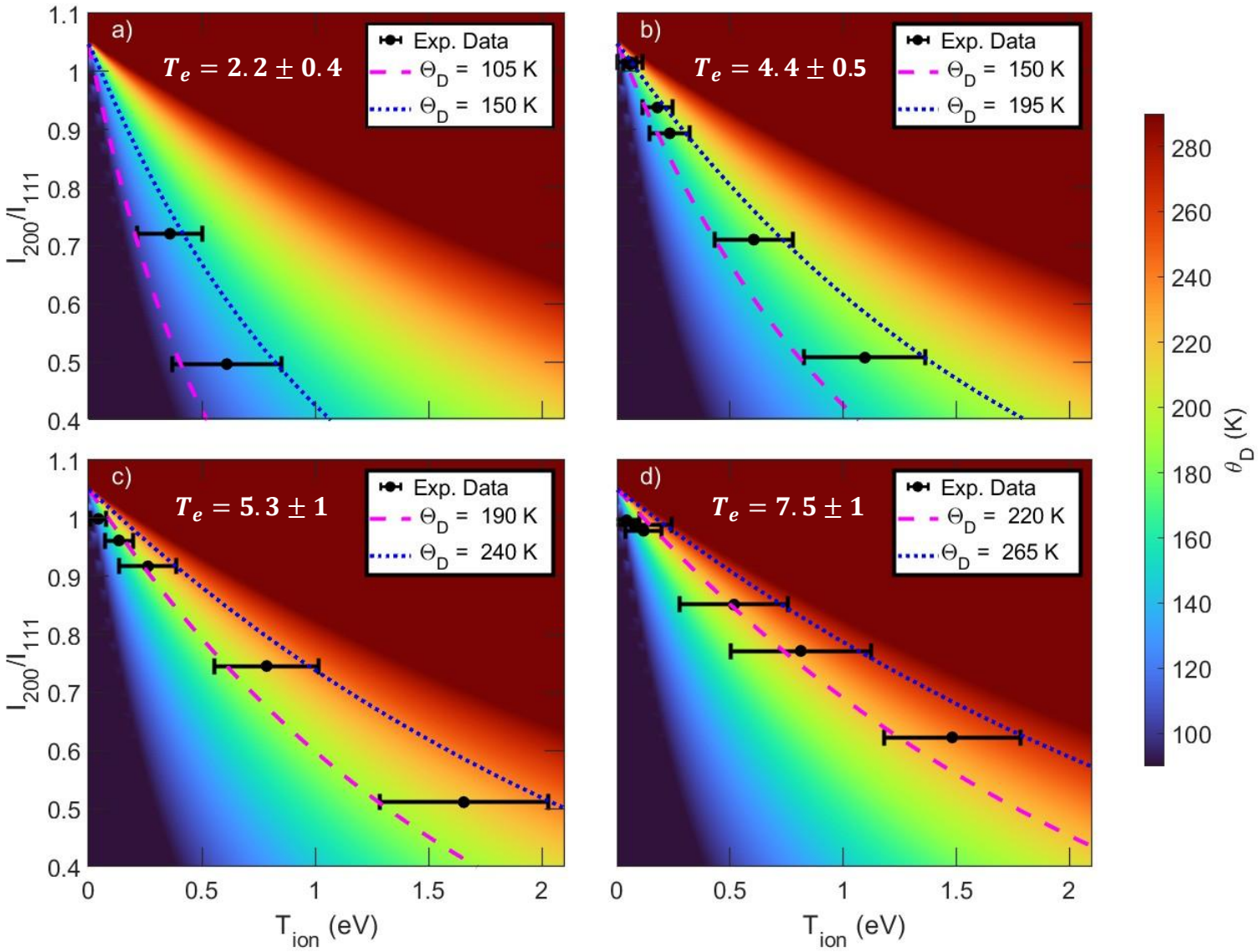

Bounds on Debye temperature can be determined using the Debye Waller equations

- Experimental data can be plotted onto the Debye Waller phase space.
- Dashed lines indicated bounds on the experimental data.
- Only the final data point is used as this differences in θ_D are easier to recognize.

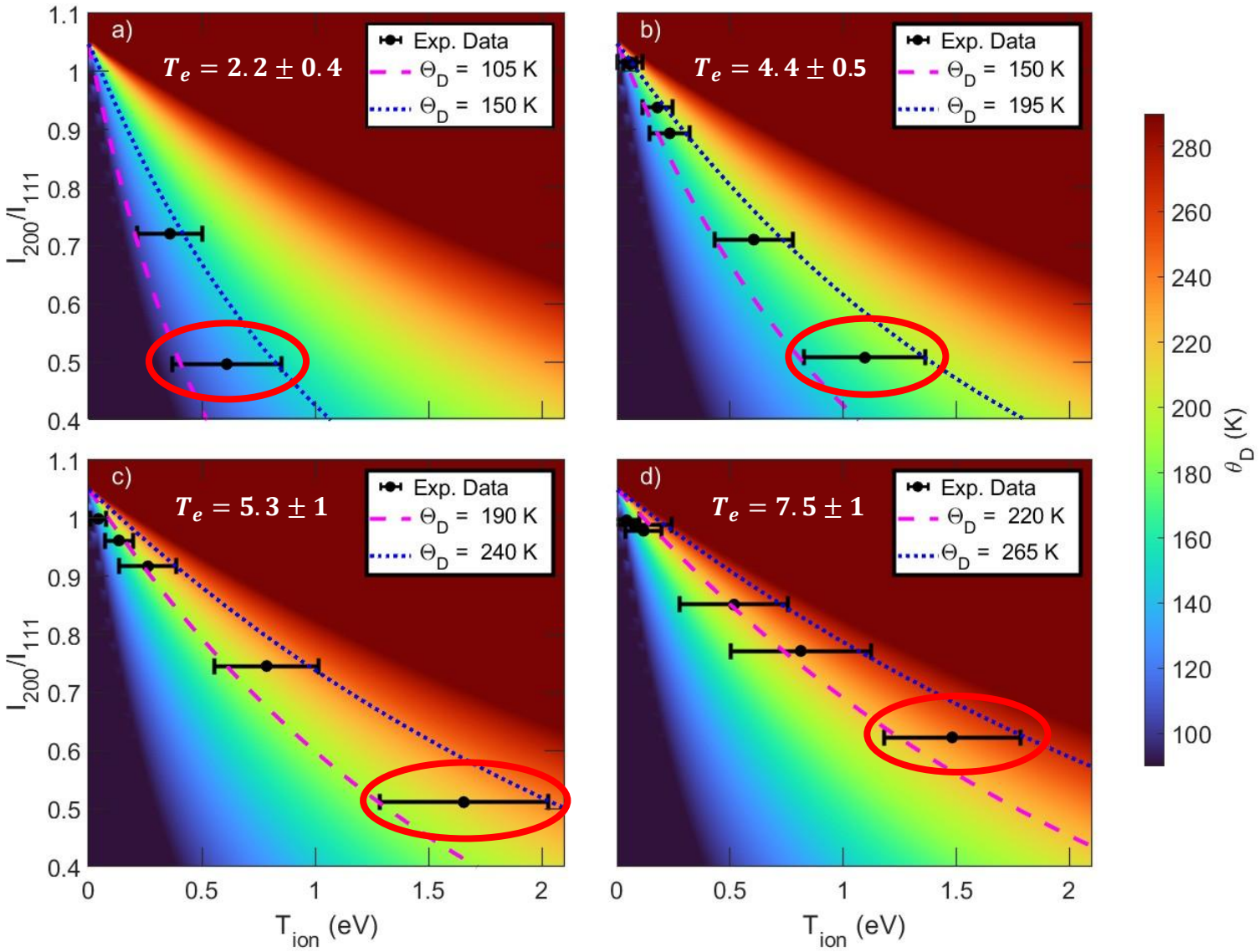

Initially results seems to disagree with theoretical predictions for bond-hardening

- Recoules *et al.*[1] bond hardening prediction agrees with ambient θ_D from Synecek *et al.*[2] ($\sim 185\ K$)
- Synecek *et al.*[2] made measurements on **bulk** sample with **single crystal** orientation

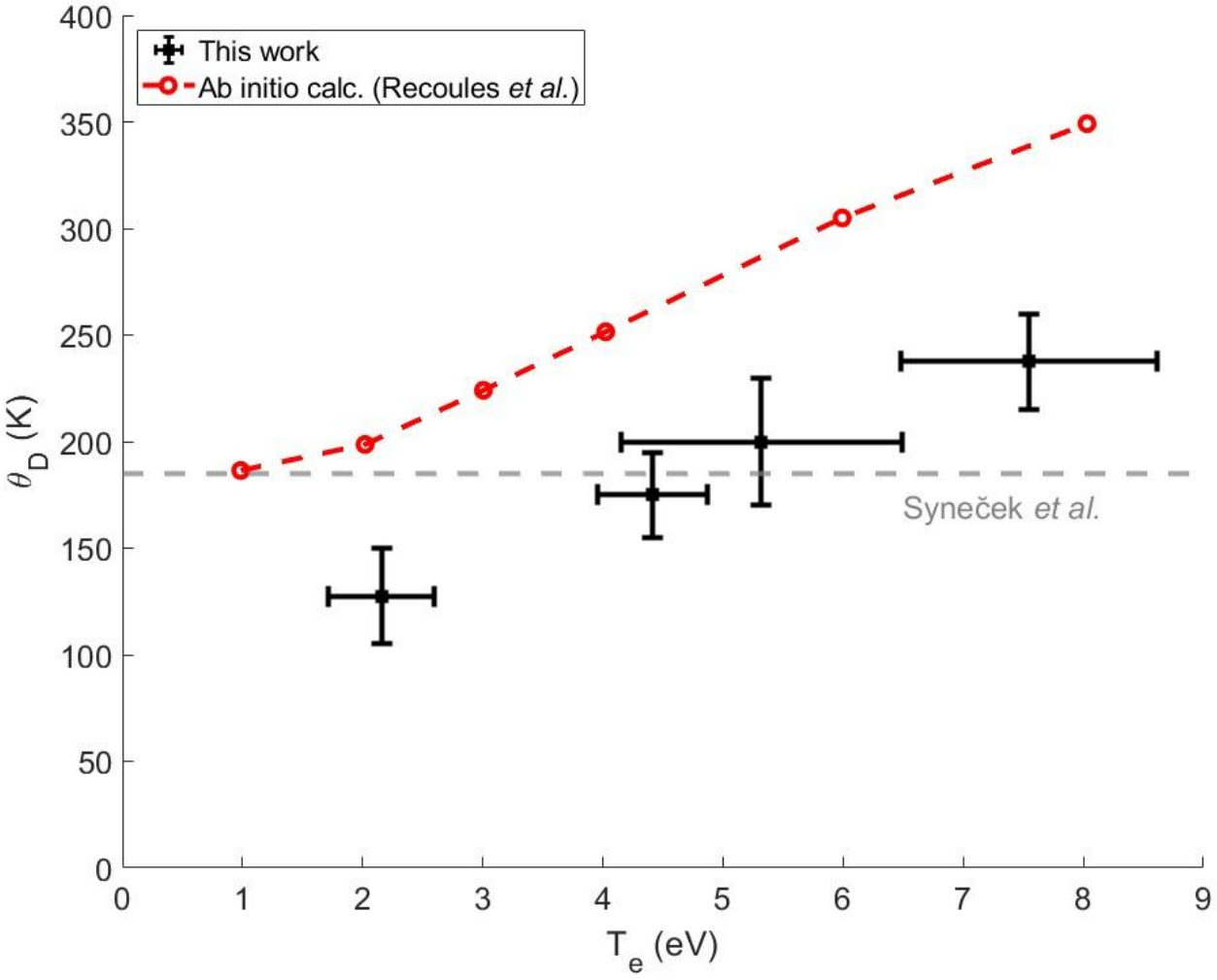

[1]V. Recoules et al. Phys. Rev. Lett. 96, 055503 (2006)
[2]V. Synecek et al. Acta Cryst. A26, 108-113 (1970)

Ambient Debye temperature reduced for thin films and polycrystal samples

- Ma et al.[3] found differences in θ_D between single crystal and polycrystal structures
- Additionally, there is clear evidence for dependence on film thickness
- For a **50 nm polycrystal** sample θ_D at ambient temperature drops to $\sim\mathbf{100\ K}$.

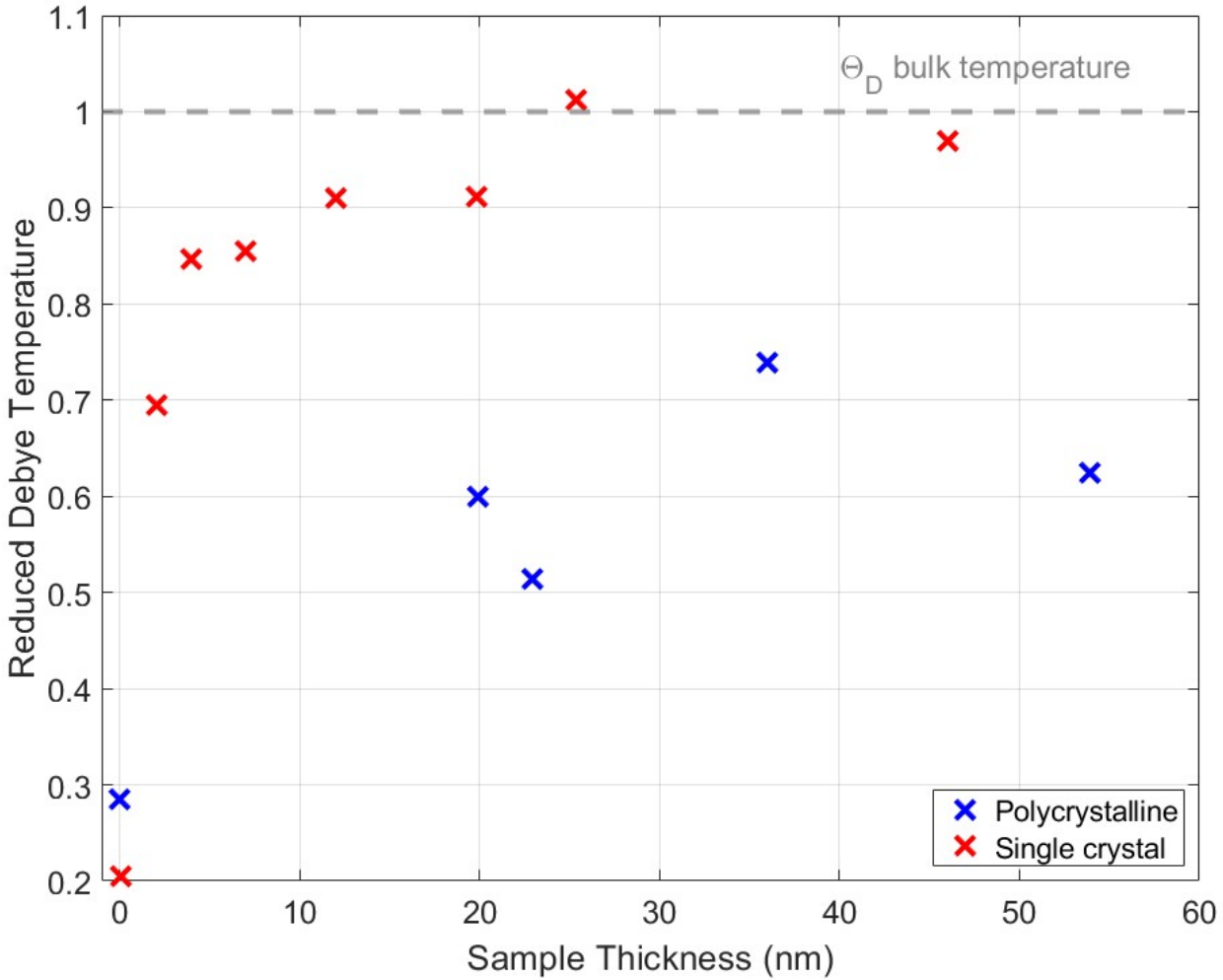

Figure adapted from[3]

[3] *W. Ma et al. J. Phys. D: Appl. Phys 43 465301 (2010)*

Ambient Debye temperature reduced for thin films and polycrystal samples

- Ma et al.[3] found differences in θ_D between single crystal and polycrystal structures.
- Additionally, there is clear evidence for dependence on film thickness
- For a **50 nm polycrystal** sample θ_D at ambient temperature drops to $\sim\mathbf{100\ K}$.

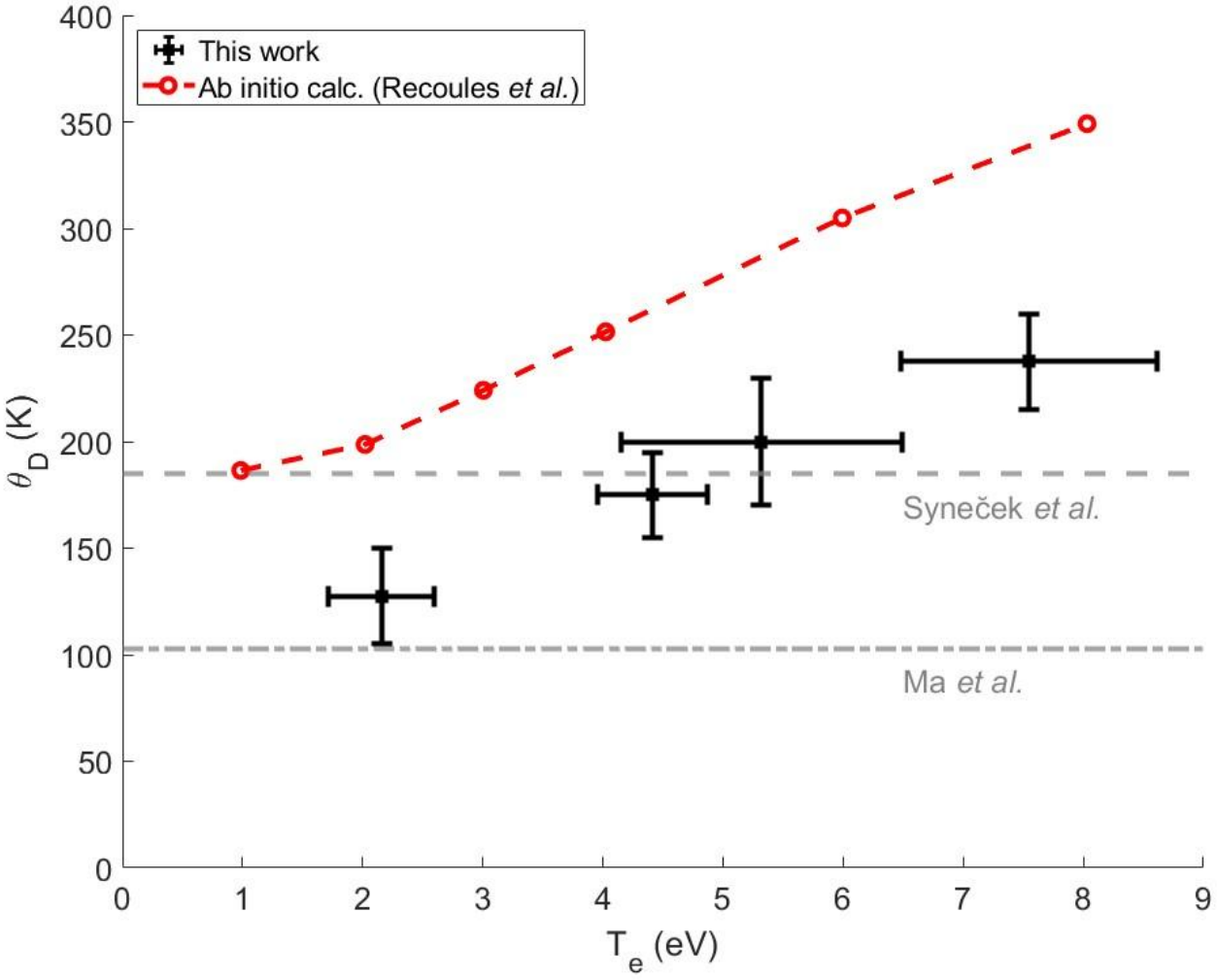

[1]V. Recoules et al. Phys. Rev. Lett. 96, 055503 (2006)
[2]V. Synecek et al. Acta Cryst. A26, 108-113 (1970)
[3]W. Ma et al. J. Phys. D: Appl. Phys 43 465301 (2010)

When accounting for thin film and polycrystalline effects results match theory

- Adjusting Recoules *et al.*[1] starting Debye temperature, predictions match experimental results
- Definitively see evidence of bond hardening as a function of electron temperature in thin polycrystalline gold films.

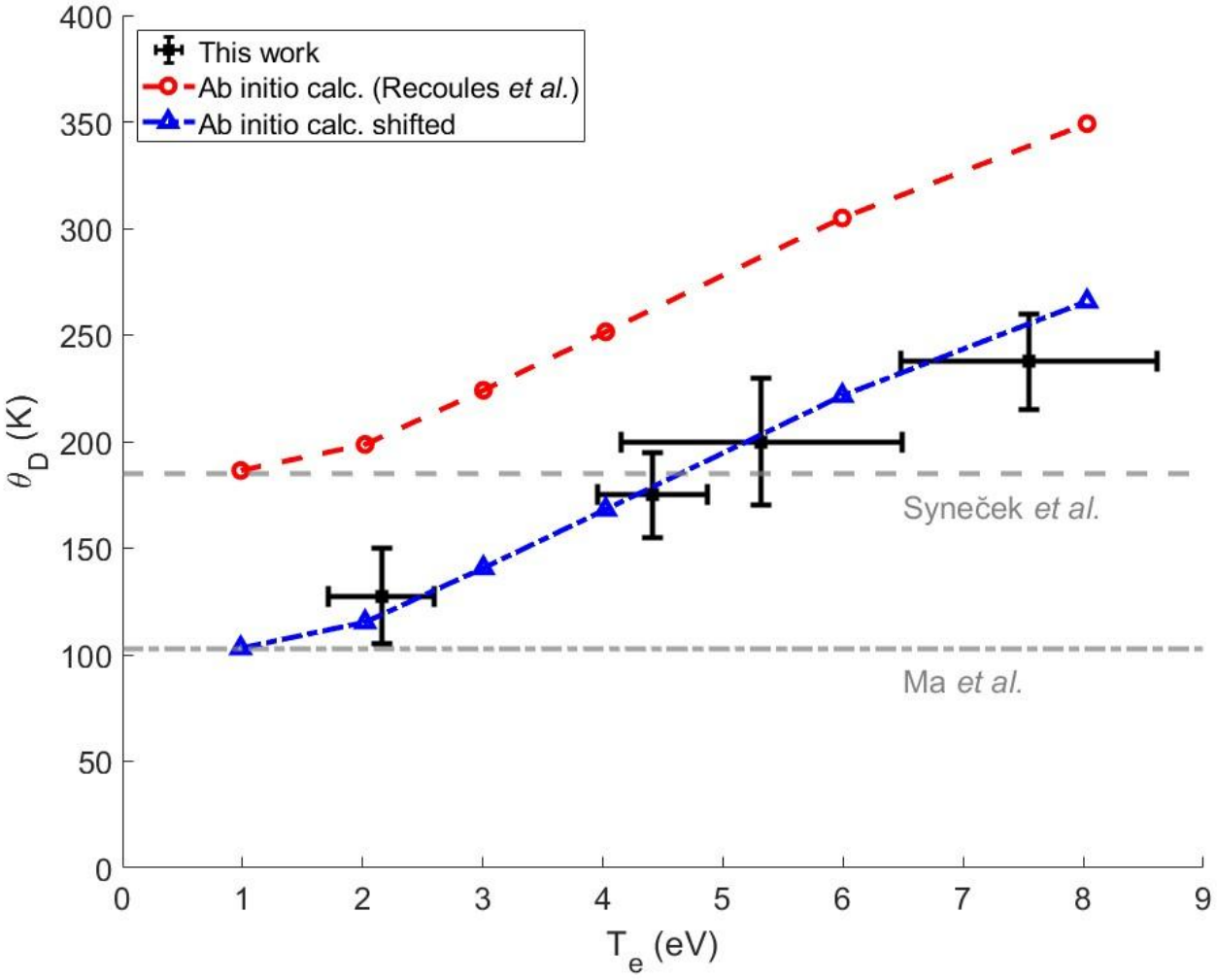

[1]V. Recoules et al. Phys. Rev. Lett. 96, 055503 (2006)
[2]V. Synecek et al. Acta Cryst. A26, 108-113 (1970)
[3]W. Ma et al. J. Phys. D: Appl. Phys 43 465301 (2010)

When accounting for thin film and polycrystalline effects results match theory

- We have successfully demonstrated the first direct measurement of the ion temperature in laser-heated metals in Au
- Ion-temperature and *in situ* Bragg peak diffraction data have been combined to calculate the Debye temperature in WDM gold.
- We have conclusively determined bond strength in this regime.

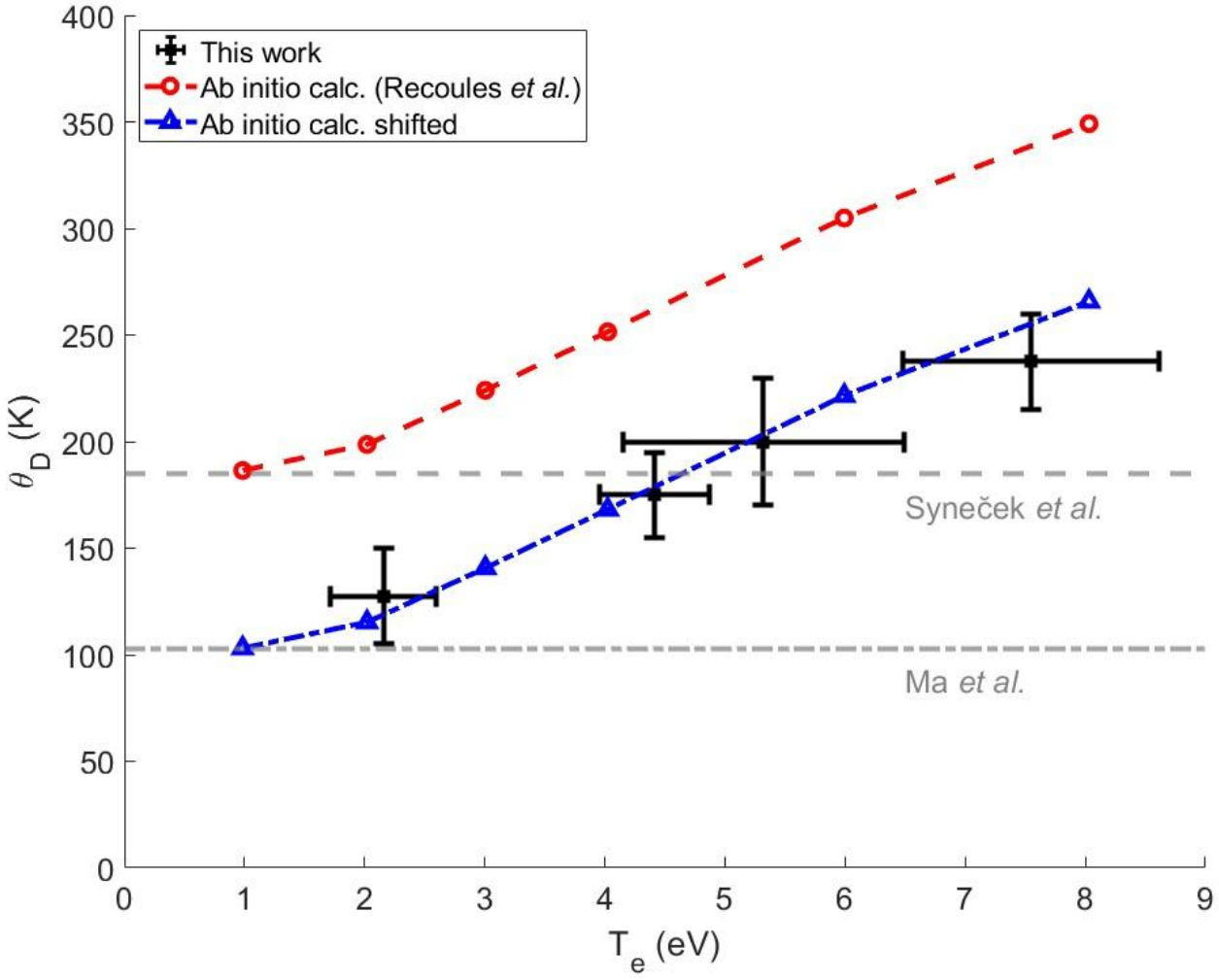

[1]V. Recoules et al. Phys. Rev. Lett. 96, 055503 (2006)
[2]V. Synecek et al. Acta Cryst. A26, 108-113 (1970)
[3]W. Ma et al. J. Phys. D: Appl. Phys 43 465301 (2010)

Discussion topics

- Heat transport across warm dense matter interfaces
  - Observation of *Interfacial Thermal Resistance* at Extreme Conditions
- **Direct ion temperature measurements at free electron lasers**
  - Bond strength in non-equilibrium gold
  - **Electron ion equilibration in warm dense matter**
  - Superheating beyond the entropy catastrophe
- Forward Scattering
  - Sound speed in warm dense methane
  - Phonon dispersion and temperature through detailed balance

Electron-Ion Equilibration

- When a high-intensity optical laser is incident on a solid target, it initiates an energy cascade
- The preferential and rapid heating of one subsystem over the other creates a highly non-equilibrium state.
- These transient, high-energy-density plasmas are a precursor to warm dense matter (WDM) and serve as a testbed where we can validate quantum mechanical theories of electron-ion interactions.
- In these transient systems, the colder ions are strongly coupled, while the electrons behave quantum mechanically.
- This complication has led to large differences in the predictions of the electron-ion equilibration rate. e.g., Spitzer, Fermi's Golden Rule, and Coupled Mode

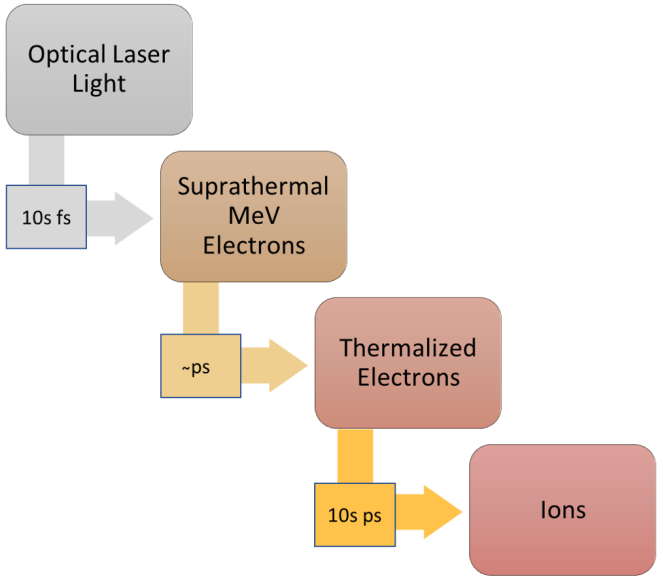

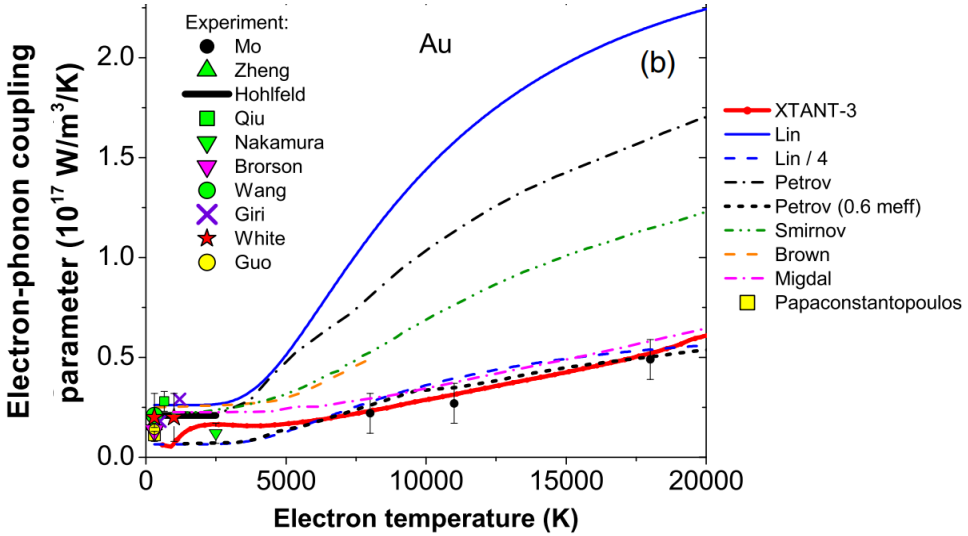

The excited state of the ions also complicates the physics of these systems in ways that are not yet fully understood. e.g., G=G(T_e, T_i, ρ)

The excited state of the ions also complicates the physics of these systems in ways that are not yet fully understood. e.g., G=G(T_e, T_i, ρ)

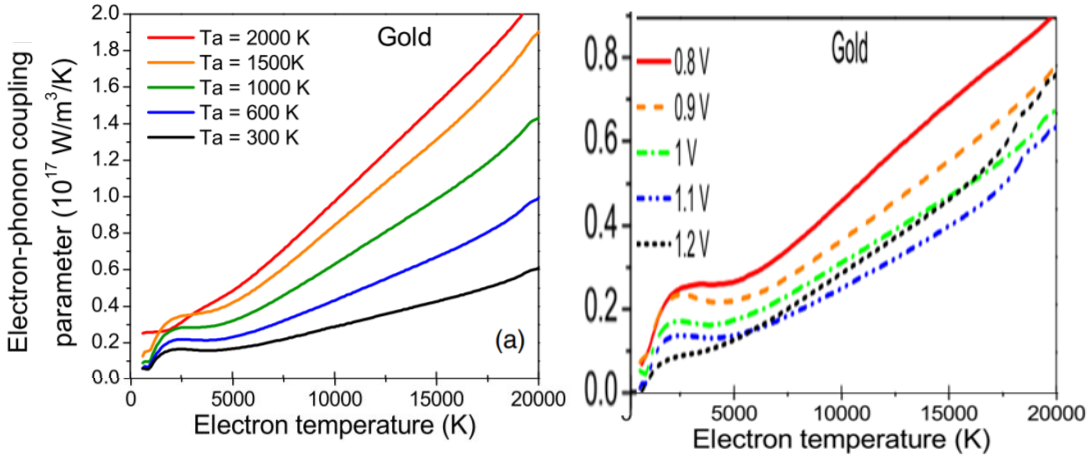

Medvedev et al. Phys. Rev. B 102, 064302 (2020)

Suppressed Electron-Ion Equilibration at High Electron Temperatures?

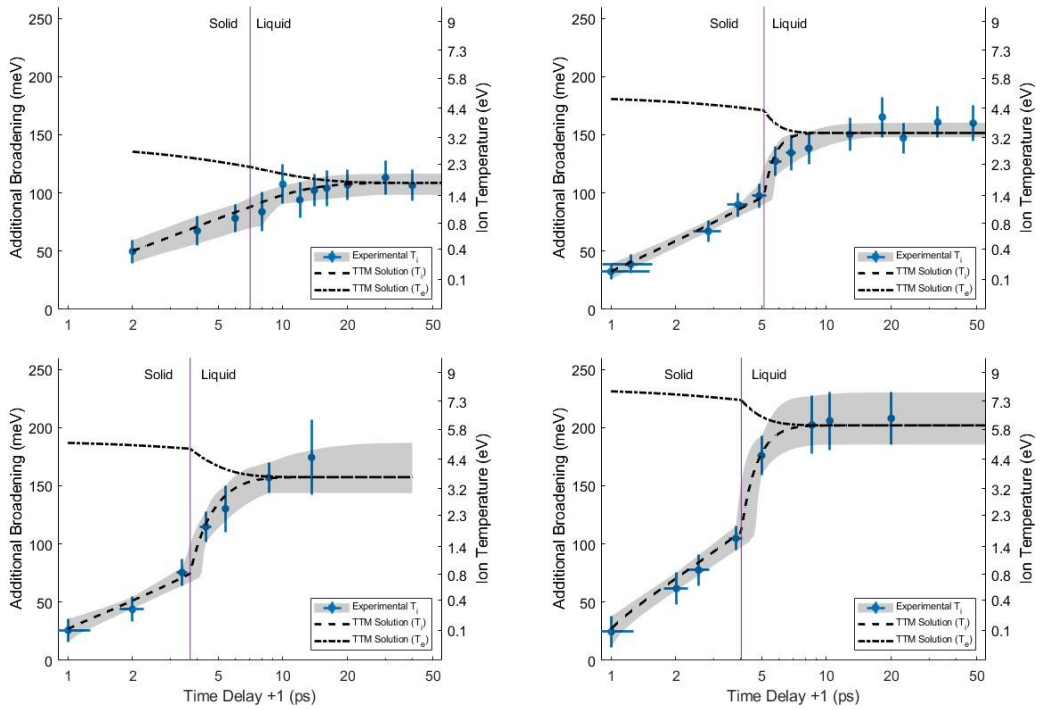

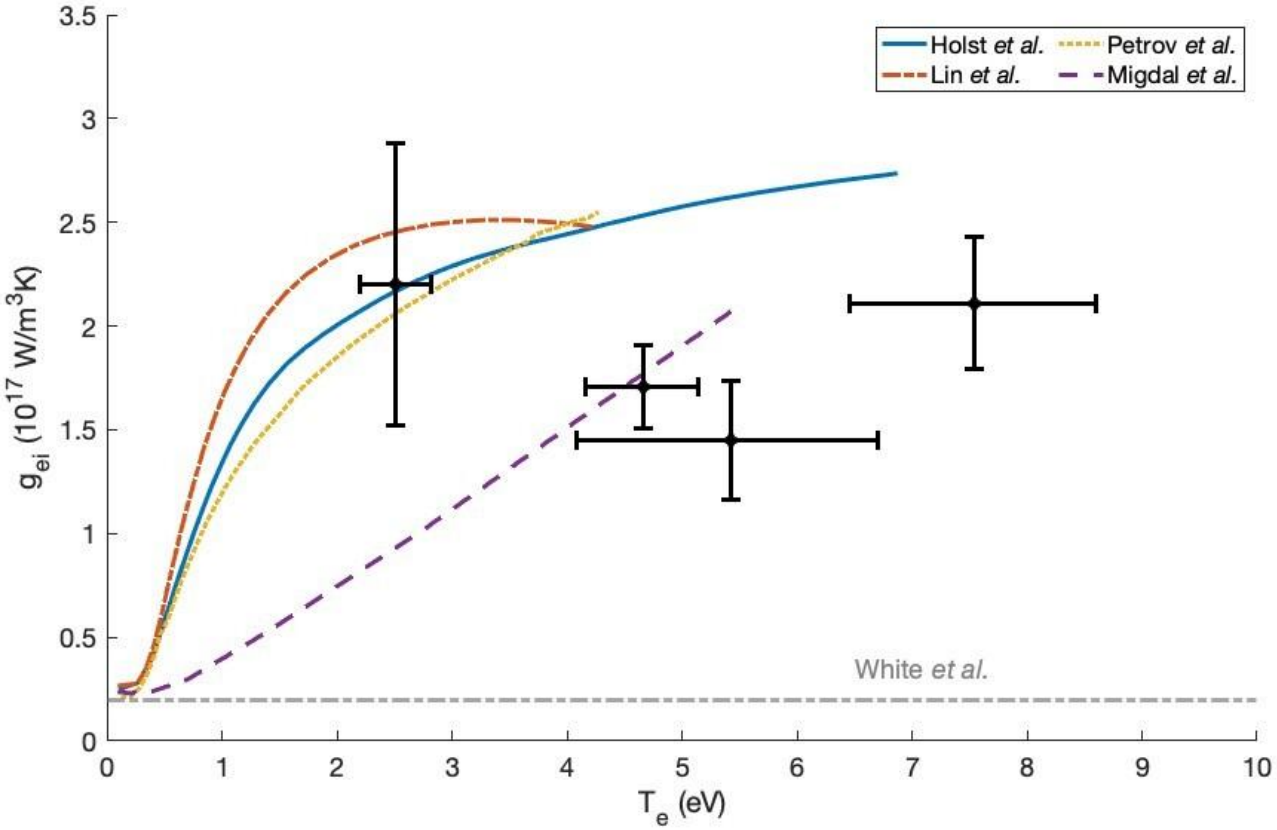

- We see signs of suppressed or inhibited electron-ion equilibration in solid-density gold at elevated electron temperatures.
- We are still working on the ‘jump’ in the data at melt. We have a number of working theories (latent heat, rapid expansion). Work is ongoing.

Discussion topics

- Heat transport across warm dense matter interfaces
  - Observation of *Interfacial Thermal Resistance* at Extreme Conditions
- **Direct ion temperature measurements at free electron lasers**
  - Bond strength in non-equilibrium gold
  - Electron ion equilibration in warm dense matter
  - **Superheating beyond the entropy catastrophe**
- Forward Scattering
  - Sound speed in warm dense methane
  - Phonon dispersion and temperature through detailed balance

What is the Ultimate Limit of Superheating?

Superheating is a complex non-equilibrium phenomenon in which materials reach temperatures higher than required for a phase transition yet remain in their original phase.

What is the Ultimate Limit of Superheating?

Superheating is a complex non-equilibrium phenomenon in which materials reach temperatures higher than required for a phase transition yet remain in their original phase.

A short history of superheating:

- 1948 - Walter Kauzmann, Chem. Rev. 43, 219
  - Supercooling limit predicted from entropy cross-over.
  - A liquid cooled below this limit will undergo spontaneous crystallization or glass formation.

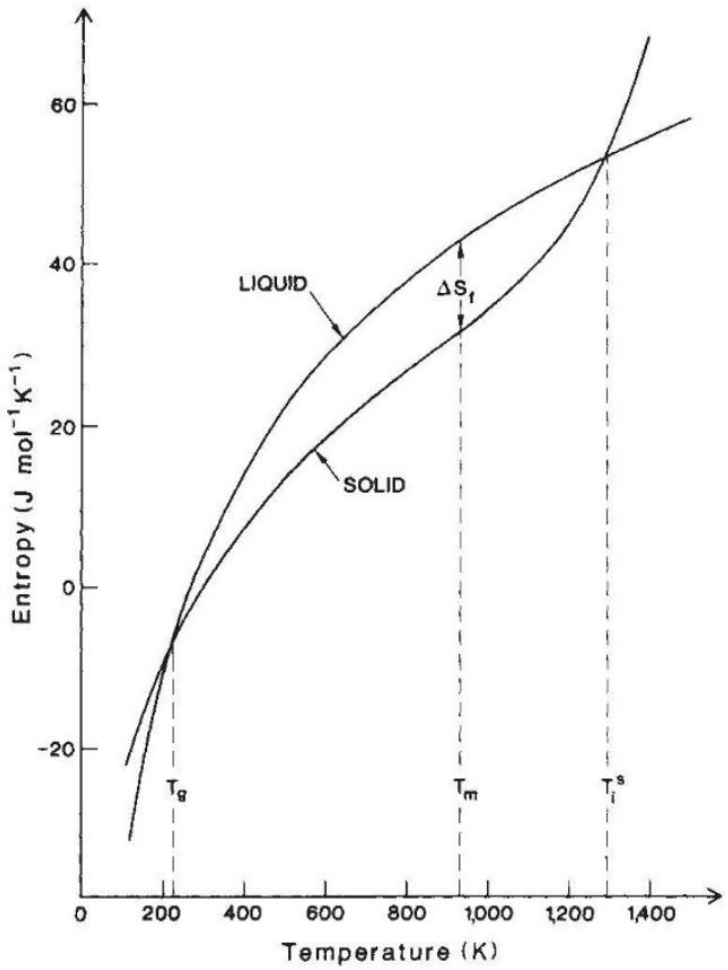

Fig. 1 The entropy of liquid and crystalline aluminium as function of temperature in the stable and metastable regime. ΔS_f denotes the entropy of fusion.

What is the Ultimate Limit of Superheating?

Superheating is a complex non-equilibrium phenomenon in which materials reach temperatures higher than required for a phase transition yet remain in their original phase.

A short history of superheating:

- 1948 - Walter Kauzmann, Chem. Rev. 43, 219
  - Supercooling limit predicted from entropy cross-over.
  - A liquid cooled below this limit will undergo spontaneous crystallization or glass formation.
- 1988 - H. J. Fecht and W. L. Johnson, Nature 334, 50
  - Introduced the notion of the entropy catastrophe
  - A solid heated above ~$3T_m$ will spontaneously melt
  - Represents a true upper limit of superheating

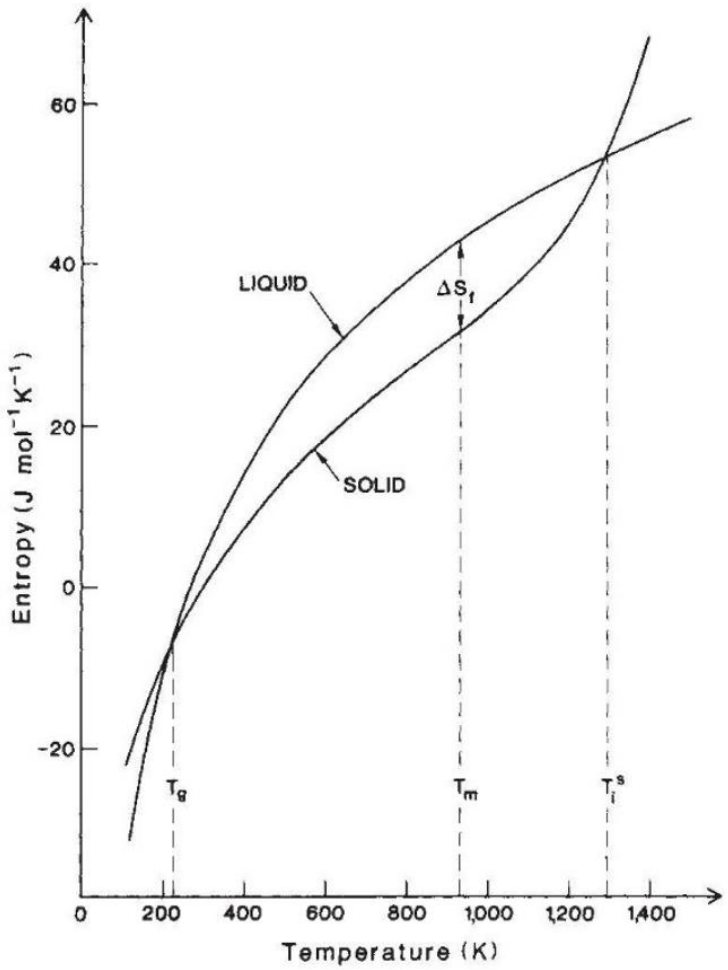

Fig. 1 The entropy of liquid and crystalline aluminium as function of temperature in the stable and metastable regime. ΔS_f denotes the entropy of fusion.

What is the Ultimate Limit of Superheating?

Superheating is a complex non-equilibrium phenomenon in which materials reach temperatures higher than required for a phase transition yet remain in their original phase.

A short history of superheating:

- 1948 - Walter Kauzmann, Chem. Rev. 43, 219
  - Supercooling limit predicted from entropy cross-over.
  - A liquid cooled below this limit will undergo spontaneous crystallization or glass formation.
- 1988 - H. J. Fecht and W. L. Johnson, Nature 334, 50
  - Introduced the notion of the entropy catastrophe
  - A solid heated above ~$3T_m$ will spontaneously melt
  - Represents a true upper limit of superheating
- 1988 S. Lele et al. Nature 336, 567
  - New entropy catastrophe limit lowered to ~$2T_m$
- 1989 - K. Lu, Y. Li, Phys. Rev. Lett. 80, 4474
  - Rigidity catastrophe ~$1.25T_m$
  - Volume/ isochoric catastrophe ~$1.3*T_m$
- 2003 - K. Lu PRL 80, 20, 4474-4477
  - Homogeneous nucleation catastrophe ~$1.2*T_m$

Hierarchy of catastrophes

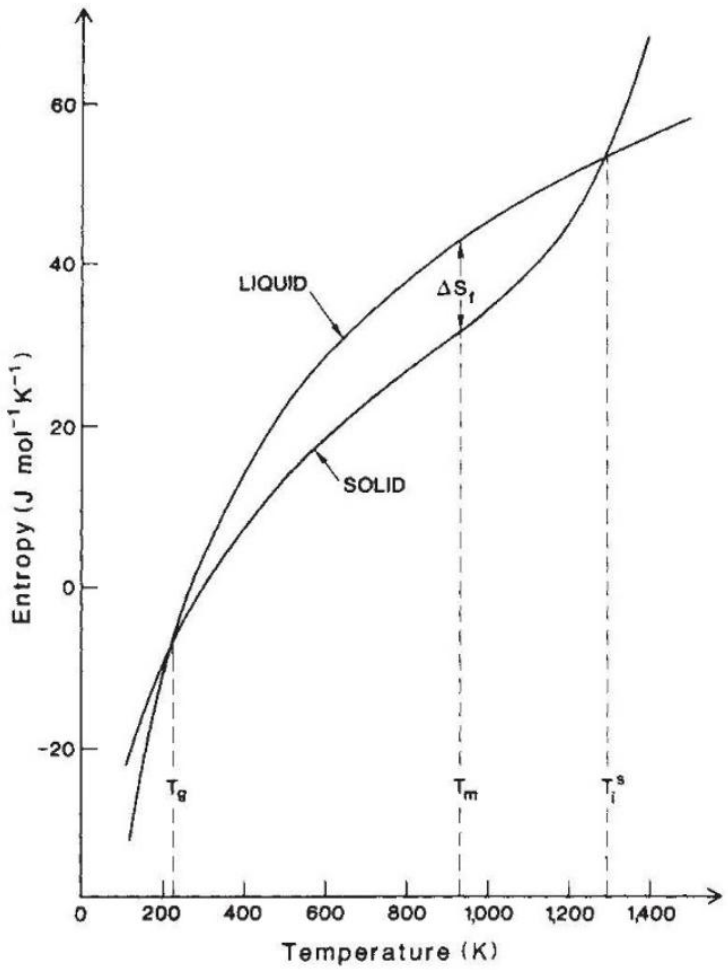

Fig. 1 The entropy of liquid and crystalline aluminium as function of temperature in the stable and metastable regime. ΔS_f denotes the entropy of fusion.

What is the Ultimate Limit of Superheating?

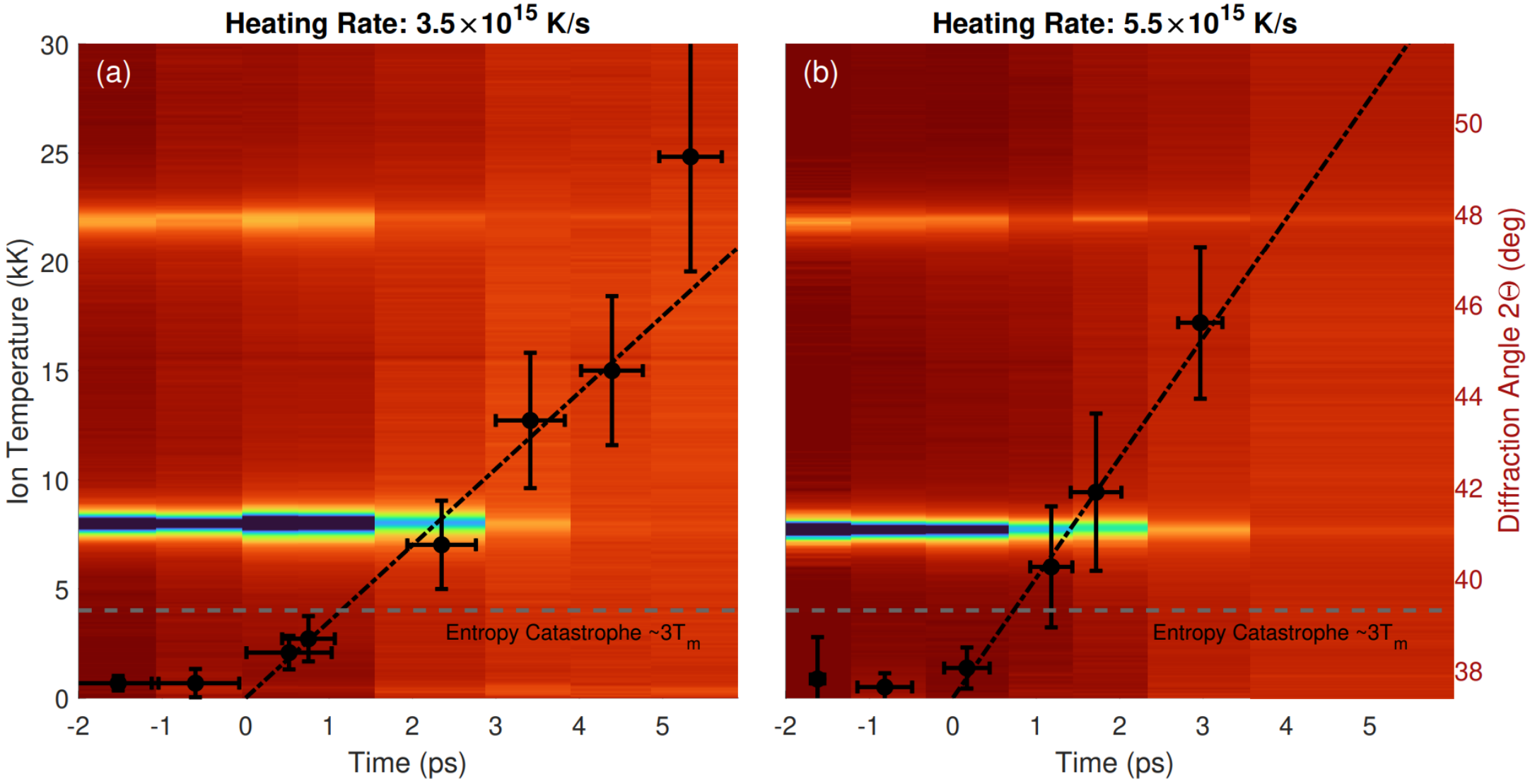

What is the Ultimate Limit of Superheating?

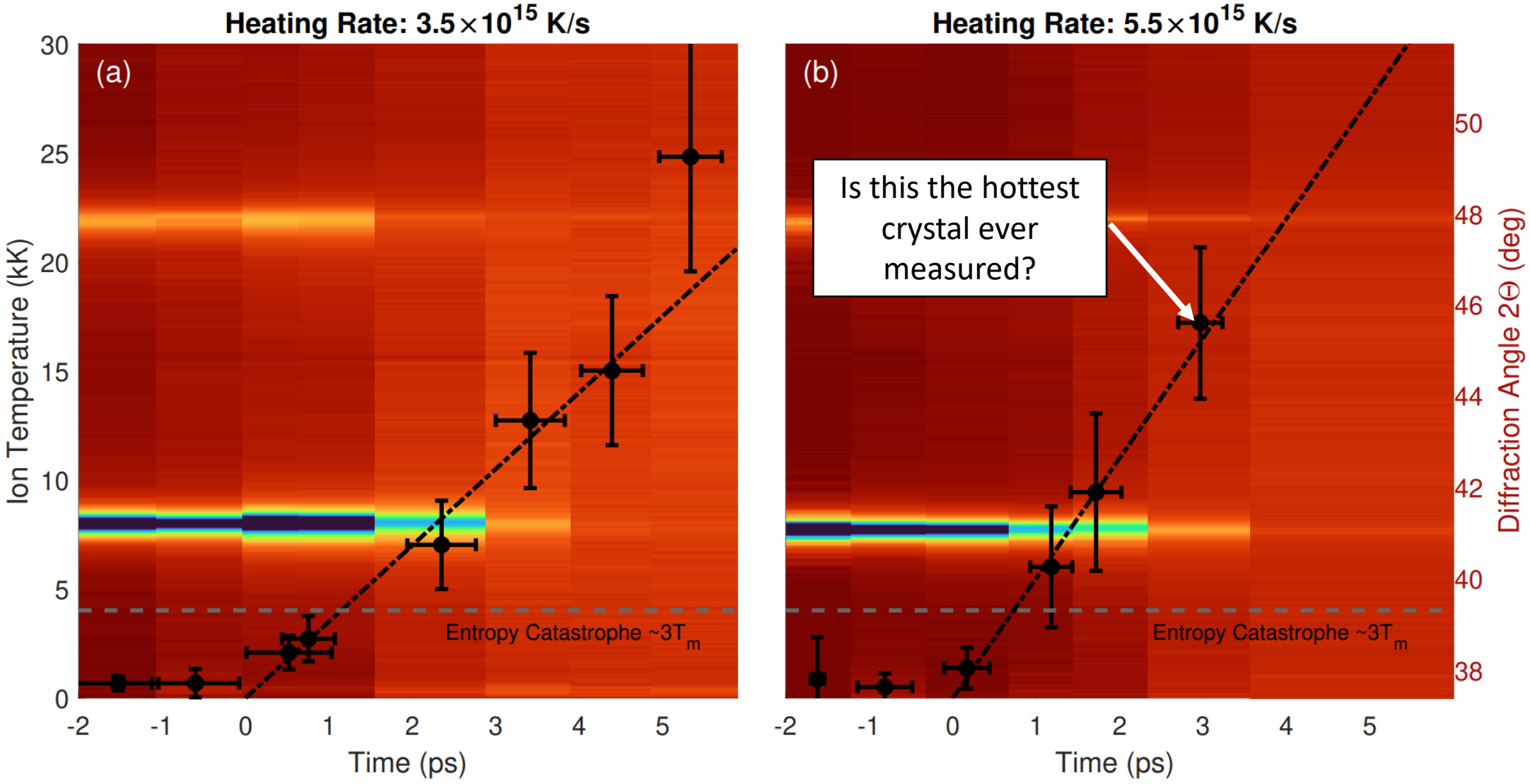

Surviving the Entropy Catastrophe: Redefining the Limit of Superheating

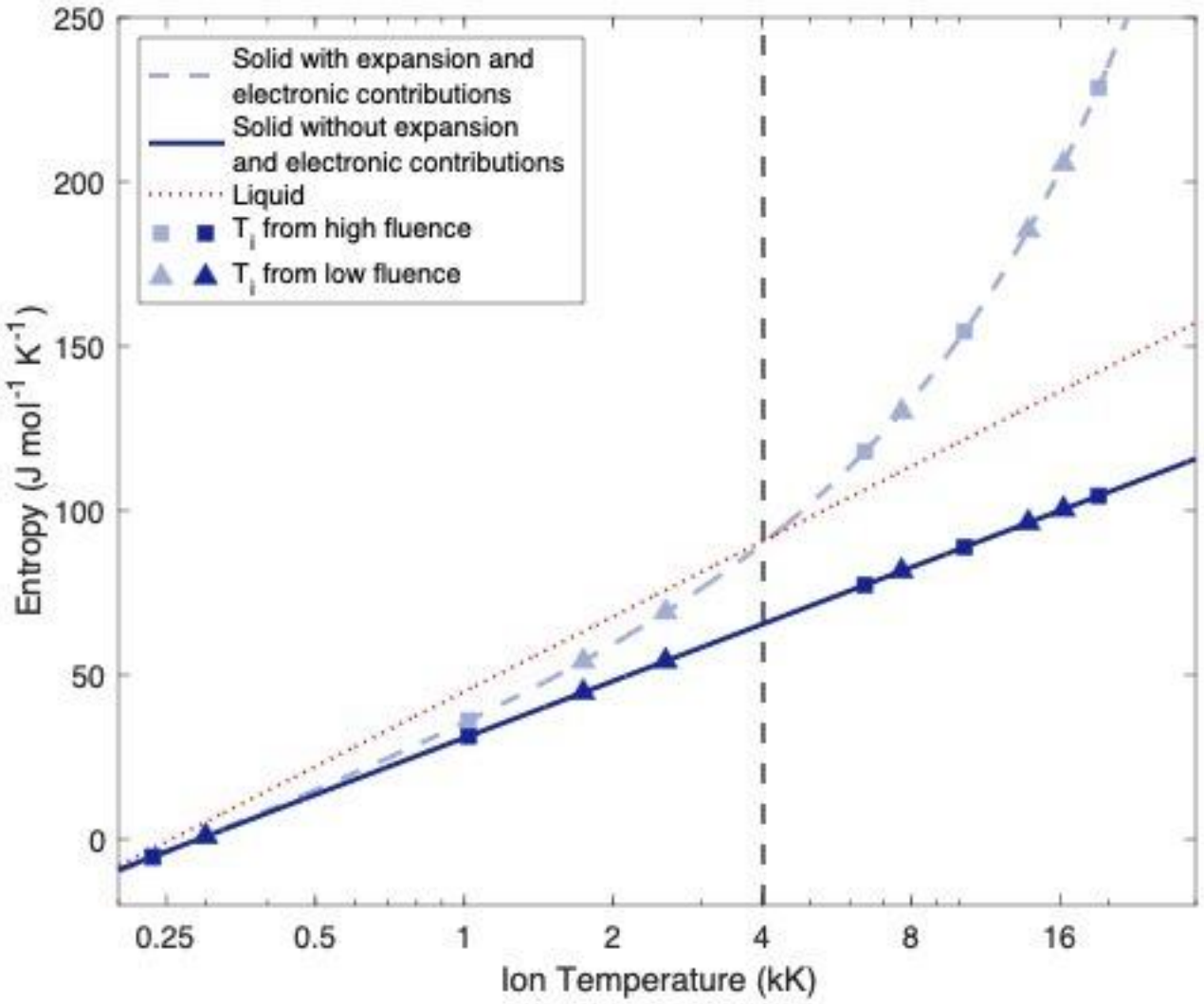

event.fourwaves.com/sccs2025

July 27 to August 1, 2025

Strongly Coupled Coulomb Systems 2025

Registration Abstract Submission

Program

SCCS 2025 will cover the following topics:

- Dense and Astrophysical Plasmas
- Plasmas in Condensed Matter
- Confined and Mesoscopic Coulomb Systems
- High-Energy Density Plasmas in the Laboratory
- Classical Charged Systems
- Developments in Theoretical Methods and Numerical Techniques
- Non-Equilibrium Systems